Published for SISSA by Springer

Received: *August 30, 2012*
Accepted: *October 1, 2012*
Published: *November 8, 2012*

Measurements of the pseudorapidity dependence of the total transverse energy in proton-proton collisions at $\sqrt{s} = 7\,\mathrm{TeV}$ with ATLAS

The ATLAS collaboration

E-mail: atlas.publications@cern.ch

Abstract: This paper describes measurements of the sum of the transverse energy of particles as a function of particle pseudorapidity, η, in proton-proton collisions at a centre-of-mass energy, $\sqrt{s} = 7\,\mathrm{TeV}$ using the ATLAS detector at the Large Hadron Collider. The measurements are performed in the region $|\eta| < 4.8$ for two event classes: those requiring the presence of particles with a low transverse momentum and those requiring particles with a significant transverse momentum. In the second dataset measurements are made in the region transverse to the hard scatter. The distributions are compared to the predictions of various Monte Carlo event generators, which generally tend to underestimate the amount of transverse energy at high $|\eta|$.

Keywords: Hadron-Hadron Scattering

ArXiv ePrint: 1208.6256

doi:10.1007/JHEP11(2012)033

JHEP11(2012)033

Contents

1 Introduction

The main aim of the Large Hadron Collider (LHC) general-purpose detectors is to explore physics in collisions around and above the electroweak symmetry-breaking scale. Such processes typically involve high momentum transfer, which distinguishes them from the dominant processes, namely low momentum transfer strong force interactions described by non-perturbative Quantum Chromodynamics (QCD). In order to collect enough data

JHEP11(2012)033

to be sensitive to rare processes it is necessary to run the LHC at high instantaneous luminosities, meaning that multiple proton-proton interactions are very likely to occur each time the proton bunches collide. It is essential that the Monte Carlo event generators used to simulate these processes have an accurate description of the soft particle kinematics in inclusive proton-proton interactions over the entire acceptance of the LHC experiments, such that reliable comparisons can be made between theoretical predictions and the data for any process of interest.

Protons are composite objects made up of partons, the longitudinal momentum distributions of which are described by parton distribution functions (PDFs). When protons interact at the LHC the dominant parton-parton interaction is t-channel gluon exchange. Due to the composite nature of the protons it is possible that multiple parton-parton interactions (MPI) occur in the same proton-proton interaction. Therefore, if a hard parton-parton interaction occurs it will likely be accompanied by additional QCD interactions, again predominately low momentum t-channel gluon exchange. Any part of the interaction not attributed to the hard parton-parton scatter is collectively termed the underlying event, which includes MPI as well as soft particle production from the beam-beam remnants. Monte Carlo event generators that simulate any hard process at the LHC must also include an accurate description of the underlying event.

At low momentum transfer, perturbative calculations in QCD are not meaningful and cross-sections cannot currently be computed from first principles. Phenomenological models are therefore used to describe the kinematics of particle production in inclusive proton-proton interactions and in the underlying event in events with a hard scatter; these must be constrained by, and tuned to, data.

This paper presents a measurement of the sum of the transverse energy, ΣE_{T}, of particles produced in proton-proton collisions at the LHC, using the ATLAS detector [1]. The ΣE_{T} distribution is measured in bins of pseudorapidity,[1] η, in the range $|\eta| < 4.8$. Distributions of the ΣE_{T} and the mean ΣE_{T} as a function of $|\eta|$ are presented. These measurements are performed with two distinct datasets. The first is as inclusive as possible, with minimal event selection applied, sufficient to ensure that an inelastic collision has occurred. This is termed the *minimum bias* dataset and is studied in order to probe the particle kinematics in inclusive proton-proton interactions. Understanding these processes is vital to ensure a good description of multiple proton-proton interactions in runs with high instantaneous luminosity. The second dataset requires the presence of two jets with high transverse energy, $E_{\mathrm{T}} > 20\,\mathrm{GeV}$, which ensures a hard parton-parton scatter has occurred and therefore allows the particle kinematics in the underlying event to be probed. This sample is termed the *dijet* dataset. Both datasets were collected during the first LHC runs at $\sqrt{s} = 7\,\mathrm{TeV}$ in 2010. The data samples correspond to integrated luminosities of 7.1 $\mu\mathrm{b}^{-1}$ for the minimum

[1] ATLAS uses a right-handed coordinate system with its origin at the nominal interaction point (IP) in the centre of the detector and the z-axis along the beam pipe. The x-axis points from the IP to the centre of the LHC ring, and the y-axis points upward. Cylindrical coordinates (r, ϕ) are used in the transverse $(x - y)$ plane, ϕ being the azimuthal angle around the beam pipe. The pseudorapidity is defined in terms of the polar angle θ with respect to the beamline as $\eta = -\ln\tan(\theta/2)$.

JHEP11(2012)033

bias measurement[2] and 590 μb^{-1} for the dijet measurement. Such small data samples are used because the early LHC runs had a very low instantaneous luminosity ensuring a negligible contribution from multiple proton-proton interactions. The larger sample for the dijet analysis is used as the cross-section for a hard scatter is significantly lower than for inclusive proton-proton interactions.

Many previous measurements of the kinematic properties of particles produced in minimum bias events [2–5] and in the underlying event [6–11] were restricted to the central region of the detectors. This is because they used tracking detectors, with limited coverage, to study charged particles, or because they used only the central region of the calorimeters, where the tracking detectors could be used for calibration. Measurements of the mean of the sum of the energy of particles as a function of $|\eta|$ in minimum bias events and in the underlying event were performed with the CMS forward calorimeter [12]; these were limited to the very forward region ($3.15 < |\eta| < 4.9$). LHCb has performed measurements of charged particle multiplicities in the regions $-2.5 < \eta < -2.0$ and $2.0 < \eta < 4.5$ [13].

The measurements described in this paper utilize the entire acceptance of the ATLAS calorimeters, $|\eta| < 4.9$, allowing the ΣE_{T} to be probed and unfolded in the region $|\eta| < 4.8$. Unless otherwise stated, the central region will refer to the range $|\eta| < 2.4$ and the forward region will refer to the range $2.4 < |\eta| < 4.8$. The measurement is performed with the ATLAS calorimeters and is corrected for detector effects so that the variables are defined at the particle-level (see section 2), which includes all stable particles (those with a proper lifetime greater than 3×10^{-11} seconds). Both the mean and distributions of the ΣE_{T} are measured. This provides additional information, giving a complete picture of both inclusive proton-proton interactions and the underlying event in dijet processes, within the entire acceptance of the general purpose LHC detectors. The relative levels of particle production in the forward and central regions may be affected by the contribution from beam-beam remnant interactions, details of the hadronization as modelled with colour reconnection between quarks and gluons, the relative contribution from diffractive processes and the parton distribution functions in this kinematic domain.

This paper is organized as follows. Section 2 defines the particle-level variables. Section 3 describes the Monte Carlo models that are used to correct the data for detector effects and to compare to the final unfolded results. The ATLAS detector is discussed in section 4, the event reconstruction in section 5 and the event selection in section 6. The method used to correct the data for detector effects is described in section 7. The systematic uncertainties are described in section 8. Section 9 presents and discusses the final results and compares them to various Monte Carlo simulations. Finally, conclusions are given in section 10.

2 Particle-level variable definitions

In data, events are selected and variables defined using calibrated detector-level quantities. Corrections for detector effects are then applied. In order to compare the corrected data with predictions from Monte Carlo event generators without passing the events through a simulation of the ATLAS detector, it is necessary to define variables at the particle-level.

[2]The run dependence of the analysis was checked in a larger sample and found to be negligible.

JHEP11(2012)033

The particle-level ΣE_{T} is defined at the generator level by summing the E_{T} of all stable charged particles with momentum $p > 500\,\mathrm{MeV}$ and all stable neutral particles with $p > 200\,\mathrm{MeV}$. Lower momentum particles are not included as they are unlikely to deposit significant energy in the ATLAS calorimeters.

The ΣE_{T} distribution is defined as $\frac{1}{N_{\mathrm{evt}}}\frac{dN_{\mathrm{evt}}}{d\Sigma E_{\mathrm{T}}}$, where N_{evt} is the number of events in the sample. It is measured in six regions: $0.0 < |\eta| < 0.8$, $0.8 < |\eta| < 1.6$, $1.6 < |\eta| < 2.4$, $2.4 < |\eta| < 3.2$, $3.2 < |\eta| < 4.0$ and $4.0 < |\eta| < 4.8$. In addition the mean ΣE_{T} over all events, per unit η–ϕ, is measured as a function of $|\eta|$. This is denoted as the transverse energy density ($E_{\mathrm{T}}^{\mathrm{density}}$) and is defined as $\langle\frac{d^2\Sigma E_{\mathrm{T}}}{d\eta d\phi}\rangle$. In the minimum bias measurement, the ΣE_{T} includes particles at any ϕ. In the dijet measurement, the ΣE_{T} is measured using only particles that are in the azimuthal region transverse to the hard scatter, namely $\frac{\pi}{3} < |\Delta\phi| < \frac{2\pi}{3}$, where $\Delta\phi$ is the azimuthal separation between the leading jet and a given particle. This region of phase space contains limited particle production from the hard parton-parton interaction and is therefore most sensitive to the underlying event.

2.1 Particle-level minimum bias event selection

The events in the minimum bias analysis contain at least two charged particles with $p_{\mathrm{T}} > 250\,\mathrm{MeV}$ and $|\eta| < 2.5$, reflecting as closely as possible the requirement of a reconstructed vertex, as will be discussed in section 6.

2.2 Particle-level dijet event selection

The events in the dijet analysis contain at least two particle-level jets.[3] Both the leading and sub-leading jets must have $E_{\mathrm{T}}^{\mathrm{jet}} > 20\,\mathrm{GeV}$ and $|\eta^{\mathrm{jet}}| < 2.5$, reconstructed with the anti-k_t [14] algorithm with radius parameter $R = 0.4$. This selection ensures that a hard scattering has occurred. A relatively small radius parameter reduces the probability of the jet algorithm collecting particles that are not associated with the hard scatter. In order to select a well balanced back-to-back dijet system, the jets satisfy $|\Delta\phi_{\mathrm{jj}}| > 2.5$ radians, where $\Delta\phi_{\mathrm{jj}}$ is the difference in azimuthal angle of the leading and sub-leading jet, and $\frac{E_{\mathrm{T}}^{\mathrm{jet2}}}{E_{\mathrm{T}}^{\mathrm{jet1}}} > 0.5$, where $E_{\mathrm{T}}^{\mathrm{jet1(2)}}$ is the E_{T} of the (sub-)leading jet. The latter requirement retains most of the dataset, but avoids topologies in which there is a large transverse energy difference between the leading and sub-leading jets. A well balanced dijet system suppresses contributions from multijet events, allowing a clearer distinction between regions with particle production dominated by the hard scatter and by the underlying event.

3 Monte Carlo event generators

This section describes the Monte Carlo event generator (MC) models used to correct the data for detector effects, to assign systematic uncertainties to the corrections due to the physics model, and for comparisons with the final unfolded data. The `PYTHIA 6` [15], `PYTHIA 8` [16], `Herwig++` [17] and `EPOS` [18] generators are used, with various tunes that are described below. First a brief introduction to the relevant parts of the event generators is given.

[3] A particle-level jet is built from all stable particles, excluding neutrinos and muons.

JHEP11(2012)033

PYTHIA 6 and PYTHIA 8 are general purpose generators that use the Lund string hadronization model [19]. In PYTHIA 6 there is an option to use a virtuality-ordered or p_{T}-ordered parton shower, with the latter used in most recent tunes. In PYTHIA 8, the p_{T}-ordered parton shower is used. The inclusive hadron-hadron interactions are described by a model that splits the total inelastic cross-section into non-diffractive processes, dominated by t-channel gluon exchange, and diffractive processes involving a colour-singlet exchange. The diffractive processes are further divided into single-diffractive dissociation, where one of the initial hadrons remains intact and the other is diffractively excited and dissociates, and double-diffractive dissociation where both hadrons dissociate. Such events tend to have large gaps in particle production at central rapidity. The smaller contribution from central diffraction, in which both hadrons remain intact and particles are produced in the central region, is neglected. The $2 \to 2$ non-diffractive processes, including MPI, are described by lowest-order perturbative QCD with the divergence of the cross-section as $p_{\mathrm{T}} \to 0$ regulated with a phenomenological model. There are many tunable parameters that control, among other things, the behaviour of this regularization, the matter distribution of partons within the hadrons, and colour reconnection. When p_{T}-ordered parton showers are used, the MPI and parton shower are interleaved in one common sequence of decreasing p_{T} values. For PYTHIA 6 the interleaving is between the initial-state shower and MPI only, while for PYTHIA 8 it also includes final-state showers. Since the p_{T}-ordered showers and interleaving with MPI are considered to be a model improvement, the most recent PYTHIA 6 tunes are made with this configuration. This is also the only configuration available in PYTHIA 8. A pomeron-based approach is used to describe diffractive events, using (by default) the Schuler and Sjöstrand [20] parameterization of the pomeron flux. In PYTHIA 6 the diffractive dissociations are treated using the Lund string model, producing final-state particles with limited p_{T}. In PYTHIA 8 the dissociations are treated like this only for events with a diffractive system with a very low mass; in higher mass systems diffractive parton distributions from H1 [21] are used to include diffractive final states which are characteristic of hard partonic interactions. In this case, the full machinery of MPI and parton showers is used. This approach yields a significantly harder p_{T} spectrum for final-state particles.

Herwig++ is another general purpose generator, but with a different approach: it uses an angular-ordered parton shower and the cluster hadronization model [22]. It has an MPI model similar to the one used by the PYTHIA generators, with tunable parameters for regularizing the behaviour at very low momentum transfer, but does not include the interleaving with the parton showers. Inclusive hadron-hadron collisions are simulated by applying the MPI model to events with no hard scattering. It is therefore possible to generate an event with zero $2 \to 2$ partonic scatters, in which only beam remnants are produced, with nothing in between them. While Herwig++ has no explicit model for diffractive processes, these zero-scatter events will look similar to double-diffractive dissociation.

EPOS is an event generator used primarily to simulate heavy ion and cosmic shower interactions, but which can also simulate proton-proton interactions. EPOS provides an implementation of a parton based Gribov-Regge [23] theory which is an effective, QCD-inspired field theory describing hard and soft scattering simultaneously. EPOS calculations

JHEP11(2012)033

Generator	Version	Tune	PDF	7 TeV data	
				MB	UE
PYTHIA 6	6.423	AMBT1 [24]	MRST LO* [25]	yes	no
PYTHIA 6	6.423	DW [26]	CTEQ 5L [27]	no	no
PYTHIA 6	6.423	Perugia0 [28]	CTEQ 5L	no	no
PYTHIA 8	8.145	4C [29]	CTEQ 6L1 [30]	yes	no
Herwig++	2.5.1	UE7-2 [31]	MRST LO** [25]	no	yes

Table 1. MC tunes used to unfold the data and to determine the physics model dependent systematic uncertainty. The last two columns indicate whether the data used in the tune included 7 TeV minimum bias (MB) and/or underlying event (UE) data.

Generator	Version	Tune	PDF	7 TeV data	
				MB	UE
PYTHIA 6	6.425	AUET2B:CTEQ6L1 [32]	CTEQ 6L1	no	yes
PYTHIA 8	8.153	A2:CTEQ6L1 [33]	CTEQ 6L1	yes	no
PYTHIA 8	8.153	A2:MSTW2008LO [33]	MSTW2008 LO [34]	yes	no
EPOS	1.99_v2965	LHC	N/A	yes	no

Table 2. Additional MC tunes used to compare to the unfolded data only. The last two columns indicate whether the data used in the tune included 7 TeV minimum bias (MB) and/or underlying event (UE) data.

thus do not rely on the standard PDFs as used in generators like PYTHIA and Herwig++. At high parton densities a hydrodynamic evolution of the initial state is calculated for the proton-proton scattering process as it would be for heavy ion interactions. The results presented here use the EPOS LHC tune, which contains a parameterized approximation of the hydrodynamic evolution. The optimal parameterization has been derived from tuning to LHC minimum bias data.

The reference MC sample used throughout this study is the AMBT1 [24] tune of PYTHIA 6. In order to check the model dependence of the data corrections, additional generators and tunes are considered. These are summarized in table 1 along with information about the PDFs used and whether minimum bias or underlying event data at $\sqrt{s} = 7$ TeV were used in the tune. Of the PYTHIA 6 tunes listed, only DW uses the old virtuality-ordered parton shower without interleaving with MPI. Some more recent tunes are also used to compare to the unfolded data; these are summarized in table 2. For these more recent tunes the PDF is explicitly given in the name as there are different instances of each tune that use different PDFs and hence have different parameters.

JHEP11(2012)033

4 The ATLAS detector

The ATLAS detector is described in detail in ref. [1]. Here only the components most relevant for this measurement are described.

Tracks and interaction vertices are reconstructed with the inner detector tracking system, which consists of a silicon pixel detector, a silicon strip detector and a transition radiation tracker, all immersed in a 2 T axial magnetic field. The calorimeter systems are of particular importance for the measurements presented in this paper. The ATLAS calorimeter system provides fine-grained measurements of shower energy depositions over a wide range of η. A highly segmented electromagnetic liquid argon (LAr) sampling calorimeter covers the region $|\eta| < 3.2$, with granularity that ranges from 0.003×0.10 or 0.025×0.025 to 0.1×0.1 in $\Delta\eta \times \Delta\phi$, depending on depth segment and pseudorapidity. It is divided into a barrel part ($|\eta| < 1.475$) and an endcap part ($1.375 < |\eta| < 3.2$). The hadronic barrel ($|\eta| < 1.7$) calorimeter consists of steel absorbers and active scintillating tiles, with a granularity of either 0.1×0.1 or 0.2×0.1 depending on the layer. The hadronic endcap ($1.5 < |\eta| < 3.2$) and forward ($3.1 < |\eta| < 4.9$) electromagnetic and hadronic calorimeters use liquid argon technology. The granularity in the hadronic endcap ranges from 0.1×0.1 to 0.2×0.2. In the forward calorimeter, the cells are not arranged in projective towers but are aligned parallel to the beam axis. As such the readout granularity is not constant in η–ϕ.

Minimum bias trigger scintillator (MBTS) detectors are mounted in front of the endcap calorimeters on both sides of the interaction point and cover the region $2.1 < |\eta| < 3.8$. The MBTS is divided into inner and outer rings, both of which have eight-fold segmentation, and is used to trigger the events analysed in this paper.

5 Event reconstruction

This analysis is based on topological clusters in the calorimeter, which represent an attempt to reconstruct three-dimensional energy depositions associated with individual particles [35]. The topological clustering algorithm proceeds through the following steps. First, seed cells are found that have $|E| > 4\sigma$ above the noise level, where E is the cell energy measured at the electromagnetic scale[4] and calibrated using test-beam data [36–39]. Next, neighbouring cells are collected into the cluster if they have $|E| > 2\sigma$ above the noise level. Finally, all surrounding cells are added to the cluster until no further cells with $|E| > 2\sigma$ are among the direct neighbours.

The detector-level ΣE_{T} is formed by summing the E_{T} of all clusters in the η–ϕ region of interest. Negative energy clusters are included, leading to a convenient cancellation of the contributions from noise, which can be either negative or positive.

To correct these clusters back to the particle-level, it is first necessary to determine the particle momenta to which the ATLAS calorimeters are sensitive. Using a `GEANT4` [40] simulation of the ATLAS detector [41], generator-level particles are propagated from

[4]The electromagnetic scale is the basic calorimeter signal scale for the ATLAS calorimeters. It gives the correct response for the energy deposited in electromagnetic showers, but does not account for the lower response to hadrons.

JHEP11(2012)033

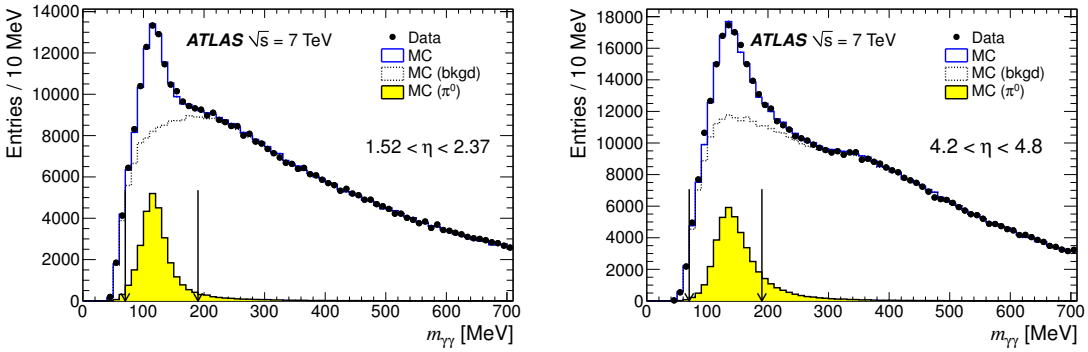

(a) **(b)**

Figure 1. The di-photon invariant mass in the region (a) $1.52 < \eta < 2.37$ and (b) $4.2 < \eta < 4.8$. The data are compared to the MC simulation with the best fit scale factor applied (this is 0.97 ± 0.02 for (a) and 1.01 ± 0.02 for (b)). The contribution from the MC signal $\pi^0 \to \gamma\gamma$ templates and background templates are also shown separately. The arrows indicate the fit range.

the primary vertex to the calorimeters and the fraction of their energy deposited in the calorimeters as clusters is studied as a function of $|\eta|$ and p of the particle. As discussed in section 2, charged particles with $p > 500\,\text{MeV}$ and neutral particles with $p > 200\,\text{MeV}$ are found to deposit enough energy in the calorimeter to be included in the particle-level definition for all $|\eta|$ regions. Particles with lower momenta contribute a negligible amount to the cluster ΣE_{T} and are therefore excluded from the particle-level ΣE_{T} definition.

In order to properly correct for detector effects, the detector simulation must accurately describe the energy response of the calorimeters to low energy particles. The simulation calibration is refined using the di-photon invariant mass distribution of $\pi^0 \to \gamma\gamma$ candidates. In data selected with the MBTS trigger, pairs of photon candidates in a given η region are formed and their invariant mass, $m_{\gamma\gamma}$, is constructed. In order to reduce combinatorial background, only events with exactly one pair in the η region are considered. The data are compared to MC signal plus background templates in η bins, which are chosen to reflect the boundaries of the calorimeter sub-systems.

The signal templates are derived from the `PYTHIA 6 AMBT1` samples, by matching pairs of clusters to generator level photons from a π^0 decay. The background templates are obtained using pairs of clusters that are not matched. The energies of the clusters in the signal template are scaled by an energy response scale factor. This is varied and the χ^2 between the data and MC distributions is minimized in order to determine the best fit value. Deviations from unity are typically 2–3% but reach values of up to 10% in some η regions. This scale factor is then applied to the energy of the MC clusters before unfolding the data. Figure 1 shows the $m_{\gamma\gamma}$ distribution in data compared to the MC in two sample $|\eta|$ regions with the best fit scale factor applied.

JHEP11(2012)033

6 Event selection

Events in the minimum bias analysis are selected with a one-sided MBTS trigger, which requires one counter on either side of the detector to be above noise threshold, suppressing contributions from empty beam crossings and beam-induced background. In order to suppress these contributions further, events are required to have a reconstructed primary vertex with at least two associated tracks with $p_{\mathrm{T}} > 150\,\mathrm{MeV}$ and $|\eta| < 2.5$. Note that the track p_{T} cut is lower than the 250 MeV particle-level cut described in section 2.1. This is because tracking and vertex reconstruction inefficiencies result in events with at least two 150 MeV reconstructed tracks having the same $E_{\mathrm{T}}^{\mathrm{density}}$ as events with at least two 250 MeV charged particles, according to the MC models considered in this analysis.

Furthermore, events having more than one reconstructed vertex with five or more tracks are vetoed to suppress contributions from multiple proton-proton interactions. Five tracks are required on the additional vertices so that events with secondary vertices from decaying particles are not vetoed.

Events in the dijet analysis are also selected with the one-sided MBTS trigger and are required to pass the same event selection criteria as the minimum bias analysis. In addition, they are required to contain two back-to-back jets passing the same kinematic selection criteria as the particle-level jets described in section 2.2.

7 Corrections for detector effects

The ΣE_{T} distributions are unfolded in each $|\eta|$ region using an iterative Bayesian unfolding technique [42]. The $E_{\mathrm{T}}^{\mathrm{density}}$ distribution is obtained by taking the mean of each unfolded ΣE_{T} distribution and dividing by the $|\eta|$ and ϕ phase space. An unfolding matrix is formed from events generated with `PYTHIA 6 AMBT1`, passed through the `GEANT4` simulation of the ATLAS detector. The detector simulation accounts for energy losses of the particles in material upstream of the calorimeter, for charged particles that bend in the magnetic field and get swept out of the calorimeter acceptance, and for the calorimeter response and resolution. Before unfolding each ΣE_{T} distribution, the MC is reweighted by a fit to the ratio of the data to the MC detector-level ΣE_{T} distribution, so that the ΣE_{T} distribution matches that seen in data. The MC significantly underestimates the ΣE_{T} in the forward region, as seen in figure 2, where the detector-level ΣE_{T} distribution in the region $4.0 < |\eta| < 4.8$ is shown for both data and MC, before and after reweighting, for both the minimum bias and dijet selections.

The unfolding matrix associates the ΣE_{T} formed from clusters with the ΣE_{T} formed from generator-level particles. Events that pass the detector-level but not the particle-level selection criteria and vice versa are also accounted for in the correction procedure. The prior distribution of the particle-level ΣE_{T} is initially taken from `PYTHIA 6 AMBT1` (reweighted to data) and the unfolding procedure is iterated twice, with the prior distribution replaced by the unfolded distribution after each iteration. A stable result is achieved after two iterations.

JHEP11(2012)033

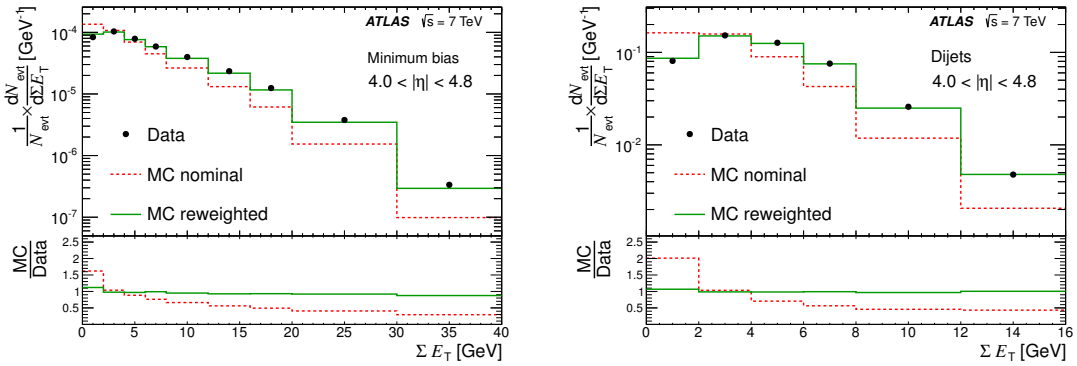

(a) **(b)**

Figure 2. The detector-level ΣE_{T} distribution in the region $4.0 < |\eta| < 4.8$ for data compared to the nominal detector-level PYTHIA 6 AMBT1 prediction and the reweighted detector-level PYTHIA 6 AMBT1 prediction in (a) the minimum bias events and (b) the dijet events.

8 Systematic uncertainties

The dominant systematic uncertainties arise from three sources: (1) the accuracy with which the MC simulates the energy response of the calorimeters to low energy particles, (2) the knowledge of the amount of material upstream of the calorimeters and (3) the MC generator model dependence in the unfolding. In the dijet analysis an additional uncertainty arises from the accuracy with which the MC simulates the jet energy scale. These sources are discussed in the following sub-sections. In each case the uncertainty on the unfolded data is obtained by shifting the MC by $\pm 1\sigma$ for the source in question and comparing with the nominal unfolded data. In order to give information about the correlations of the systematic uncertainties between bins and between the different distributions in this paper, each source is split into different components. These systematic uncertainties are summarized in tabular form in appendix A.

The following additional potential sources of systematic uncertainty are found to be negligible: energy resolution, multiple proton-proton interactions, contributions from noise and beam-induced backgrounds, simulation of the primary vertex position, simulation of the trigger selection, and simulation of the position of the forward calorimeter.

8.1 Calorimeter energy response

The systematic uncertainty on the calorimeter energy response is determined separately for electromagnetic and hadronic particles. An average is then obtained, using the PYTHIA 6 AMBT1 prediction of the relative contributions to the ΣE_{T} by different particle types. For electromagnetic particles the systematic error comes from uncertainties on the extraction of the energy scale from fits to the $m_{\gamma\gamma}$ distributions in $\pi^0 \to \gamma\gamma$ candidates. These are obtained from variations in the fit range, the background shape, the criteria for matching reconstructed photons to generator-level photons in the production of the

JHEP11(2012)033

signal template, variations in the simulation of the calorimeter resolution, and consistency with a similar analysis using tighter kinematic and photon identification cuts. The total uncertainty depends on the $|\eta|$ region and is generally at the level of 2–4%, but increases up to 15% in the regions where different calorimeter sub-systems overlap.

The uncertainty on the energy response for hadronic particles in the central region, where there is good coverage from the inner tracking detector, is obtained from studies of the ratio of the calorimeter energy measurement to the inner detector track momentum measurement, for isolated charged pions [43]. The uncertainty is obtained by taking the difference between data and MC in p and $|\eta|$ bins and is found to be 3.5% for $|\eta| < 0.8$ and 5% for $0.8 < |\eta| < 2.4$. In the forward region the energy response uncertainty for hadrons is taken from the difference between the MC and data in test-beam studies of charged pions [44]. This leads to a one-sided uncertainty for hadrons relative to electromagnetic particles of +5% in the region $2.5 < |\eta| < 3.2$ and +9% in the forward calorimeter ($|\eta| > 3.2$).

The only component of the systematic uncertainty on the energy response assumed to be correlated between $|\eta|$ bins is that of the forward calorimeter (determined from test-beam results), which affects the bins $3.2 < |\eta| < 4.0$ and $4.0 < |\eta| < 4.8$. The systematic uncertainties from the $\pi^0 \to \gamma\gamma$ fits are assumed to be uncorrelated as the $m_{\gamma\gamma}$ shapes are rather different in the different $|\eta|$ regions, resulting in different possible systematic shifts. Similarly, the difference between data and MC for the ratio of calorimeter energy to inner detector track momentum does not show systematic shifts in one direction and is assumed to be uncorrelated.

Appendix A gives both the uncorrelated and correlated uncertainties in each bin of each distribution. The former vary between 2.4% and 5.4% for the $E_{\mathrm{T}}^{\mathrm{density}}$ in the minimum bias data, depending on the $|\eta|$ region. The largest uncertainty is in the region $0.8 < |\eta| < 1.6$, which contains the region of overlap between the barrel and endcap electromagnetic calorimeters ($1.375 < |\eta| < 1.475$). The correlated source is about −6% for the two highest $|\eta|$ bins in the minimum bias data and about −8% in the dijet data. Note that a positive uncertainty on the energy scale in the MC leads to a negative uncertainty on the corrected result in the data. The uncertainty is higher in the dijet data, due to a larger contribution from events where the detector-level jets pass the selection criteria but the generator-level jets do not. Their ΣE_{T} distribution is taken from the MC so a shift in the energy scale leads to an additional bias in the corrected result.

8.2 Material description

The amount of material upstream of the calorimeters affects the ΣE_{T} distributions because particles can interact and lose some of their energy before reaching the calorimeter. It is therefore important to have a realistic description of the material in the MC simulation used to perform the detector corrections.

In order to assess the systematic uncertainty arising from possible discrepancies in the material description, detector corrections are recalculated using a special `PYTHIA 6 AMBT1` sample with additional material. The sample is based on a similar one described in section 3 of ref. [45], but with additional material introduced in the forward region. The results are compared to the nominal unfolded data and the difference is taken as

JHEP11(2012)033

a symmetric systematic uncertainty to account for the possibility of the MC simulation either underestimating or overestimating the amount of material.

In order to understand the correlations between the uncertainties in different $|\eta|$ bins, the additional material is split into three components: (1) extra material upstream of the barrel calorimeter, (2) an increase in material density in the barrel-endcap overlap region and (3) additional material in the inner detector, the inner detector services and the forward region, as well as an increase in the material density in some detector volumes in the forward region. The systematic uncertainties arising from components (1) and (2) are assumed to be correlated between $|\eta|$ bins, whereas the uncertainty arising from component (3) is assumed to be uncorrelated, due to the fine structure of these detectors with respect to the wide bins used in this analysis.

Source (1) affects only the first two $|\eta|$ bins, at the level of about 3% in the minimum bias data and 1.3–2.5% in the dijet data. The uncertainty is generally smaller in the dijet data as the particles in these events tend to have larger momenta. Source (2) affects only the second and third bins and is less than 1%. Source (3) affects all $|\eta|$ bins and ranges between 0.23% and 5.5%, with the largest uncertainty in the region $1.6 < |\eta| < 2.4$, where there is a large amount of material associated with the inner detector.

8.3 Physics model dependence

The MC model used to correct the data can affect the results as a realistic description of particle kinematics is needed. The model dependence is minimized by first reweighting the detector-level MC to the data and then by iterating the unfolding, using the unfolded data as the new prior distribution after each iteration. This reduces the dependence on the ΣE_{T} spectrum itself; however, other kinematic distributions can also affect the unfolding. One important variable is the E_{T} of the individual particles, as the calorimeter response to a particle is energy dependent. The dependence on the model is investigated by performing the unfolding with other MC models. The following MC models and tunes are considered: `PYTHIA 6 AMBT1` (nominal), `PYTHIA 6 DW`, `PYTHIA 6 Perugia0`, `PYTHIA 8 4C` and `Herwig++ UE7-2`. Details of these tunes are given in table 1. The MC model used to assess the systematic uncertainty is chosen to ensure a reasonable spread in the particle kinematics with respect to the reference `PYTHIA 6 AMBT1` model. Figure 3 shows distributions of $\frac{1}{E_{\mathrm{T}}^{\mathrm{tot}}} \times \frac{dE_{\mathrm{T}}^{\mathrm{tot}}}{d|E_{\mathrm{T}}|}$, where $E_{\mathrm{T}}^{\mathrm{tot}}$ is the sum over events of the detector-level ΣE_{T}, and E_{T} is the detector-level cluster transverse energy. These distributions show the relative contribution to the ΣE_{T} from clusters with a given E_{T}. $|E_{\mathrm{T}}|$ is plotted instead of E_{T} since the former leads to a cancellation in the contribution from noise. Figure 3a shows the distribution in minimum bias events for the region $3.2 < |\eta| < 4.0$. This region is shown as it has significant differences between data and MC. The contribution to the ΣE_{T} from high E_{T} clusters is smaller in data than in `PYTHIA 6 AMBT1`. The model with the largest deviations from `PYTHIA 6 AMBT1` is `Herwig++ UE7-2`, indicating that this model can be used to assess possible biases in the unfolding due to this effect. It should be noted that at high $|E_{\mathrm{T}}|$ `Herwig++ UE7-2` lies above `PYTHIA 6 AMBT1` while the data lie below it, but the final systematic uncertainty is symmetrized. The same distribution is shown in figure 3b for the sub-sample of events with $\Sigma E_{\mathrm{T}} > 15\,\mathrm{GeV}$. Again, the data have a softer cluster $|E_{\mathrm{T}}|$ distribution. Here `PYTHIA 6`

JHEP11(2012)033

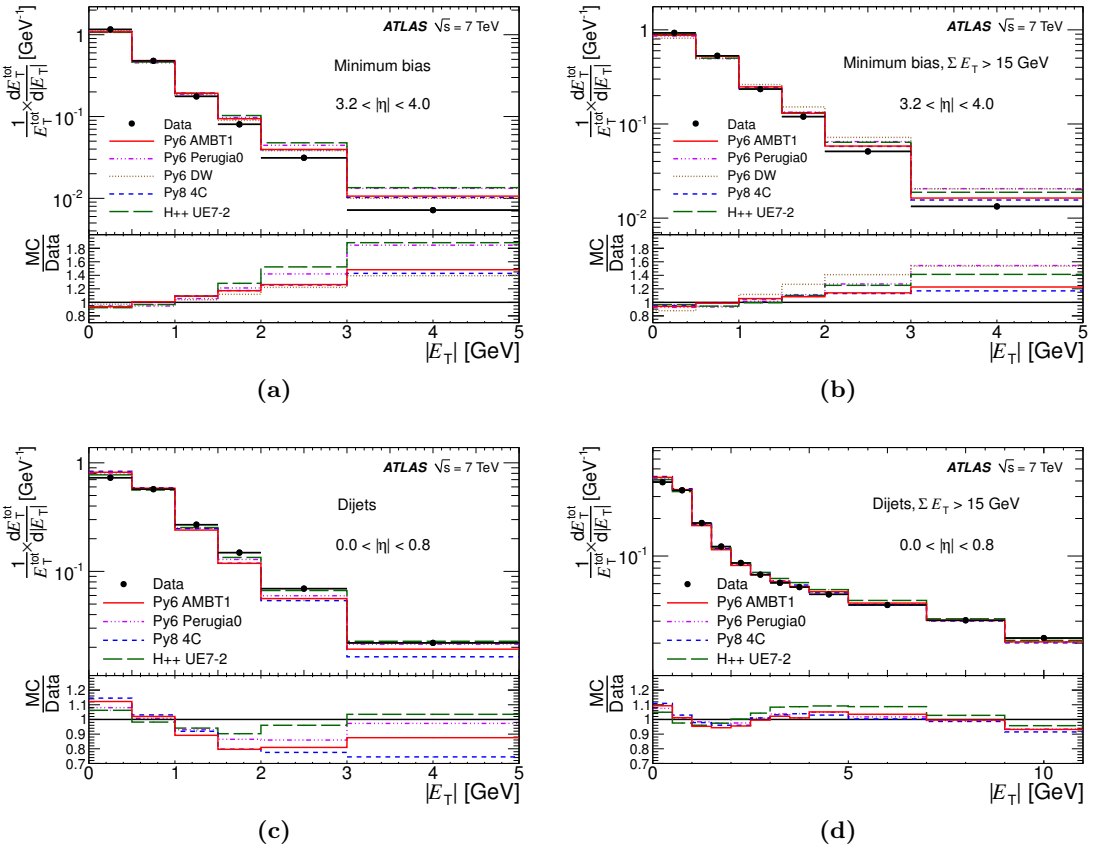

Figure 3. Distribution of $\frac{1}{E_{\mathrm{T}}^{\mathrm{tot}}} \times \frac{dE_{\mathrm{T}}^{\mathrm{tot}}}{d|E_{\mathrm{T}}|}$, where $E_{\mathrm{T}}^{\mathrm{tot}}$ is the sum over events of the detector-level ΣE_{T}, and E_{T} is the detector-level cluster transverse energy (a) in minimum bias events in the region $3.2 < |\eta| < 4.0$; (b) as in (a) but for events with $\Sigma E_{\mathrm{T}} > 15\,\mathrm{GeV}$; (c) in dijet events in the region $0.0 < |\eta| < 0.8$; (d) as in (c) but for events with $\Sigma E_{\mathrm{T}} > 15\,\mathrm{GeV}$. The data are compared to various MC predictions.

DW shows the largest deviations from PYTHIA 6 AMBT1. Since unfolding with PYTHIA 6 DW results in a larger shift in the corrected data than unfolding with Herwig++ UE7-2, the former is used to assess the systematic uncertainty in the minimum bias events.

Figure 3c shows the same distribution in dijet events; the most central region is shown as the differences between data and MC are largest in this region. This time the data distribution is harder than PYTHIA 6 AMBT1. Again Herwig++ UE7-2 has the largest deviations. Figure 3d shows the same distribution for events with $\Sigma E_{\mathrm{T}} > 15\,\mathrm{GeV}$; all the models agree well with the data, but Herwig++ UE7-2 has the largest deviations. For the dijet selection Herwig++ UE7-2 is therefore used to assess the systematic uncertainty.

For both the minimum bias and dijet analyses, this systematic uncertainty is symmetrized and treated as correlated between $|\eta|$ bins (although not correlated between the two analyses). The uncertainties on the $E_{\mathrm{T}}^{\mathrm{density}}$ range from 2–4% for the minimum bias data and are 2% or less for the dijet data.

JHEP11(2012)033

8.4 Jet energy scale

In the dijet selection, events are required to contain at least two jets with $E_{\mathrm{T}} > 20\,\mathrm{GeV}$. It is possible that events that satisfy the detector-level criteria do not satisfy the criteria at the particle-level, and vice versa. This is accounted for in the correction procedure, but if there are differences in the jet energy scale between data and MC simulation this could result in a bias in the correction procedure. The uncertainty on the jet energy scale is described in ref. [46]. The corresponding uncertainty on the $E_{\mathrm{T}}^{\mathrm{density}}$ is at the level of 1.6% in the most central bin and decreases to 0.13% in the most forward bin. It is treated as correlated between $|\eta|$ bins. For the ΣE_{T} distributions this source of uncertainty is negligible and therefore neglected in the region $|\eta| > 2.4$.

9 Results

9.1 Nominal results

The unfolded $E_{\mathrm{T}}^{\mathrm{density}}$ distributions are shown in figure 4 for both the minimum bias and the dijet selections. The filled bands indicate the systematic and statistical uncertainties on the data, added in quadrature. In all bins the systematic uncertainty is significantly larger than the statistical uncertainty. The $E_{\mathrm{T}}^{\mathrm{density}}$ distribution in the minimum bias data dips in the central region. Since the relative fraction of low momentum particles is higher in the central region than in the forward region, fewer central particles pass the selection criteria described in section 2, hence reducing the ΣE_{T} in the central region. The dip in the central region is less prominent in the dijet data; this feature is discussed below.

Figure 5 shows the ratio of the $E_{\mathrm{T}}^{\mathrm{density}}$ in the dijet transverse region to the $E_{\mathrm{T}}^{\mathrm{density}}$ in minimum bias events. The correlations between the systematic uncertainties for the dijet and minimum bias distributions are taken into account. All systematic uncertainties but the physics model dependence and jet energy scale are taken as correlated between the two. The $E_{\mathrm{T}}^{\mathrm{density}}$ in the transverse region for the dijet selection is larger than the $E_{\mathrm{T}}^{\mathrm{density}}$ in the minimum bias data. This increase is expected, due primarily to the presence of a hard scatter, which will bias the selected events away from peripheral proton scatters and towards small impact parameter ("head-on") proton-proton interactions. This means that more parton-parton interactions are likely to occur in the underlying event in the dijet data than in the collisions with a larger impact parameter that characterize the events in the minimum bias dataset.

The unfolded data are compared to various MC models. In the minimum bias sample the $E_{\mathrm{T}}^{\mathrm{density}}$ distribution in figure 4a is well described by `PYTHIA 6 AMBT1` in the central region. This is expected as this tune was prepared with ATLAS 7 TeV minimum bias data in the region $|\eta| < 2.5$ [3]. At higher $|\eta|$ values, however, the $E_{\mathrm{T}}^{\mathrm{density}}$ is underestimated and is approximately 25% too low in the highest $|\eta|$ bin. The `PYTHIA 6 AUET2B:CTEQ6L1` prediction is very similar to that from `PYTHIA 6 AMBT1`, with slightly more energy in the central region and less in the forward region, meaning that the description of the $|\eta|$ dependence is even worse. `PYTHIA 6 DW` underestimates the $E_{\mathrm{T}}^{\mathrm{density}}$ in all $|\eta|$ bins. Despite this it provides an improved description of the $|\eta|$ dependence of the $E_{\mathrm{T}}^{\mathrm{density}}$. `PYTHIA 8`

JHEP11(2012)033

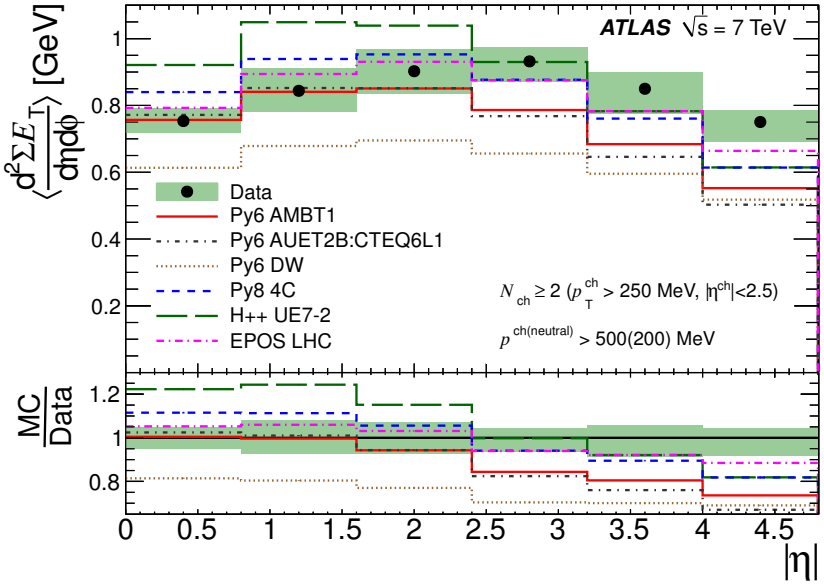

(a)

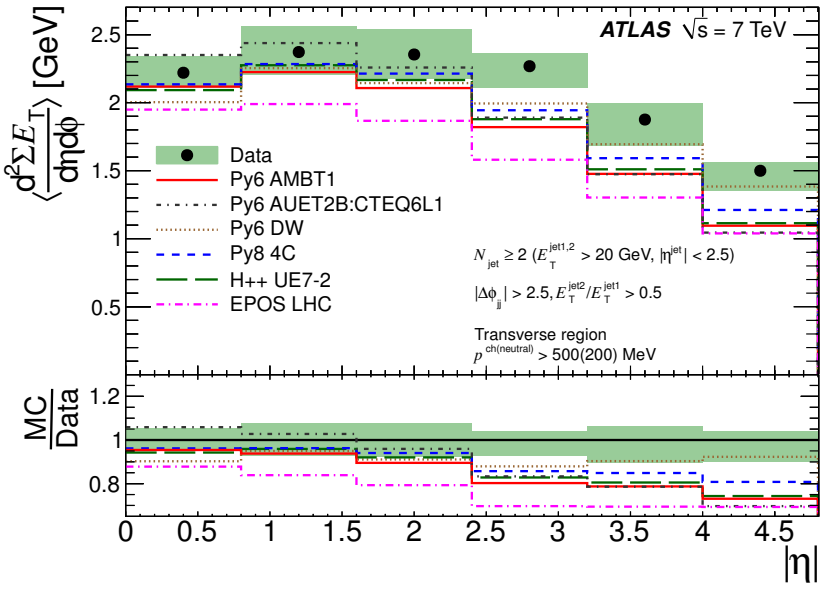

(b)

Figure 4. Unfolded $E_{\mathrm{T}}^{\mathrm{density}}$ distribution compared to various MC models and tunes for (a) the minimum bias selection and (b) the dijet selection in the transverse region. The filled band represents the total uncertainty on the unfolded data. N_{ch} refers to the number of charged particles in the event, and $p_{\mathrm{T}}^{\mathrm{ch}}$ and η^{ch} are, respectively, the p_{T} and η of those particles. N_{jet} refers to the number of jets, $E_{\mathrm{T}}^{\mathrm{jet1(2)}}$ is the E_{T} of the (sub-)leading jet, η^{jet} is the jet pseudorapidity, and $\Delta\phi_{\mathrm{jj}}$ is the azimuthal angle difference between the two leading jets. $p^{\mathrm{ch(neutral)}}$ refers to the momentum of the charged(neutral) particles used in the ΣE_{T} calculation.

JHEP11(2012)033

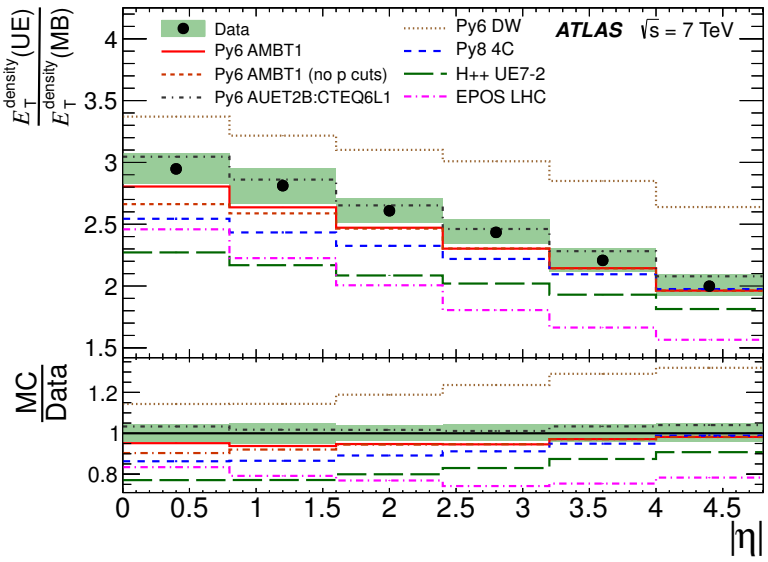

Figure 5. Unfolded $E_{\mathrm{T}}^{\mathrm{density}}$ distribution in the dijet data transverse region divided by that in the minimum bias data, compared to various MC models and tunes. The filled band represents the total uncertainty on the unfolded data.

4C overestimates the $E_{\mathrm{T}}^{\mathrm{density}}$ in the central region. The agreement improves in the region $1.6 < |\eta| < 3.2$, but in the higher $|\eta|$ bins the $E_{\mathrm{T}}^{\mathrm{density}}$ is underestimated. Herwig++ UE7-2 overestimates the $E_{\mathrm{T}}^{\mathrm{density}}$ in the central region, describes the data well in the region $2.4 < |\eta| < 3.2$, and undershoots the data at higher $|\eta|$. The EPOS LHC prediction provides the best description over the entire $|\eta|$ region, although it does fall slightly too fast with $|\eta|$. It should be noted that, with the exception of EPOS LHC and PYTHIA 6 DW, while some models and tunes appear to agree better in some regions than others, this is generally due to differences in the total level of particle production. The overall pattern remains the same: the $E_{\mathrm{T}}^{\mathrm{density}}$ in the forward region is too low relative to the central region.

In the dijet selection in figure 4b, all of the MC models and tunes perform reasonably well in the central region, apart from EPOS LHC which underestimates the $E_{\mathrm{T}}^{\mathrm{density}}$ in all $|\eta|$ bins. PYTHIA 6 AUET2B:CTEQ6L1 slightly overestimates the energy in the most central bins, and all the other predictions are slightly too low. As was the case in the minimum bias analysis, the $E_{\mathrm{T}}^{\mathrm{density}}$ in the forward region is underestimated. PYTHIA 8 4C is approximately 20% too low in the most forward bin, while PYTHIA 6 AMBT1, Herwig++ UE7-2 and PYTHIA 6 AUET2B:CTEQ6L1 are 25–30% too low. PYTHIA 6 DW provides the best description of the $|\eta|$ dependence, although the overall amount of energy is too low.

The fall-off with $|\eta|$ of the ratio of the $E_{\mathrm{T}}^{\mathrm{density}}$ in dijet and minimum bias events seen in figure 5 is reproduced by the models, with PYTHIA 6 AMBT1 and AUET2B:CTEQ6L1 describing the data the best. The reduction in the ratio with $|\eta|$ is partly due to the momentum cuts on the particles included in the ΣE_{T} calculation. In the dijet data, the particles tend to have larger momenta and so fewer are removed from the ΣE_{T} calculation. According to PYTHIA 6 AMBT1, the momentum cuts remove 25(18)% of the $E_{\mathrm{T}}^{\mathrm{density}}$ in the most central

JHEP11(2012)033

bin and a negligble amount in the most forward bin for the minimum bias (dijet) selections. The PYTHIA 6 AMBT1 (no p cuts) curve in figure 5, shows the ratio when the momentum cuts on the particles contributing to the ΣE_{T} have been removed. There is still a residual decrease with $|\eta|$ which may be due to a contribution to the underlying event in the central region coming from particles associated with the hard scatter.

The unfolded ΣE_{T} distributions are shown in figures 6 and 7 for the minimum bias and dijet selections, respectively. The distribution peaks at higher values of ΣE_{T} in the forward region due to the particle momentum cuts discussed above. In the region $|\eta| < 3.2$ the distribution is broader than in the forward region, with more events populating the high ΣE_{T} tails. There is therefore more event-by-event variation in the ΣE_{T} in the central part of the detector. These features are reproduced by the MC predictions. PYTHIA 6 AMBT1 provides the best description of the ΣE_{T} shape in the central region for the minimum bias data. For the dijet data, most of the tunes do a reasonable job, although PYTHIA 8 4C and EPOS LHC underestimate the high ΣE_{T} tails. As with the $E_{\mathrm{T}}^{\mathrm{density}}$ distributions, the ΣE_{T} in the forward region is underestimated for all but the dijet PYTHIA 6 DW prediction.

In summary, all of the MCs underestimate the amount of energy in the forward region relative to the central region, in both the minimum bias data and the underlying event, with the exception of PYTHIA 6 DW which provides a reasonable description of the dijet data, although the prediction is approximately one standard deviation below the central values measured in the data in all $|\eta|$ bins. EPOS LHC provides the best overall description of the minimum bias data. PYTHIA 6 AMBT1 provides the best description in the most central region ($|\eta| < 1.6$), while at higher $|\eta|$ values PYTHIA 8 4C and Herwig++ UE7-2 reflect the data more accurately. In the dijet analysis, all the MCs provide a reasonable description in the central region, apart from EPOS LHC.

9.2 Variation in diffractive contributions

In order to investigate the sensitivity of the $E_{\mathrm{T}}^{\mathrm{density}}$ to the fraction of diffractive events, figure 8 compares the unfolded $E_{\mathrm{T}}^{\mathrm{density}}$ distribution in the minimum bias data to PYTHIA 8 4C with the nominal diffractive cross-sections (50.9 mb, 12.4 mb and 8.1 mb for non-diffractive, single-diffractive and double-diffractive processes, respectively) and to samples where the diffractive cross-sections have been doubled or halved, with the non-diffractive cross-section held constant. This is achieved by combining the separate MC samples for the different processes with adjusted weights, rather than by changing the relevant parameters when generating the samples. Diffractive processes tend to have less particle production than non-diffractive processes. As expected, increasing the diffractive contribution decreases the $E_{\mathrm{T}}^{\mathrm{density}}$. However, the shape of the $E_{\mathrm{T}}^{\mathrm{density}}$ distribution is not significantly affected.

9.3 Variation in parton distribution functions

The overall energy as well as its $|\eta|$ dependence are affected by the PDFs used as input to the MC model. In order to investigate the dependence on the PDFs, comparisons are made between the data and the PYTHIA 8 A2 family of tunes, which use different input PDFs [33], with the following variations:

JHEP11(2012)033

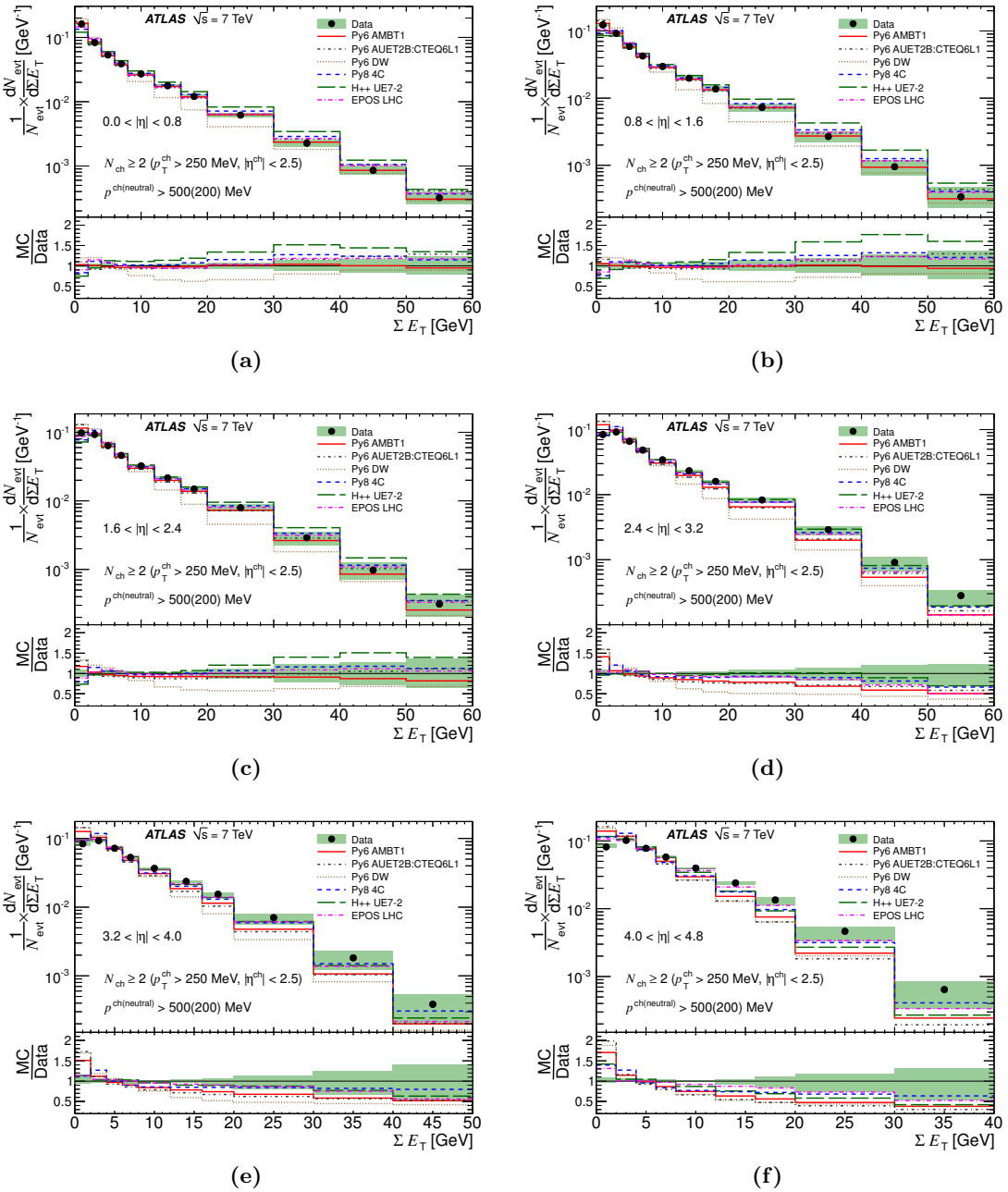

Figure 6. Unfolded ΣE_{T} distributions compared to various MC models and tunes for the minimum bias selection in the following $|\eta|$ regions: (a) $0.0 < |\eta| < 0.8$, (b) $0.8 < |\eta| < 1.6$, (c) $1.6 < |\eta| < 2.4$, (d) $2.4 < |\eta| < 3.2$, (e) $3.2 < |\eta| < 4.0$ and (f) $4.0 < |\eta| < 4.8$. The filled band in each plot represents the total uncertainty on the unfolded data. N_{ch} refers to the number of charged particles in the event, and $p_{\mathrm{T}}^{\mathrm{ch}}$ and η^{ch} are, respectively, the p_{T} and η of those particles. $p^{\mathrm{ch(neutral)}}$ refers to the momentum of the charged(neutral) particles used in the ΣE_{T} calculation.

JHEP11(2012)033

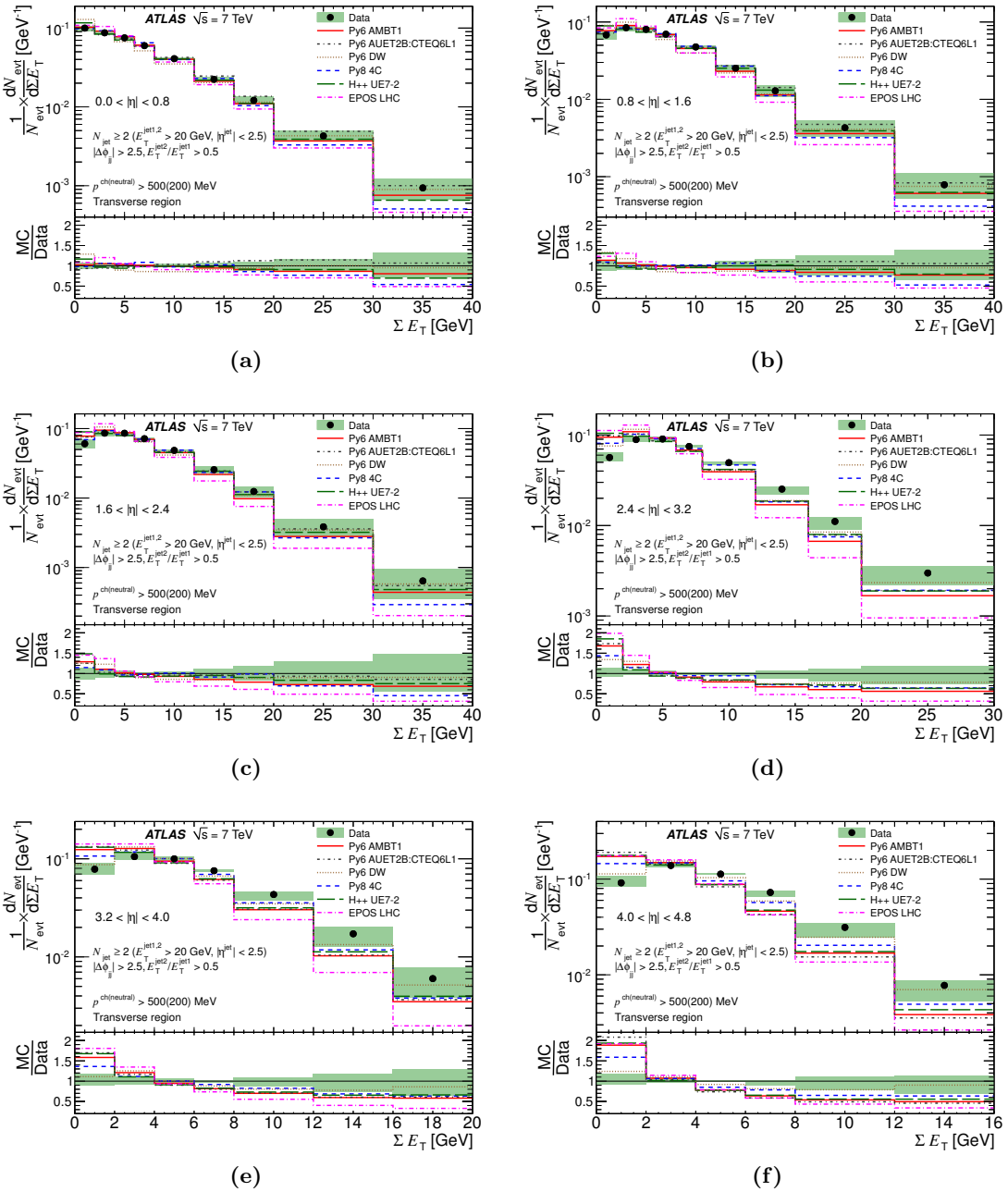

Figure 7. Unfolded ΣE_{T} distributions compared to various MC models and tunes for the dijet selection in the transverse region in the following $|\eta|$ regions: (a) $0.0 < |\eta| < 0.8$, (b) $0.8 < |\eta| < 1.6$, (c) $1.6 < |\eta| < 2.4$, (d) $2.4 < |\eta| < 3.2$, (e) $3.2 < |\eta| < 4.0$ and (f) $4.0 < |\eta| < 4.8$. The filled band in each plot represents the total uncertainty on the unfolded data. N_{jet} refers to the number of jets, $E_{\mathrm{T}}^{\mathrm{jet1(2)}}$ is the E_{T} of the (sub-)leading jet, η^{jet} is the jet pseudorapidity, and $\Delta\phi_{\mathrm{jj}}$ is the azimuthal angle difference between the two leading jets. $p^{\mathrm{ch(neutral)}}$ refers to the momentum of the charged(neutral) particles used in the ΣE_{T} calculation.

JHEP11(2012)033

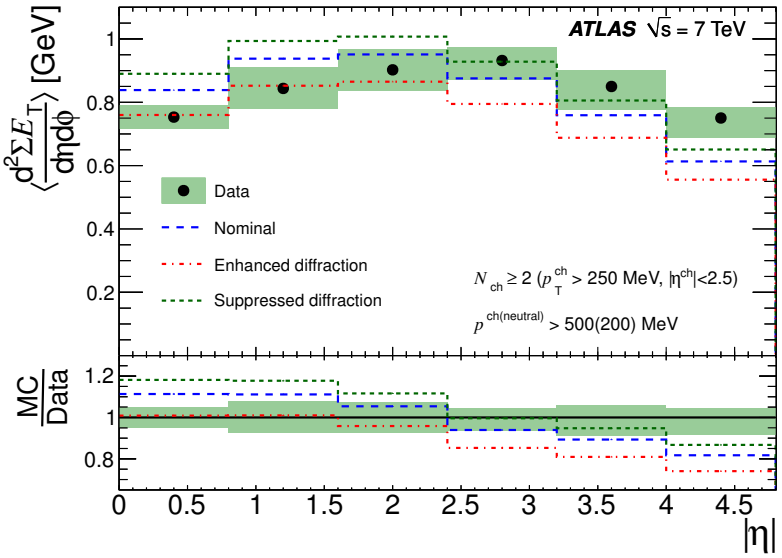

Figure 8. Final unfolded $E_{\mathrm{T}}^{\mathrm{density}}$ distribution for the minimum bias selection compared to PYTHIA 8 4C with the nominal diffractive cross-sections, as well as enhanced and suppressed diffractive cross-sections, as described in the text. The filled band represents the total uncertainty on the unfolded data. N_{ch} refers to the number of charged particles in the event, and $p_{\mathrm{T}}^{\mathrm{ch}}$ and η^{ch} are, respectively, the p_{T} and η of those particles. $p^{\mathrm{ch(neutral)}}$ refers to the momentum of the charged(neutral) particles used in the ΣE_{T} calculation.

1. Tune A2:CTEQ6L1.

2. The A2:CTEQ6L1 tune parameters, but with the MSTW2008LO PDFs.

3. Tune A2:MSTW2008LO.

4. Tune A2:CTEQ6L1 where the $E_{\mathrm{T}}^{\mathrm{density}}$ has been scaled by 0.93(0.96) for the minimum bias (dijet) selection so that it matches A2:MSTW2008LO in the most central bin.

These comparisons are shown in figure 9. The first thing to note is that moving from the CTEQ6L1 to the MSTW2008LO PDFs (and keeping all tune parameters the same) decreases the amount of energy in the central region, but increases it in the forward region, presumably due to the increase in both the high-x and low-x gluon PDF with respect to the mid-x region, where x is the proton momentum fraction carried by the gluon. When the parameters are tuned to data in the central region, the energy increases for the minimum bias prediction. If the $E_{\mathrm{T}}^{\mathrm{density}}$ obtained using A2:CTEQ6L1 is scaled down to match A2:MSTW2008LO in the most central bin, it is clear that the latter provides a better description of the data in the forward region, with the underestimation in the most forward bin improving from about 30% to 15%.

JHEP11(2012)033

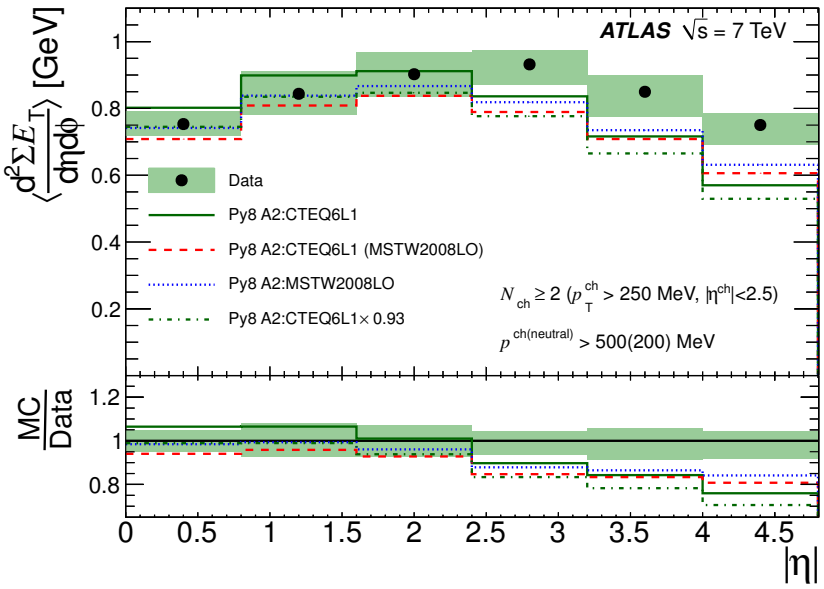

(a)

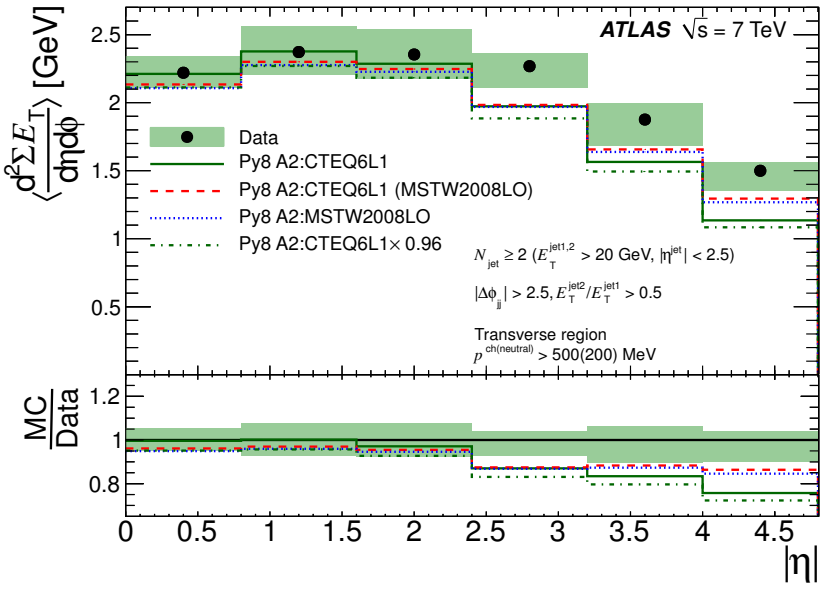

(b)

Figure 9. Final unfolded $E_{\mathrm{T}}^{\mathrm{density}}$ distribution compared to PYTHIA 8 with variations of the PDFs used, as discussed in the text for (a) the minimum bias selection and (b) the dijet selection. The filled band represents the total uncertainty on the unfolded data. N_{ch} refers to the number of charged particles in the event, and $p_{\mathrm{T}}^{\mathrm{ch}}$ and η^{ch} are, respectively, the p_{T} and η of those particles. N_{jet} refers to the number of jets, $E_{\mathrm{T}}^{\mathrm{jet1(2)}}$ is the E_{T} of the (sub-)leading jet, η^{jet} is the jet pseudorapidity, and $\Delta\phi_{\mathrm{jj}}$ is the azimuthal angle difference between the two leading jets. $p^{\mathrm{ch(neutral)}}$ refers to the momentum of the charged(neutral) particles used in the ΣE_{T} calculation.

JHEP11(2012)033

10 Conclusions

Measurements of the $E_{\mathrm{T}}^{\mathrm{density}}$ and the ΣE_{T} distributions as functions of $|\eta|$ have been presented for two event classes: those requiring the presence of particles with a low transverse momentum (minimum bias) and those requiring particles with a significant transverse momentum (dijets), using proton-proton collision data at $\sqrt{s}$ =7 TeV recorded by the ATLAS detector. In the dijet selection the distributions are measured in the region transverse in ϕ to the hard scatter, in order to probe the particle production from the underlying event. The measurements are performed in the region $|\eta| < 4.8$ for charged particles with $p > 500$ MeV and neutral particles with $p > 200$ MeV, and are the first to utilize the entire acceptance of the ATLAS calorimeters to probe the overall properties of inclusive proton-proton collisions, as well as the underlying event. The distributions are compared to various MC models and tunes. In general all MC predictions are found to underestimate the amount of energy in the forward region relative to the central region by 20–30%, with the exception of the PYTHIA 6 DW tune and EPOS LHC for the minimum bias data, although PYTHIA 6 DW underpredicts the overall energy by 20–30%. For the PYTHIA 8 A2 tune series, this is improved if the MSTW2008 LO PDFs are used instead of the CTEQ 6L1 PDFs.

Acknowledgments

We thank CERN for the very successful operation of the LHC, as well as the support staff from our institutions without whom ATLAS could not be operated efficiently.

We acknowledge the support of ANPCyT, Argentina; YerPhI, Armenia; ARC, Australia; BMWF, Austria; ANAS, Azerbaijan; SSTC, Belarus; CNPq and FAPESP, Brazil; NSERC, NRC and CFI, Canada; CERN; CONICYT, Chile; CAS, MOST and NSFC, China; COLCIENCIAS, Colombia; MSMT CR, MPO CR and VSC CR, Czech Republic; DNRF, DNSRC and Lundbeck Foundation, Denmark; EPLANET and ERC, European Union; IN2P3-CNRS, CEA-DSM/IRFU, France; GNSF, Georgia; BMBF, DFG, HGF, MPG and AvH Foundation, Germany; GSRT, Greece; ISF, MINERVA, GIF, DIP and Benoziyo Center, Israel; INFN, Italy; MEXT and JSPS, Japan; CNRST, Morocco; FOM and NWO, Netherlands; RCN, Norway; MNiSW, Poland; GRICES and FCT, Portugal; MERYS (MECTS), Romania; MES of Russia and ROSATOM, Russian Federation; JINR; MSTD, Serbia; MSSR, Slovakia; ARRS and MVZT, Slovenia; DST/NRF, South Africa; MICINN, Spain; SRC and Wallenberg Foundation, Sweden; SER, SNSF and Cantons of Bern and Geneva, Switzerland; NSC, Taiwan; TAEK, Turkey; STFC, the Royal Society and Leverhulme Trust, United Kingdom; DOE and NSF, United States of America.

The crucial computing support from all WLCG partners is acknowledged gratefully, in particular from CERN and the ATLAS Tier-1 facilities at TRIUMF (Canada), NDGF (Denmark, Norway, Sweden), CC-IN2P3 (France), KIT/GridKA (Germany), INFN-CNAF (Italy), NL-T1 (Netherlands), PIC (Spain), ASGC (Taiwan), RAL (U.K.) and BNL (U.S.A.) and in the Tier-2 facilities worldwide.

JHEP11(2012)033

$\lvert\eta\rvert$	$\langle\frac{d^2\Sigma E_T}{d\eta d\phi}\rangle$ [GeV]	Stat. [%]	E_1^* [%]	E_2 [%]	M_1 [%]	M_2 [%]	M_3^* [%]	P_1 [%]	Total [%]
0.0–0.8	0.753	±0.19	$^{+3.2}_{-2.9}$	—	±2.9	—	±0.51	±2.6	$^{+5.1}_{-4.9}$
0.8–1.6	0.844	±0.17	$^{+5.4}_{-4.9}$	—	±3.2	±0.49	±1.2	±4.6	$^{+7.9}_{-7.5}$
1.6–2.4	0.902	±0.16	$^{+4.0}_{-3.8}$	—	—	±0.89	±5.0	±3.4	$^{+7.4}_{-7.2}$
2.4–3.2	0.932	±0.16	$^{+2.4}_{-5.0}$	—	—	—	±3.0	±2.5	$^{+4.6}_{-6.4}$
3.2–4.0	0.850	±0.15	$^{+4.3}_{-4.4}$	−6.2	—	—	±2.7	±3.2	$^{+6.0}_{-8.7}$
4.0–4.8	0.750	±0.14	$^{+2.7}_{-2.7}$	−6.8	—	—	±0.8	±3.6	$^{+4.6}_{-8.2}$

Table 3. Measured E_T^{density} and systematic uncertainty breakdown for the minimum bias data. The systematic uncertainties marked with a $*$ are uncorrelated between $|\eta|$ bins.

$\lvert\eta\rvert$	$\langle\frac{d^2\Sigma E_T}{d\eta d\phi}\rangle$ [GeV]	Stat. [%]	E_1^* [%]	E_2 [%]	M_1 [%]	M_2 [%]	M_3^* [%]	P_2 [%]	J [%]	Total [%]
0.0–0.8	2.22	±0.61	$^{+4.3}_{-4.2}$	—	±1.3	—	±0.23	±2.2	$^{+1.6}_{-1.3}$	$^{+5.3}_{-5.1}$
0.8–1.6	2.37	±0.54	$^{+7.2}_{-6.4}$	—	±2.5	±0.38	±0.96	±0.12	$^{+1.3}_{-1.3}$	$^{+7.8}_{-7.1}$
1.6–2.4	2.35	±0.52	$^{+5.3}_{-5.0}$	—	—	±0.97	±5.5	±0.41	$^{+0.98}_{-0.92}$	$^{+7.8}_{-7.6}$
2.4–3.2	2.27	±0.50	$^{+3.8}_{-7.0}$	—	—	—	±0.64	±0.55	$^{+0.80}_{-0.37}$	$^{+4.0}_{-7.1}$
3.2–4.0	1.88	±0.51	$^{+6.1}_{-5.8}$	−8.2	—	—	±1.1	±1.3	$^{+0.46}_{-0.17}$	$^{+6}_{-10}$
4.0–4.8	1.50	±0.47	$^{+3.8}_{-3.6}$	−9.0	—	—	±0.6	±1.6	$^{+0.13}_{-0.03}$	$^{+4.2}_{-9.8}$

Table 4. Measured E_T^{density} and systematic uncertainty breakdown for the dijet data. The systematic uncertainties marked with a $*$ are uncorrelated between $|\eta|$ bins.

A Tabulated results and uncertainties

The unfolded data are presented in tabular form in this appendix for the E_T^{density} and the six ΣE_T distributions, for both the minimum bias and dijet selections. Tables 3, 4 and 5 give the unfolded data and systematic uncertainties for the E_T^{density} for the minimum bias selection, the dijet selection, and the ratio between them, respectively. Tables 6–11 give the unfolded data and systematic uncertainties for the ΣE_T distributions for the minimum bias selection and tables 12–17 give the corresponding information for the dijet analysis. In each case, the breakdown of the systematic uncertainties by source is also given. Each systematic source is described in section 8. The uncorrelated calorimeter energy scale systematic is denoted as $E_1^{a,b,c,d,e,f}$ for each of the six $|\eta|$ regions, respectively. The correlated calorimeter energy scale systematic is denoted as E_2. The two correlated material systematic sources are denoted as M_1 and M_2 and the uncorrelated source is denoted as $M_3^{a,b,c,d,e,f}$ for the six $|\eta|$ regions. All the above sources are correlated between the minimum bias data and the dijet data and therefore have the same symbol.

JHEP11(2012)033

$\lvert\eta\rvert$	$\frac{\langle\frac{d^2\Sigma E_T}{d\eta d\phi}\rangle(UE)}{\langle\frac{d^2\Sigma E_T}{d\eta d\phi}\rangle(MB)}$	Stat.	E_1^*	E_2	M_1	M_2	M_3^*	P	J	Total
		[%]	[%]	[%]	[%]	[%]	[%]	[%]	[%]	[%]
0.0–0.8	2.95	±0.64	$^{+1.1}_{-1.3}$	—	$^{+1.5}_{-1.6}$	—	$^{+0.27}_{-0.28}$	±3.4	$^{+1.6}_{-1.3}$	$^{+4.3}_{-4.2}$
0.8–1.6	2.81	±0.57	$^{+1.7}_{-1.6}$	—	$^{+0.64}_{-0.69}$	$^{+0.10}_{-0.11}$	$^{+0.25}_{-0.26}$	±4.6	$^{+1.3}_{-1.3}$	$^{+5.1}_{-5.1}$
1.6–2.4	2.61	±0.55	$^{+1.2}_{-1.2}$	—	—	$^{+0.08}_{-0.08}$	$^{+0.43}_{-0.47}$	±3.5	$^{+0.98}_{-0.92}$	$^{+3.9}_{-3.9}$
2.4–3.2	2.43	±0.52	$^{+1.4}_{-2.1}$	—	—	—	$^{+2.3}_{-2.5}$	±2.6	$^{+0.80}_{-0.37}$	$^{+3.8}_{-4.2}$
3.2–4.0	2.21	±0.53	$^{+1.7}_{-1.6}$	−2.2	—	—	$^{+1.5}_{-1.6}$	±3.4	$^{+0.46}_{-0.17}$	$^{+4.1}_{-4.6}$
4.0–4.8	2.00	±0.49	$^{+1.1}_{-1.0}$	−2.4	—	—	$^{+0.19}_{-0.20}$	±3.9	$^{+0.13}_{-0.03}$	$^{+4.1}_{-4.7}$

Table 5. Ratio of measured E_T^{density} for the dijet data to that for the the minimum bias data, and systematic uncertainty breakdown. The systematic uncertainties marked with a $*$ are uncorrelated between $|\eta|$ bins.

ΣE_T	$\frac{1}{N_{evt}}\frac{dN_{evt}}{d\Sigma E_T}$	Stat.	E_1^a	E_2	M_1	M_2	M_3^a	P_1	Total
[GeV]	[GeV^{-1}]	[%]	[%]	[%]	[%]	[%]	[%]	[%]	[%]
0–2	0.161	0.35	$^{+2.0}_{-2.1}$	—	∓ 2.1	—	∓ 0.38	±0.07	$^{+3.0}_{-3.1}$
2–4	0.0835	0.32	$^{+1.3}_{-1.4}$	—	∓ 1.2	—	∓ 0.21	∓4.5	$^{+4.8}_{-4.8}$
4–6	0.0533	0.40	$^{+0.24}_{-0.39}$	—	∓ 0.90	—	∓ 0.16	∓3.8	$^{+3.9}_{-3.9}$
6–8	0.039	0.46	$^{-0.20}_{+0.00}$	—	± 0.23	—	± 0.04	∓0.44	$^{+0.68}_{-0.71}$
8–12	0.0271	0.49	$^{-0.57}_{+0.56}$	—	± 1.4	—	± 0.24	±2.2	$^{+2.7}_{-2.7}$
12–16	0.0177	0.57	$^{-1.3}_{+1.5}$	—	± 1.8	—	± 0.31	±3.5	$^{+4.3}_{-4.2}$
16–20	0.0121	0.67	$^{-2.5}_{+2.5}$	—	± 2.4	—	± 0.43	±3.6	$^{+5.1}_{-5.1}$
20–30	0.00619	0.75	$^{-4.6}_{+4.8}$	—	± 4.1	—	± 0.73	±4.2	$^{+7.7}_{-7.5}$
30–40	0.00226	1.2	$^{-7.5}_{+8.4}$	—	± 7.9	—	± 1.4	±5.5	$^{+13}_{-12}$
40–50	0.000855	1.9	$^{-10}_{+12}$	—	± 8.7	—	± 1.5	±8.1	$^{+17}_{-16}$
50–60	0.000321	2.5	$^{-13}_{+15}$	—	± 13	—	± 2.3	±10	$^{+22}_{-21}$

Table 6. Measured $\frac{1}{N_{evt}}\frac{dN_{evt}}{d\Sigma E_T}$ and systematic uncertainty breakdown for the minimum bias data in the region $0.0 < |\eta| < 0.8$.

The physics model systematic uncertainty on the minimum bias and dijet results, and on their ratio, are denoted as, P_1, P_2 and P, respectively. The jet energy scale systematic uncertainty is denoted as J. The physics model and jet energy scale systematic sources are uncorrelated between the minimum bias and dijet data. For the ΣE_T distributions J is negligible and therefore neglected in the region $|\eta| > 2.4$.

The correlations between bins of a given distribution are indicated by the sign of the uncertainty. For example, in table 6 the uncertainty E_1^a is ± in the first three bins and ∓

JHEP11(2012)033

ΣE_{T}	$\frac{1}{N_{\mathrm{evt}}}\frac{dN_{\mathrm{evt}}}{d\Sigma E_{\mathrm{T}}}$	Stat.	E_1^b	E_2	M_1	M_2	M_3^b	P_1	Total
[GeV]	[GeV^{-1}]	[%]	[%]	[%]	[%]	[%]	[%]	[%]	[%]
0–2	0.123	0.38	$^{+4.7}_{-4.8}$	—	$\mp$ 3.0	$\mp$ 0.46	$\mp$ 1.1	$\pm$0.64	$^{+5.7}_{-5.8}$
2–4	0.092	0.30	$^{+2.5}_{-2.9}$	—	$\mp$ 1.6	$\mp$ 0.25	$\mp$ 0.62	$\mp$5.3	$^{+6.1}_{-6.2}$
4–6	0.0588	0.35	$^{+0.55}_{-0.85}$	—	$\mp$ 0.65	$\mp$ 0.1	$\mp$ 0.25	$\mp$9	$^{+9.0}_{-9.1}$
6–8	0.0425	0.42	$^{-0.29}_{+0.21}$	—	$\pm$ 0.07	$\pm$ 0.01	$\pm$ 0.03	$\mp$3.8	$^{+3.8}_{-3.8}$
8–12	0.0296	0.44	$^{-1.0}_{+1.1}$	—	$\pm$ 0.76	$\pm$ 0.12	$\pm$ 0.29	$\pm$1.3	$^{+1.9}_{-1.9}$
12–16	0.0198	0.51	$^{-2.2}_{+2.0}$	—	$\pm$ 1.9	$\pm$ 0.29	$\pm$ 0.73	$\pm$5.7	$^{+6.4}_{-6.4}$
16–20	0.0137	0.58	$^{-3.9}_{+3.8}$	—	$\pm$ 2.1	$\pm$ 0.32	$\pm$ 0.80	$\pm$8.3	$^{+9.4}_{-9.4}$
20–30	0.00726	0.67	$^{-7.3}_{+7.6}$	—	$\pm$ 4.7	$\pm$ 0.72	$\pm$ 1.8	$\pm$10	$^{+14}_{-13}$
30–40	0.00268	1.1	$^{-13}_{+14}$	—	$\pm$ 7.3	$\pm$ 1.1	$\pm$ 2.8	$\pm$9	$^{+19}_{-17}$
40–50	0.000951	1.7	$^{-18}_{+21}$	—	$\pm$ 13	$\pm$ 1.9	$\pm$ 4.9	$\pm$10	$^{+27}_{-25}$
50–60	0.000339	2.4	$^{-22}_{+30}$	—	$\pm$ 17	$\pm$ 2.6	$\pm$ 6.5	$\pm$15	$^{+38}_{-32}$

Table 7. Measured $\frac{1}{N_{\mathrm{evt}}}\frac{dN_{\mathrm{evt}}}{d\Sigma E_{\mathrm{T}}}$ and systematic uncertainty breakdown for the minimum bias data in the region $0.8 < |\eta| < 1.6$.

ΣE_{T}	$\frac{1}{N_{\mathrm{evt}}}\frac{dN_{\mathrm{evt}}}{d\Sigma E_{\mathrm{T}}}$	Stat.	E_1^c	E_2	M_1	M_2	M_3^c	P_1	Total
[GeV]	[GeV^{-1}]	[%]	[%]	[%]	[%]	[%]	[%]	[%]	[%]
0–2	0.0980	0.41	$^{+4.4}_{-4.3}$	—	—	$\mp$ 1.2	$\mp$ 6.8	$\pm$1.1	$^{+8.2}_{-8.2}$
2–4	0.0931	0.32	$^{+2.5}_{-2.6}$	—	—	$\mp$ 0.48	$\mp$ 2.7	$\mp$2.0	$^{+4.2}_{-4.3}$
4–6	0.0639	0.36	$^{+0.57}_{-0.76}$	—	—	$\mp$ 0.18	$\mp$ 1.0	$\mp$6.2	$^{+6.3}_{-6.4}$
6–8	0.0460	0.45	$^{-0.15}_{+0.05}$	—	—	$\pm$ 0.27	$\pm$ 1.6	$\mp$4.8	$^{+5.1}_{-5.1}$
8–12	0.0323	0.46	$^{-0.61}_{+0.55}$	—	—	$\pm$ 0.26	$\pm$ 1.5	$\mp$0.75	$^{+1.8}_{-1.8}$
12–16	0.0216	0.54	$^{-1.6}_{+1.5}$	—	—	$\pm$ 0.33	$\pm$ 1.9	$\pm$2.1	$^{+3.2}_{-3.3}$
16–20	0.0149	0.62	$^{-2.9}_{+2.7}$	—	—	$\pm$ 0.59	$\pm$ 3.4	$\pm$3.5	$^{+5.6}_{-5.7}$
20–30	0.00792	0.68	$^{-5.6}_{+5.6}$	—	—	$\pm$ 1.2	$\pm$ 7.1	$\pm$6.8	$^{+11}_{-11}$
30–40	0.00290	1.1	$^{-11}_{+11}$	—	—	$\pm$ 2.6	$\pm$ 15	$\pm$12	$^{+22}_{-22}$
40–50	0.000977	1.8	$^{-15}_{+17}$	—	—	$\pm$ 3.2	$\pm$ 18	$\pm$14	$^{+29}_{-28}$
50–60	0.000312	2.5	$^{-19}_{+24}$	—	—	$\pm$ 4.3	$\pm$ 25	$\pm$14	$^{+37}_{-34}$

Table 8. Measured $\frac{1}{N_{\mathrm{evt}}}\frac{dN_{\mathrm{evt}}}{d\Sigma E_{\mathrm{T}}}$ and systematic uncertainty breakdown for the minimum bias data in the region $1.6 < |\eta| < 2.4$.

in the remaining bins. This means that the first three bins are correlated with each other and anti-correlated with the remaining bins (a downward shift in the ΣE_{T} will shift the low ΣE_{T} bins up and the high ΣE_{T} bins down). Since the individual sources within a

JHEP11(2012)033

ΣE_{T}	$\frac{1}{N_{\mathrm{evt}}}\frac{dN_{\mathrm{evt}}}{d\Sigma E_{\mathrm{T}}}$	Stat.	E_1^d	E_2	M_1	M_2	M_3^d	P_1	Total
[GeV]	[GeV^{-1}]	[%]	[%]	[%]	[%]	[%]	[%]	[%]	[%]
0–2	0.0840	0.48	$^{+6.9}_{-3.1}$	—	—	—	$\mp$ 5.3	$\pm$0.72	$^{+8.8}_{-6.2}$
2–4	0.0920	0.33	$^{+3.1}_{-1.6}$	—	—	—	$\mp$ 1.7	$\mp$1.5	$^{+3.9}_{-2.8}$
4–6	0.0660	0.46	$^{+0.65}_{-0.41}$	—	—	—	$\pm$ 0.46	$\mp$5.3	$^{+5.3}_{-5.3}$
6–8	0.0485	0.47	$^{-0.16}_{+0.07}$	—	—	—	$\pm$ 0.47	$\mp$3.5	$^{+3.5}_{-3.5}$
8–12	0.0343	0.50	$^{-0.46}_{+0.25}$	—	—	—	$\pm$ 0.33	$\mp$0.57	$^{+0.86}_{-0.95}$
12–16	0.0232	0.57	$^{-1.5}_{+0.6}$	—	—	—	$\pm$ 1.1	$\pm$3.1	$^{+3.4}_{-3.7}$
16–20	0.0160	0.61	$^{-3.7}_{+1.6}$	—	—	—	$\pm$ 2.7	$\pm$3.3	$^{+4.6}_{-5.7}$
20–30	0.00829	0.72	$^{-7.8}_{+3.6}$	—	—	—	$\pm$ 4.6	$\pm$5.3	$^{+8}_{-11}$
30–40	0.00290	1.2	$^{-14}_{+7}$	—	—	—	$\pm$ 7.6	$\pm$6.9	$^{+12}_{-17}$
40–50	0.000908	1.6	$^{-22}_{+12}$	—	—	—	$\pm$ 12	$\pm$11	$^{+20}_{-27}$
50–60	0.000281	3.2	$^{-27}_{+14}$	—	—	—	$\pm$ 15	$\pm$7.3	$^{+22}_{-32}$

Table 9. Measured $\frac{1}{N_{\mathrm{evt}}}\frac{dN_{\mathrm{evt}}}{d\Sigma E_{\mathrm{T}}}$ and systematic uncertainty breakdown for the minimum bias data in the region $2.4 < |\eta| < 3.2$.

ΣE_{T}	$\frac{1}{N_{\mathrm{evt}}}\frac{dN_{\mathrm{evt}}}{d\Sigma E_{\mathrm{T}}}$	Stat.	E_1^e	E_2	M_1	M_2	M_3^e	P_1	Total
[GeV]	[GeV^{-1}]	[%]	[%]	[%]	[%]	[%]	[%]	[%]	[%]
0–2	0.0837	0.46	$^{+5.2}_{-4.3}$	7.3	—	—	$\mp$ 4.0	$\mp$1.5	$^{+9.9}_{-6.1}$
2–4	0.0931	0.33	$^{+3.5}_{-3.4}$	4.9	—	—	$\mp$ 2.1	$\pm$0.64	$^{+6.4}_{-4.0}$
4–6	0.0720	0.38	$^{+1.1}_{-1.3}$	1.6	—	—	$\mp$ 0.18	$\mp$4.1	$^{+4.5}_{-4.3}$
6–8	0.0530	0.44	$^{+0.23}_{-0.30}$	0.33	—	—	$\mp$ 0.57	$\mp$4.5	$^{+4.6}_{-4.6}$
8–12	0.0367	0.47	$^{-0.69}_{+0.36}$	-0.98	—	—	$\pm$ 1.6	$\mp$2.2	$^{+2.8}_{-3.0}$
12–16	0.0237	0.54	$^{-2.4}_{+1.9}$	-3.3	—	—	$\pm$ 1.1	$\pm$2.3	$^{+3.2}_{-4.9}$
16–20	0.0154	0.66	$^{-4.6}_{+3.8}$	-6.4	—	—	$\pm$ 2.6	$\pm$5.3	$^{+7.0}_{-9.9}$
20–30	0.00704	0.77	$^{-9.3}_{+8.6}$	-13	—	—	$\pm$ 5.7	$\pm$9.5	$^{+14}_{-20}$
30–40	0.00183	1.4	$^{-18}_{+19}$	-25	—	—	$\pm$ 7.5	$\pm$13	$^{+24}_{-34}$
40–50	0.000385	2.4	$^{-24}_{+31}$	-33	—	—	$\pm$ 20	$\pm$13	$^{+39}_{-48}$

Table 10. Measured $\frac{1}{N_{\mathrm{evt}}}\frac{dN_{\mathrm{evt}}}{d\Sigma E_{\mathrm{T}}}$ and systematic uncertainty breakdown for the minimum bias data in the region $3.2 < |\eta| < 4.0$.

given distribution are uncorrelated, the relationship between $\pm$ and $\mp$ between sources is not relevant to the calculation of the total error in a given bin.

The uncertainties are given to two significant figures or a precision of 0.01%, whichever is smaller. In cases where the + and − uncertainty have a different precision the lowest

JHEP11(2012)033

ΣE_{T}	$\frac{1}{N_{\mathrm{evt}}}\frac{dN_{\mathrm{evt}}}{d\Sigma E_{\mathrm{T}}}$	Stat.	E_1^f	E_2	M_1	M_2	M_3^f	P_1	Total
[GeV]	[GeV^{-1}]	[%]	[%]	[%]	[%]	[%]	[%]	[%]	[%]
0–2	0.0818	0.54	$^{+3.6}_{-3.2}$	9.0	—	—	$\mp$ 1.7	$\mp$0.37	$^{+9.9}_{-3.7}$
2–4	0.102	0.42	$^{+2.0}_{-2.0}$	5.1	—	—	$\mp$ 0.58	$\mp$1.1	$^{+5.7}_{-2.4}$
4–6	0.0777	0.44	$^{+0.60}_{-0.77}$	1.5	—	—	$\pm$ 0.54	$\mp$5.3	$^{+5.6}_{-5.4}$
6–8	0.0577	0.48	$^{+0.06}_{-0.04}$	0.16	—	—	$\mp$ 0.14	$\mp$4.5	$^{+4.5}_{-4.5}$
8–12	0.0397	0.49	$^{-0.60}_{+0.43}$	-1.5	—	—	$\pm$ 0.50	$\mp$0.26	$^{+0.9}_{-1.8}$
12–16	0.0239	0.58	$^{-2.4}_{+2.0}$	-6.0	—	—	$\pm$ 0.33	$\pm$3.6	$^{+4.1}_{-7.5}$
16–20	0.0135	0.75	$^{-4.8}_{+4.5}$	-12	—	—	$\pm$ 1.6	$\pm$9.1	$^{+10}_{-16}$
20–30	0.00464	0.96	$^{-8.7}_{+8.9}$	-22	—	—	$\pm$ 2.5	$\pm$14	$^{+17}_{-28}$
30–40	0.000642	2.3	$^{-15}_{+19}$	-39	—	—	$\pm$ 3.4	$\pm$24	$^{+31}_{-48}$

Table 11. Measured $\frac{1}{N_{\mathrm{evt}}}\frac{dN_{\mathrm{evt}}}{d\Sigma E_{\mathrm{T}}}$ and systematic uncertainty breakdown for the minimum bias data in the region $4.0 < |\eta| < 4.8$.

ΣE_{T}	$\frac{1}{N_{\mathrm{evt}}}\frac{dN_{\mathrm{evt}}}{d\Sigma E_{\mathrm{T}}}$	Stat.	E_1^a	E_2	M_1	M_2	M_3^a	P_2	J	Total
[GeV]	[GeV^{-1}]	[%]	[%]	[%]	[%]	[%]	[%]	[%]	[%]	[%]
0–2	0.0998	2.1	$^{+4.3}_{-4.4}$	—	$\mp$ 2.1	—	$\mp$ 0.37	$\mp$5.1	$^{-1.2}_{+1.2}$	$^{+7.4}_{-7.4}$
2–4	0.0870	1.5	$^{+3.4}_{-3.7}$	—	$\mp$ 1.4	—	$\mp$ 0.24	$\pm$2.6	$^{-0.61}_{+0.35}$	$^{+4.8}_{-5.0}$
4–6	0.0751	1.4	$^{+2.0}_{-1.8}$	—	$\mp$ 0.67	—	$\mp$ 0.12	$\pm$2.7	$^{-0.38}_{+0.08}$	$^{+3.7}_{-3.6}$
6–8	0.0598	1.6	$^{+0.46}_{-0.59}$	—	$\pm$ 0.05	—	$\pm$ 0.01	$\mp$1.8	$^{-0.34}_{+0.14}$	$^{+2.5}_{-2.5}$
8–12	0.0409	1.7	$^{-1.9}_{+1.9}$	—	$\pm$ 1.1	—	$\pm$ 0.20	$\mp$2.0	$^{-0.23}_{+0.25}$	$^{+3.4}_{-3.4}$
12–16	0.0224	2.2	$^{-4.9}_{+5.3}$	—	$\pm$ 2.5	—	$\pm$ 0.45	$\mp$0.15	$^{+0.14}_{+0.21}$	$^{+6.3}_{-6.0}$
16–20	0.0121	3.0	$^{-7.7}_{+7.0}$	—	$\pm$ 4.0	—	$\pm$ 0.70	$\pm$6.0	$^{+1.0}_{-0.8}$	$^{+11}_{-11}$
20–30	0.00428	4.3	$^{-11}_{+13}$	—	$\pm$ 6.5	—	$\pm$ 1.1	$\pm$3.9	$^{+5.4}_{-4.5}$	$^{+16}_{-15}$
30–40	0.000939	8.7	$^{-16}_{+18}$	—	$\pm$ 10	—	$\pm$ 1.8	$\pm$16	$^{+13}_{-11}$	$^{+31}_{-28}$

Table 12. Measured $\frac{1}{N_{\mathrm{evt}}}\frac{dN_{\mathrm{evt}}}{d\Sigma E_{\mathrm{T}}}$ and systematic uncertainty breakdown for the dijet data in the region $0.0 < |\eta| < 0.8$.

precision is chosen for both. In cases where the uncertainty is not applicable, this is indicated with a dash.

JHEP11(2012)033

ΣE_{T}	$\frac{1}{N_{\mathrm{evt}}}\frac{dN_{\mathrm{evt}}}{d\Sigma E_{\mathrm{T}}}$	Stat.	E_1^b	E_2	M_1	M_2	M_3^b	P_2	J	Total
[GeV]	[GeV^{-1}]	[%]	[%]	[%]	[%]	[%]	[%]	[%]	[%]	[%]
0–2	0.0680	2.2	$^{+9.7}_{-9.6}$	—	$\mp$ 4.0	$\mp$ 0.62	$\mp$ 1.5	$\mp$7.7	$^{-0.79}_{+0.89}$	$^{+13}_{-13}$
2–4	0.0844	1.5	$^{+7.1}_{-7.4}$	—	$\mp$ 2.8	$\mp$ 0.44	$\mp$ 1.1	$\pm$4.8	$^{-0.80}_{+0.81}$	$^{+9.2}_{-9.4}$
4–6	0.0804	1.4	$^{+4.1}_{-4.4}$	—	$\mp$ 1.7	$\mp$ 0.25	$\mp$ 0.64	$\pm$3.7	$^{-0.83}_{+0.91}$	$^{+6.0}_{-6.2}$
6–8	0.0695	1.4	$^{+0.9}_{-1.6}$	—	$\mp$ 0.48	$\mp$ 0.07	$\mp$ 0.19	$\pm$2.0	$^{-0.62}_{+0.69}$	$^{+2.7}_{-3.0}$
8–12	0.0476	1.6	$^{-3.4}_{+2.7}$	—	$\pm$ 1.3	$\pm$ 0.20	$\pm$ 0.49	$\mp$0.86	$^{-0.01}_{+0.09}$	$^{+3.5}_{-4.1}$
12–16	0.0252	2.0	$^{-8.9}_{+8.9}$	—	$\pm$ 3.6	$\pm$ 0.56	$\pm$ 1.4	$\mp$4.2	$^{+0.69}_{-1.1}$	$^{+11}_{-11}$
16–20	0.0129	2.8	$^{-13}_{+15}$	—	$\pm$ 6.0	$\pm$ 0.92	$\pm$ 2.3	$\mp$4.8	$^{+1.3}_{-2.3}$	$^{+17}_{-16}$
20–30	0.00429	4.2	$^{-19}_{+23}$	—	$\pm$ 10	$\pm$ 1.6	$\pm$ 3.9	$\pm$3.5	$^{+4.2}_{-4.2}$	$^{+26}_{-23}$
30–40	0.000785	9.5	$^{-26}_{+32}$	—	$\pm$ 16	$\pm$ 2.5	$\pm$ 6.1	$\pm$6.9	$^{+13}_{-10}$	$^{+40}_{-35}$

Table 13. Measured $\frac{1}{N_{\mathrm{evt}}}\frac{dN_{\mathrm{evt}}}{d\Sigma E_{\mathrm{T}}}$ and systematic uncertainty breakdown for the dijet data in the region $0.8 < |\eta| < 1.6$.

ΣE_{T}	$\frac{1}{N_{\mathrm{evt}}}\frac{dN_{\mathrm{evt}}}{d\Sigma E_{\mathrm{T}}}$	Stat.	E_1^c	E_2	M_1	M_2	M_3^c	P_2	J	Total
[GeV]	[GeV^{-1}]	[%]	[%]	[%]	[%]	[%]	[%]	[%]	[%]	[%]
0–2	0.0604	2.4	$^{+7.6}_{-7.5}$	—	—	$\mp$ 1.6	$\mp$ 9.2	$\mp$8.2	$^{+0.01}_{+0.52}$	$^{+15}_{-15}$
2–4	0.0859	1.6	$^{+6.1}_{-6.0}$	—	—	$\mp$ 1.2	$\mp$ 6.6	$\pm$2.6	$^{-0.43}_{+0.51}$	$^{+9.6}_{-9.5}$
4–6	0.0857	1.5	$^{+3.4}_{-3.3}$	—	—	$\mp$ 0.70	$\mp$ 4.0	$\pm$2.1	$^{-0.47}_{+0.27}$	$^{+5.8}_{-5.8}$
6–8	0.0715	1.6	$^{+0.8}_{-1.3}$	—	—	$\mp$ 0.24	$\mp$ 1.3	$\pm$2.5	$^{-0.40}_{+0.22}$	$^{+3.3}_{-3.5}$
8–12	0.0485	1.7	$^{-2.7}_{+2.2}$	—	—	$\pm$ 0.46	$\pm$ 2.6	$\pm$0.51	$^{-0.63}_{+0.33}$	$^{+3.9}_{-4.2}$
12–16	0.0256	2.3	$^{-7.3}_{+7.4}$	—	—	$\pm$ 1.4	$\pm$ 7.9	$\mp$3	$^{-0.30}_{+0.10}$	$^{+12}_{-11}$
16–20	0.0124	3.3	$^{-12}_{+12}$	—	—	$\pm$ 2.3	$\pm$ 13	$\mp$1.2	$^{+0.75}_{-0.51}$	$^{+18}_{-18}$
20–30	0.00385	4.8	$^{-17}_{+18}$	—	—	$\pm$ 4.0	$\pm$ 22	$\pm$1.3	$^{+4.7}_{-3.9}$	$^{+30}_{-29}$
30–40	0.000641	11	$^{-20}_{+25}$	—	—	$\pm$ 6.3	$\pm$ 36	$\mp$2.0	$^{+17}_{-14}$	$^{+48}_{-45}$

Table 14. Measured $\frac{1}{N_{\mathrm{evt}}}\frac{dN_{\mathrm{evt}}}{d\Sigma E_{\mathrm{T}}}$ and systematic uncertainty breakdown for the dijet data in the region $1.6 < |\eta| < 2.4$.

JHEP11(2012)033

ΣE_{T}	$\frac{1}{N_{\mathrm{evt}}}\frac{dN_{\mathrm{evt}}}{d\Sigma E_{\mathrm{T}}}$	Stat.	E_1^d	E_2	M_1	M_2	M_3^d	P_2	Total
[GeV]	[GeV^{-1}]	[%]	[%]	[%]	[%]	[%]	[%]	[%]	[%]
0–2	0.0565	2.9	$^{+11}_{-5}$	—	—	—	$\mp$ 2.6	$\mp$6.0	$^{+13}_{-9}$
2–4	0.0892	1.7	$^{+8.5}_{-3.8}$	—	—	—	$\mp$ 1.8	$\pm$0.53	$^{+8.9}_{-4.5}$
4–6	0.0905	1.7	$^{+5.1}_{-2.5}$	—	—	—	$\mp$ 0.9	$\pm$2.7	$^{+6.1}_{-4.2}$
6–8	0.0748	1.7	$^{+1.1}_{-1.0}$	—	—	—	$\mp$ 0.03	$\pm$1.3	$^{+2.4}_{-2.3}$
8–12	0.0495	1.8	$^{-4.6}_{+1.1}$	—	—	—	$\pm$ 1.3	$\mp$1.2	$^{+2.8}_{-5.3}$
12–16	0.0253	2.6	$^{-12}_{+6}$	—	—	—	$\pm$ 3.0	$\pm$1.5	$^{+7}_{-13}$
16–20	0.0111	3.5	$^{-18}_{+10}$	—	—	—	$\pm$ 4.8	$\mp$2.1	$^{+12}_{-19}$
20–30	0.00298	5.8	$^{-25}_{+15}$	—	—	—	$\pm$ 7.8	$\pm$1.2	$^{+18}_{-27}$

Table 15. Measured $\frac{1}{N_{\mathrm{evt}}}\frac{dN_{\mathrm{evt}}}{d\Sigma E_{\mathrm{T}}}$ and systematic uncertainty breakdown for the dijet data in the region $2.4 < |\eta| < 3.2$.

ΣE_{T}	$\frac{1}{N_{\mathrm{evt}}}\frac{dN_{\mathrm{evt}}}{d\Sigma E_{\mathrm{T}}}$	Stat.	E_1^e	E_2	M_1	M_2	M_3^e	P_2	Total
[GeV]	[GeV^{-1}]	[%]	[%]	[%]	[%]	[%]	[%]	[%]	[%]
0–2	0.0784	2.5	$^{+8.3}_{-7.3}$	12	—	—	$\mp$ 5.1	$\mp$6.6	$^{+17}_{-11}$
2–4	0.105	1.7	$^{+6.7}_{-6.2}$	9.5	—	—	$\mp$ 2.9	$\pm$1.7	$^{+12}_{-7.3}$
4–6	0.0999	1.6	$^{+2.8}_{-3.1}$	3.9	—	—	$\mp$ 0.8	$\pm$2.0	$^{+5.5}_{-4.1}$
6–8	0.0756	1.7	$^{-1.4}_{+0.3}$	-2.0	—	—	$\pm$ 1.3	$\pm$0.47	$^{+2.2}_{-3.3}$
8–12	0.0433	2.0	$^{-7.1}_{+5.6}$	-10	—	—	$\pm$ 4.5	$\pm$0.46	$^{+8}_{-13}$
12–16	0.0172	2.9	$^{-15}_{+15}$	-21	—	—	$\pm$ 8.8	$\pm$0.25	$^{+17}_{-27}$
16–20	0.00601	4.7	$^{-19}_{+25}$	-27	—	—	$\pm$ 13	$\mp$0.76	$^{+29}_{-36}$

Table 16. Measured $\frac{1}{N_{\mathrm{evt}}}\frac{dN_{\mathrm{evt}}}{d\Sigma E_{\mathrm{T}}}$ and systematic uncertainty breakdown for the dijet data in the region $3.2 < |\eta| < 4.0$.

JHEP11(2012)033

ΣE_{T} [GeV]	$\frac{1}{N_{\mathrm{evt}}}\frac{dN_{\mathrm{evt}}}{d\Sigma E_{\mathrm{T}}}$ [GeV^{-1}]	Stat. [%]	E_1^f [%]	E_2 [%]	M_1 [%]	M_2 [%]	M_3^f [%]	P_2 [%]	Total [%]
0–2	0.0915	2.5	$^{+6.2}_{-5.4}$	16	—	—	$\mp$ 0.63	$\mp$6.2	$^{+18}_{-9}$
2–4	0.139	1.6	$^{+3.4}_{-3.5}$	8.5	—	—	$\mp$ 0.12	$\pm$1.3	$^{+9.3}_{-4.1}$
4–6	0.113	1.6	$^{-0.13}_{-0.51}$	-0.33	—	—	$\pm$ 0.38	$\pm$0.38	$^{+1.7}_{-1.7}$
6–8	0.0726	1.8	$^{-3.6}_{+2.7}$	-9.0	—	—	$\pm$ 0.88	$\mp$0.18	$^{+3.4}_{-9.8}$
8–12	0.0313	2.5	$^{-7.9}_{+8.4}$	-20	—	—	$\pm$ 1.6	$\pm$4.7	$^{+10}_{-22}$
12–16	0.00775	4.4	$^{-11}_{+13}$	-28	—	—	$\pm$ 2.6	$\pm$2.2	$^{+14}_{-31}$

Table 17. Measured $\frac{1}{N_{\mathrm{evt}}}\frac{dN_{\mathrm{evt}}}{d\Sigma E_{\mathrm{T}}}$ and systematic uncertainty breakdown for the dijet data in the region $4.0 < |\eta| < 4.8$.

References

[1] ATLAS collaboration, G. Aad et al., *The ATLAS experiment at the CERN Large Hadron Collider*, 2008 *JINST* **3** S08003 [INSPIRE].

[2] CDF collaboration, T. Aaltonen et al., *Measurement of particle production and inclusive differential cross sections in $p\bar{p}$ collisions at $\sqrt{s} = 1.96$ TeV*, *Phys. Rev.* **D 79** (2009) 112005 [*Erratum ibid.* **D 82** (2010) 119903] [arXiv:0904.1098] [INSPIRE].

[3] ATLAS collaboration, G. Aad et al., *Charged-particle multiplicities in pp interactions measured with the ATLAS detector at the LHC*, *New J. Phys.* **13** (2011) 053033 [arXiv:1012.5104] [INSPIRE].

[4] ALICE collaboration, K. Aamodt et al., *First proton-proton collisions at the LHC as observed with the ALICE detector: measurement of the charged particle pseudorapidity density at $\sqrt{s} = 900$ GeV*, *Eur. Phys. J.* **C 65** (2010) 111 [arXiv:0911.5430] [INSPIRE].

[5] CMS collaboration, V. Khachatryan et al., *Charged particle multiplicities in pp interactions at $\sqrt{s} = 0.9$, 2.36 and 7 TeV*, *JHEP* **01** (2011) 079 [arXiv:1011.5531] [INSPIRE].

[6] CDF collaboration, D. Acosta et al., *The underlying event in hard interactions at the Tevatron $\bar{p}p$ collider*, *Phys. Rev.* **D 70** (2004) 072002 [hep-ex/0404004] [INSPIRE].

[7] CDF collaboration, T. Aaltonen et al., *Studying the underlying event in Drell-Yan and high transverse momentum jet production at the Tevatron*, *Phys. Rev.* **D 82** (2010) 034001 [arXiv:1003.3146] [INSPIRE].

[8] ATLAS collaboration, G. Aad et al., *Measurement of underlying event characteristics using charged particles in pp collisions at $\sqrt{s} = 900$ GeV and 7 TeV with the ATLAS detector*, *Phys. Rev.* **D 83** (2011) 112001 [arXiv:1012.0791] [INSPIRE].

[9] ALICE collaboration, B. Abelev et al., *Underlying event measurements in pp collisions at $\sqrt{s} = 0.9$ and 7 TeV with the ALICE experiment at the LHC*, *JHEP* **07** (2012) 116 [arXiv:1112.2082] [INSPIRE].

JHEP11(2012)033

[10] CMS collaboration, S. Chatrchyan et al., *Measurement of the underlying event activity at the LHC with $\sqrt{s} = 7$ TeV and comparison with $\sqrt{s} = 0.9$ TeV*, *JHEP* **09** (2011) 109 [arXiv:1107.0330] [INSPIRE].

[11] ATLAS collaboration, G. Aad et al., *Measurements of underlying-event properties using neutral and charged particles in pp collisions at 900 GeV and 7 TeV with the ATLAS detector at the LHC*, *Eur. Phys. J.* **C 71** (2011) 1636 [arXiv:1103.1816] [INSPIRE].

[12] CMS collaboration, S. Chatrchyan et al., *Measurement of energy flow at large pseudorapidities in pp collisions at $\sqrt{s} = 0.9$ and 7 TeV*, *JHEP* **11** (2011) 148 [*Erratum ibid.* **02** (2012) 055] [arXiv:1110.0211] [INSPIRE].

[13] LHCb collaboration, R. Aaij et al., *Measurement of charged particle multiplicities in pp collisions at $\sqrt{s} = 7$ TeV in the forward region*, *Eur. Phys. J.* **C 72** (2012) 1947 [arXiv:1112.4592] [INSPIRE].

[14] M. Cacciari, G.P. Salam and G. Soyez, *The anti-k_t jet clustering algorithm*, *JHEP* **04** (2008) 063 [arXiv:0802.1189] [INSPIRE].

[15] T. Sjöstrand, S. Mrenna and P.Z. Skands, *PYTHIA* 6.4 *physics and manual*, *JHEP* **05** (2006) 026 [hep-ph/0603175] [INSPIRE].

[16] T. Sjöstrand, S. Mrenna and P.Z. Skands, *A brief introduction to PYTHIA* 8.1, *Comput. Phys. Commun.* **178** (2008) 852 [arXiv:0710.3820] [INSPIRE].

[17] M. Bähr et al., *HERWIG++ physics and manual*, *Eur. Phys. J.* **C 58** (2008) 639 [arXiv:0803.0883] [INSPIRE].

[18] K. Werner, I. Karpenko, T. Pierog, M. Bleicher and K. Mikhailov, *Evidence for hydrodynamic evolution in proton-proton scattering at 900 GeV*, *Phys. Rev.* **C 83** (2011) 044915 [arXiv:1010.0400] [INSPIRE].

[19] B. Andersson, G. Gustafson, G. Ingelman and T. Sjöstrand, *Parton fragmentation and string dynamics*, *Phys. Rept.* **97** (1983) 31 [INSPIRE].

[20] G.A. Schuler and T. Sjöstrand, *Hadronic diffractive cross-sections and the rise of the total cross-section*, *Phys. Rev.* **D 49** (1994) 2257 [INSPIRE].

[21] H1 collaboration, A. Aktas et al., *Measurement and QCD analysis of the diffractive deep-inelastic scattering cross-section at HERA*, *Eur. Phys. J.* **C 48** (2006) 715 [hep-ex/0606004] [INSPIRE].

[22] B. Webber, *A QCD model for jet fragmentation including soft gluon interference*, *Nucl. Phys.* **B 238** (1984) 492 [INSPIRE].

[23] H. Drescher, M. Hladik, S. Ostapchenko, T. Pierog and K. Werner, *Parton based Gribov-Regge theory*, *Phys. Rept.* **350** (2001) 93 [hep-ph/0007198] [INSPIRE].

[24] ATLAS collaboration, *Charged particle multiplicities in pp interactions at $\sqrt{s} = 0.9$ and 7 TeV in a diffractive limited phase-space measured with the ATLAS detector at the LHC and new PYTHIA 6 tune*, ATLAS-CONF-2010-031, CERN, Geneva Switzerland (2010).

[25] A. Sherstnev and R. Thorne, *Parton distributions for LO generators*, *Eur. Phys. J.* **C 55** (2008) 553 [arXiv:0711.2473] [INSPIRE].

[26] TeV4LHC QCD Working Group collaboration, M.G. Albrow et al., *Tevatron-for-LHC report of the QCD working group*, hep-ph/0610012 [INSPIRE].

[27] CTEQ collaboration, H. Lai et al., *Global QCD analysis of parton structure of the nucleon: CTEQ5 parton distributions*, *Eur. Phys. J.* **C 12** (2000) 375 [hep-ph/9903282] [INSPIRE].

JHEP11(2012)033

[28] P.Z. Skands, *Tuning Monte Carlo generators: the Perugia tunes*, *Phys. Rev.* **D 82** (2010) 074018 [arXiv:1005.3457] [INSPIRE].

[29] R. Corke and T. Sjöstrand, *Interleaved parton showers and tuning prospects*, *JHEP* **03** (2011) 032 [arXiv:1011.1759] [INSPIRE].

[30] J. Pumplin et al., *New generation of parton distributions with uncertainties from global QCD analysis*, *JHEP* **07** (2002) 012 [hep-ph/0201195] [INSPIRE].

[31] S. Gieseke, C. Rohr and A. Siodmok, *Multiple partonic interaction developments in HERWIG++*, arXiv:1110.2675 [INSPIRE].

[32] ATLAS collaboration, *ATLAS tunes of PYTHIA 6 and PYTHIA 8 for MC11*, ATL-PHYS-PUB-2011-009, CERN, Geneva Switzerland (2011) [INSPIRE].

[33] ATLAS collaboration, *Further ATLAS tunes of PYTHIA 6 and PYTHIA 8*, ATL-PHYS-PUB-2011-014, CERN, Geneva Switzerland (2011) [INSPIRE].

[34] A. Martin, W. Stirling, R. Thorne and G. Watt, *Parton distributions for the LHC*, *Eur. Phys. J.* **C 63** (2009) 189 [arXiv:0901.0002] [INSPIRE].

[35] ATLAS collaboration, *Calorimeter clustering algorithms: description and performance*, ATLAS-LARG-PUB-2008-002, CERN, Geneva Switzerland (2008).

[36] E. Abat et al., *Study of the response of the ATLAS central calorimeter to pions of energies from 3 to 9 GeV*, *Nucl. Instrum. Meth.* **A 607** (2009) 372 [INSPIRE].

[37] P. Adragna et al., *Testbeam studies of production modules of the ATLAS tile calorimeter*, *Nucl. Instrum. Meth.* **A 606** (2009) 362 [INSPIRE].

[38] M. Aharrouche et al., *Measurement of the response of the ATLAS liquid argon barrel calorimeter to electrons at the 2004 combined test-beam*, *Nucl. Instrum. Meth.* **A 614** (2010) 400 [INSPIRE].

[39] J. Archambault et al., *Energy calibration of the ATLAS liquid argon forward calorimeter*, 2008 *JINST* **3** P02002 [INSPIRE].

[40] GEANT4 collaboration, S. Agostinelli et al., *GEANT4: a simulation toolkit*, *Nucl. Instrum. Meth.* **A 506** (2003) 250 [INSPIRE].

[41] ATLAS collaboration, G. Aad et al., *The ATLAS simulation infrastructure*, *Eur. Phys. J.* **C 70** (2010) 823 [arXiv:1005.4568] [INSPIRE].

[42] G. D'Agostini, *A multidimensional unfolding method based on Bayes' theorem*, *Nucl. Instrum. Meth.* **A 362** (1995) 487 [INSPIRE].

[43] ATLAS collaboration, G. Aad et al., *Single hadron response measurement and calorimeter jet energy scale uncertainty with the ATLAS detector at the LHC*, arXiv:1203.1302 [INSPIRE].

[44] J. Pinfold et al., *Evaluation of the local hadronic calibration with combined beam-test data for the endcap and forward calorimeters of ATLAS in the pseudorapidity region* $2.5 < |\eta| < 4.0$, *Nucl. Instrum. Meth.* **A 693** (2012) 74.

[45] ATLAS collaboration, G. Aad et al., *Electron performance measurements with the ATLAS detector using the 2010 LHC proton-proton collision data*, *Eur. Phys. J.* **C 72** (2012) 1909 [arXiv:1110.3174] [INSPIRE].

[46] ATLAS collaboration, G. Aad et al., *Jet energy measurement with the ATLAS detector in proton-proton collisions at* $\sqrt{s} = 7$ *TeV*, arXiv:1112.6426 [INSPIRE].

JHEP11(2012)033

The ATLAS collaboration

G. Aad[47], T. Abajyan[20], B. Abbott[110], J. Abdallah[11], S. Abdel Khalek[114], A.A. Abdelalim[48], O. Abdinov[10], R. Aben[104], B. Abi[111], M. Abolins[87], O.S. AbouZeid[157], H. Abramowicz[152], H. Abreu[135], E. Acerbi[88a,88b], B.S. Acharya[163a,163b], L. Adamczyk[37], D.L. Adams[24], T.N. Addy[55], J. Adelman[175], S. Adomeit[97], P. Adragna[74], T. Adye[128], S. Aefsky[22], J.A. Aguilar-Saavedra[123b,a], M. Agustoni[16], M. Aharrouche[80], S.P. Ahlen[21], F. Ahles[47], A. Ahmad[147], M. Ahsan[40], G. Aielli[132a,132b], T. Akdogan[18a], T.P.A. Åkesson[78], G. Akimoto[154], A.V. Akimov[93], M.S. Alam[1], M.A. Alam[75], J. Albert[168], S. Albrand[54], M. Aleksa[29], I.N. Aleksandrov[63], F. Alessandria[88a], C. Alexa[25a], G. Alexander[152], G. Alexandre[48], T. Alexopoulos[9], M. Alhroob[163a,163c], M. Aliev[15], G. Alimonti[88a], J. Alison[119], B.M.M. Allbrooke[17], P.P. Allport[72], S.E. Allwood-Spiers[52], J. Almond[81], A. Aloisio[101a,101b], R. Alon[171], A. Alonso[78], F. Alonso[69], B. Alvarez Gonzalez[87], M.G. Alviggi[101a,101b], K. Amako[64], C. Amelung[22], V.V. Ammosov[127,*], A. Amorim[123a,b], N. Amram[152], C. Anastopoulos[29], L.S. Ancu[16], N. Andari[114], T. Andeen[34], C.F. Anders[57b], G. Anders[57a], K.J. Anderson[30], A. Andreazza[88a,88b], V. Andrei[57a], X.S. Anduaga[69], P. Anger[43], A. Angerami[34], F. Anghinolfi[29], A. Anisenkov[106], N. Anjos[123a], A. Annovi[46], A. Antonaki[8], M. Antonelli[46], A. Antonov[95], J. Antos[143b], F. Anulli[131a], M. Aoki[100], S. Aoun[82], L. Aperio Bella[4], R. Apolle[117,c], G. Arabidze[87], I. Aracena[142], Y. Arai[64], A.T.H. Arce[44], S. Arfaoui[147], J-F. Arguin[14], E. Arik[18a,*], M. Arik[18a], A.J. Armbruster[86], O. Arnaez[80], V. Arnal[79], C. Arnault[114], A. Artamonov[94], G. Artoni[131a,131b], D. Arutinov[20], S. Asai[154], R. Asfandiyarov[172], S. Ask[27], B. Åsman[145a,145b], L. Asquith[5], K. Assamagan[24], A. Astbury[168], M. Atkinson[164], B. Aubert[4], E. Auge[114], K. Augsten[126], M. Aurousseau[144a], G. Avolio[162], R. Avramidou[9], D. Axen[167], G. Azuelos[92,d], Y. Azuma[154], M.A. Baak[29], G. Baccaglioni[88a], C. Bacci[133a,133b], A.M. Bach[14], H. Bachacou[135], K. Bachas[29], M. Backes[48], M. Backhaus[20], E. Badescu[25a], P. Bagnaia[131a,131b], S. Bahinipati[2], Y. Bai[32a], D.C. Bailey[157], T. Bain[157], J.T. Baines[128], O.K. Baker[175], M.D. Baker[24], S. Baker[76], E. Banas[38], P. Banerjee[92], Sw. Banerjee[172], D. Banfi[29], A. Bangert[149], V. Bansal[168], H.S. Bansil[17], L. Barak[171], S.P. Baranov[93], A. Barbaro Galtieri[14], T. Barber[47], E.L. Barberio[85], D. Barberis[49a,49b], M. Barbero[20], D.Y. Bardin[63], T. Barillari[98], M. Barisonzi[174], T. Barklow[142], N. Barlow[27], B.M. Barnett[128], R.M. Barnett[14], A. Baroncelli[133a], G. Barone[48], A.J. Barr[117], F. Barreiro[79], J. Barreiro Guimarães da Costa[56], P. Barrillon[114], R. Bartoldus[142], A.E. Barton[70], V. Bartsch[148], A. Basye[164], R.L. Bates[52], L. Batkova[143a], J.R. Batley[27], A. Battaglia[16], M. Battistin[29], F. Bauer[135], H.S. Bawa[142,e], S. Beale[97], T. Beau[77], P.H. Beauchemin[160], R. Beccherle[49a], P. Bechtle[20], H.P. Beck[16], A.K. Becker[174], S. Becker[97], M. Beckingham[137], K.H. Becks[174], A.J. Beddall[18c], A. Beddall[18c], S. Bedikian[175], V.A. Bednyakov[63], C.P. Bee[82], L.J. Beemster[104], M. Begel[24], S. Behar Harpaz[151], M. Beimforde[98], C. Belanger-Champagne[84], P.J. Bell[48], W.H. Bell[48], G. Bella[152], L. Bellagamba[19a], F. Bellina[29], M. Bellomo[29], A. Belloni[56], O. Beloborodova[106,f], K. Belotskiy[95], O. Beltramello[29], O. Benary[152], D. Benchekroun[134a], K. Bendtz[145a,145b], N. Benekos[164], Y. Benhammou[152], E. Benhar Noccioli[48], J.A. Benitez Garcia[158b], D.P. Benjamin[44], M. Benoit[114], J.R. Bensinger[22], K. Benslama[129], S. Bentvelsen[104], D. Berge[29],

JHEP11(2012)033

E. Bergeaas Kuutmann[41], N. Berger[4], F. Berghaus[168], E. Berglund[104], J. Beringer[14], P. Bernat[76], R. Bernhard[47], C. Bernius[24], T. Berry[75], C. Bertella[82], A. Bertin[19a,19b], F. Bertolucci[121a,121b], M.I. Besana[88a,88b], G.J. Besjes[103], N. Besson[135], S. Bethke[98], W. Bhimji[45], R.M. Bianchi[29], M. Bianco[71a,71b], O. Biebel[97], S.P. Bieniek[76], K. Bierwagen[53], J. Biesiada[14], M. Biglietti[133a], H. Bilokon[46], M. Bindi[19a,19b], S. Binet[114], A. Bingul[18c], C. Bini[131a,131b], C. Biscarat[177], B. Bittner[98], K.M. Black[21], R.E. Blair[5], J.-B. Blanchard[135], G. Blanchot[29], T. Blazek[143a], C. Blocker[22], J. Blocki[38], A. Blondel[48], W. Blum[80], U. Blumenschein[53], G.J. Bobbink[104], V.B. Bobrovnikov[106], S.S. Bocchetta[78], A. Bocci[44], C.R. Boddy[117], M. Boehler[47], J. Boek[174], N. Boelaert[35], J.A. Bogaerts[29], A. Bogdanchikov[106], A. Bogouch[89,*], C. Bohm[145a], J. Bohm[124], V. Boisvert[75], T. Bold[37], V. Boldea[25a], N.M. Bolnet[135], M. Bomben[77], M. Bona[74], M. Boonekamp[135], C.N. Booth[138], S. Bordoni[77], C. Borer[16], A. Borisov[127], G. Borissov[70], I. Borjanovic[12a], M. Borri[81], S. Borroni[86], V. Bortolotto[133a,133b], K. Bos[104], D. Boscherini[19a], M. Bosman[11], H. Boterenbrood[104], J. Bouchami[92], J. Boudreau[122], E.V. Bouhova-Thacker[70], D. Boumediene[33], C. Bourdarios[114], N. Bousson[82], A. Boveia[30], J. Boyd[29], I.R. Boyko[63], I. Bozovic-Jelisavcic[12b], J. Bracinik[17], P. Branchini[133a], A. Brandt[7], G. Brandt[117], O. Brandt[53], U. Bratzler[155], B. Brau[83], J.E. Brau[113], H.M. Braun[174,*], S.F. Brazzale[163a,163c], B. Brelier[157], J. Bremer[29], K. Brendlinger[119], R. Brenner[165], S. Bressler[171], D. Britton[52], F.M. Brochu[27], I. Brock[20], R. Brock[87], F. Broggi[88a], C. Bromberg[87], J. Bronner[98], G. Brooijmans[34], T. Brooks[75], W.K. Brooks[31b], G. Brown[81], H. Brown[7], P.A. Bruckman de Renstrom[38], D. Bruncko[143b], R. Bruneliere[47], S. Brunet[59], A. Bruni[19a], G. Bruni[19a], M. Bruschi[19a], T. Buanes[13], Q. Buat[54], F. Bucci[48], J. Buchanan[117], P. Buchholz[140], R.M. Buckingham[117], A.G. Buckley[45], S.I. Buda[25a], I.A. Budagov[63], B. Budick[107], V. Büscher[80], L. Bugge[116], O. Bulekov[95], A.C. Bundock[72], M. Bunse[42], T. Buran[116], H. Burckhart[29], S. Burdin[72], T. Burgess[13], S. Burke[128], E. Busato[33], P. Bussey[52], C.P. Buszello[165], B. Butler[142], J.M. Butler[21], C.M. Buttar[52], J.M. Butterworth[76], W. Buttinger[27], S. Cabrera Urbán[166], D. Caforio[19a,19b], O. Cakir[3a], P. Calafiura[14], G. Calderini[77], P. Calfayan[97], R. Calkins[105], L.P. Caloba[23a], R. Caloi[131a,131b], D. Calvet[33], S. Calvet[33], R. Camacho Toro[33], P. Camarri[132a,132b], D. Cameron[116], L.M. Caminada[14], R. Caminal Armadans[11], S. Campana[29], M. Campanelli[76], V. Canale[101a,101b], F. Canelli[30,g], A. Canepa[158a], J. Cantero[79], R. Cantrill[75], L. Capasso[101a,101b], M.D.M. Capeans Garrido[29], I. Caprini[25a], M. Caprini[25a], D. Capriotti[98], M. Capua[36a,36b], R. Caputo[80], R. Cardarelli[132a], T. Carli[29], G. Carlino[101a], L. Carminati[88a,88b], B. Caron[84], S. Caron[103], E. Carquin[31b], G.D. Carrillo Montoya[172], A.A. Carter[74], J.R. Carter[27], J. Carvalho[123a,h], D. Casadei[107], M.P. Casado[11], M. Cascella[121a,121b], C. Caso[49a,49b,*], A.M. Castaneda Hernandez[172,i], E. Castaneda-Miranda[172], V. Castillo Gimenez[166], N.F. Castro[123a], G. Cataldi[71a], P. Catastini[56], A. Catinaccio[29], J.R. Catmore[29], A. Cattai[29], G. Cattani[132a,132b], S. Caughron[87], V. Cavaliere[164], P. Cavalleri[77], D. Cavalli[88a], M. Cavalli-Sforza[11], V. Cavasinni[121a,121b], F. Ceradini[133a,133b], A.S. Cerqueira[23b], A. Cerri[29], L. Cerrito[74], F. Cerutti[46], S.A. Cetin[18b], A. Chafaq[134a], D. Chakraborty[105], I. Chalupkova[125], K. Chan[2], P. Chang[164], B. Chapleau[84], J.D. Chapman[27], J.W. Chapman[86], E. Chareyre[77], D.G. Charlton[17], V. Chavda[81], C.A. Chavez Barajas[29], S. Cheatham[84], S. Chekanov[5],

JHEP11(2012)033

S.V. Chekulaev[158a], G.A. Chelkov[63], M.A. Chelstowska[103], C. Chen[62], H. Chen[24], S. Chen[32c], X. Chen[172], Y. Chen[34], A. Cheplakov[63], R. Cherkaoui El Moursli[134e], V. Chernyatin[24], E. Cheu[6], S.L. Cheung[157], L. Chevalier[135], G. Chiefari[101a,101b], L. Chikovani[50a,*], J.T. Childers[29], A. Chilingarov[70], G. Chiodini[71a], A.S. Chisholm[17], R.T. Chislett[76], A. Chitan[25a], M.V. Chizhov[63], G. Choudalakis[30], S. Chouridou[136], I.A. Christidi[76], A. Christov[47], D. Chromek-Burckhart[29], M.L. Chu[150], J. Chudoba[124], G. Ciapetti[131a,131b], A.K. Ciftci[3a], R. Ciftci[3a], D. Cinca[33], V. Cindro[73], C. Ciocca[19a,19b], A. Ciocio[14], M. Cirilli[86], P. Cirkovic[12b], M. Citterio[88a], M. Ciubancan[25a], A. Clark[48], P.J. Clark[45], R.N. Clarke[14], W. Cleland[122], J.C. Clemens[82], B. Clement[54], C. Clement[145a,145b], Y. Coadou[82], M. Cobal[163a,163c], A. Coccaro[137], J. Cochran[62], J.G. Cogan[142], J. Coggeshall[164], E. Cogneras[177], J. Colas[4], S. Cole[105], A.P. Colijn[104], N.J. Collins[17], C. Collins-Tooth[52], J. Collot[54], T. Colombo[118a,118b], G. Colon[83], P. Conde Muiño[123a], E. Coniavitis[117], M.C. Conidi[11], S.M. Consonni[88a,88b], V. Consorti[47], S. Constantinescu[25a], C. Conta[118a,118b], G. Conti[56], F. Conventi[101a,j], M. Cooke[14], B.D. Cooper[76], A.M. Cooper-Sarkar[117], K. Copic[14], T. Cornelissen[174], M. Corradi[19a], F. Corriveau[84,k], A. Cortes-Gonzalez[164], G. Cortiana[98], G. Costa[88a], M.J. Costa[166], D. Costanzo[138], T. Costin[30], D. Côté[29], L. Courneyea[168], G. Cowan[75], C. Cowden[27], B.E. Cox[81], K. Cranmer[107], F. Crescioli[121a,121b], M. Cristinziani[20], G. Crosetti[36a,36b], S. Crépé-Renaudin[54], C.-M. Cuciuc[25a], C. Cuenca Almenar[175], T. Cuhadar Donszelmann[138], M. Curatolo[46], C.J. Curtis[17], C. Cuthbert[149], P. Cwetanski[59], H. Czirr[140], P. Czodrowski[43], Z. Czyczula[175], S. D'Auria[52], M. D'Onofrio[72], A. D'Orazio[131a,131b], M.J. Da Cunha Sargedas De Sousa[123a], C. Da Via[81], W. Dabrowski[37], A. Dafinca[117], T. Dai[86], C. Dallapiccola[83], M. Dam[35], M. Dameri[49a,49b], D.S. Damiani[136], H.O. Danielsson[29], V. Dao[48], G. Darbo[49a], G.L. Darlea[25b], J.A. Dassoulas[41], W. Davey[20], T. Davidek[125], N. Davidson[85], R. Davidson[70], E. Davies[117,c], M. Davies[92], O. Davignon[77], A.R. Davison[76], Y. Davygora[57a], E. Dawe[141], I. Dawson[138], R.K. Daya-Ishmukhametova[22], K. De[7], R. de Asmundis[101a], S. De Castro[19a,19b], S. De Cecco[77], J. de Graat[97], N. De Groot[103], P. de Jong[104], C. De La Taille[114], H. De la Torre[79], F. De Lorenzi[62], L. de Mora[70], L. De Nooij[104], D. De Pedis[131a], A. De Salvo[131a], U. De Sanctis[163a,163c], A. De Santo[148], J.B. De Vivie De Regie[114], G. De Zorzi[131a,131b], W.J. Dearnaley[70], R. Debbe[24], C. Debenedetti[45], B. Dechenaux[54], D.V. Dedovich[63], J. Degenhardt[119], C. Del Papa[163a,163c], J. Del Peso[79], T. Del Prete[121a,121b], T. Delemontex[54], M. Deliyergiyev[73], A. Dell'Acqua[29], L. Dell'Asta[21], M. Della Pietra[101a,j], D. della Volpe[101a,101b], M. Delmastro[4], P.A. Delsart[54], C. Deluca[104], S. Demers[175], M. Demichev[63], B. Demirkoz[11,l], J. Deng[162], S.P. Denisov[127], D. Derendarz[38], J.E. Derkaoui[134d], F. Derue[77], P. Dervan[72], K. Desch[20], E. Devetak[147], P.O. Deviveiros[104], A. Dewhurst[128], B. DeWilde[147], S. Dhaliwal[157], R. Dhullipudi[24,m], A. Di Ciaccio[132a,132b], L. Di Ciaccio[4], A. Di Girolamo[29], B. Di Girolamo[29], S. Di Luise[133a,133b], A. Di Mattia[172], B. Di Micco[29], R. Di Nardo[46], A. Di Simone[132a,132b], R. Di Sipio[19a,19b], M.A. Diaz[31a], E.B. Diehl[86], J. Dietrich[41], T.A. Dietzsch[57a], S. Diglio[85], K. Dindar Yagci[39], J. Dingfelder[20], F. Dinut[25a], C. Dionisi[131a,131b], P. Dita[25a], S. Dita[25a], F. Dittus[29], F. Djama[82], T. Djobava[50b], M.A.B. do Vale[23c], A. Do Valle Wemans[123a,n], T.K.O. Doan[4], M. Dobbs[84], R. Dobinson[29,*], D. Dobos[29], E. Dobson[29,o], J. Dodd[34], C. Doglioni[48], T. Doherty[52],

JHEP11(2012)033

Y. Doi[64,*], J. Dolejsi[125], I. Dolenc[73], Z. Dolezal[125], B.A. Dolgoshein[95,*], T. Dohmae[154], M. Donadelli[23d], J. Donini[33], J. Dopke[29], A. Doria[101a], A. Dos Anjos[172], A. Dotti[121a,121b], M.T. Dova[69], A.D. Doxiadis[104], A.T. Doyle[52], M. Dris[9], J. Dubbert[98], S. Dube[14], E. Duchovni[171], G. Duckeck[97], D. Duda[174], A. Dudarev[29], F. Dudziak[62], M. Dührssen[29], I.P. Duerdoth[81], L. Duflot[114], M-A. Dufour[84], L. Duguid[75], M. Dunford[29], H. Duran Yildiz[3a], R. Duxfield[138], M. Dwuznik[37], F. Dydak[29], M. Düren[51], J. Ebke[97], S. Eckweiler[80], K. Edmonds[80], W. Edson[1], C.A. Edwards[75], N.C. Edwards[52], W. Ehrenfeld[41], T. Eifert[142], G. Eigen[13], K. Einsweiler[14], E. Eisenhandler[74], T. Ekelof[165], M. El Kacimi[134c], M. Ellert[165], S. Elles[4], F. Ellinghaus[80], K. Ellis[74], N. Ellis[29], J. Elmsheuser[97], M. Elsing[29], D. Emeliyanov[128], R. Engelmann[147], A. Engl[97], B. Epp[60], J. Erdmann[53], A. Ereditato[16], D. Eriksson[145a], J. Ernst[1], M. Ernst[24], J. Ernwein[135], D. Errede[164], S. Errede[164], E. Ertel[80], M. Escalier[114], H. Esch[42], C. Escobar[122], X. Espinal Curull[11], B. Esposito[46], F. Etienne[82], A.I. Etienvre[135], E. Etzion[152], D. Evangelakou[53], H. Evans[59], L. Fabbri[19a,19b], C. Fabre[29], R.M. Fakhrutdinov[127], S. Falciano[131a], Y. Fang[172], M. Fanti[88a,88b], A. Farbin[7], A. Farilla[133a], J. Farley[147], T. Farooque[157], S. Farrell[162], S.M. Farrington[169], P. Farthouat[29], F. Fassi[166], P. Fassnacht[29], D. Fassouliotis[8], B. Fatholahzadeh[157], A. Favareto[88a,88b], L. Fayard[114], S. Fazio[36a,36b], R. Febbraro[33], P. Federic[143a], O.L. Fedin[120], W. Fedorko[87], M. Fehling-Kaschek[47], L. Feligioni[82], D. Fellmann[5], C. Feng[32d], E.J. Feng[5], A.B. Fenyuk[127], J. Ferencei[143b], W. Fernando[5], S. Ferrag[52], J. Ferrando[52], V. Ferrara[41], A. Ferrari[165], P. Ferrari[104], R. Ferrari[118a], D.E. Ferreira de Lima[52], A. Ferrer[166], D. Ferrere[48], C. Ferretti[86], A. Ferretto Parodi[49a,49b], M. Fiascaris[30], F. Fiedler[80], A. Filipčič[73], F. Filthaut[103], M. Fincke-Keeler[168], M.C.N. Fiolhais[123a,h], L. Fiorini[166], A. Firan[39], G. Fischer[41], M.J. Fisher[108], M. Flechl[47], I. Fleck[140], J. Fleckner[80], P. Fleischmann[173], S. Fleischmann[174], T. Flick[174], A. Floderus[78], L.R. Flores Castillo[172], M.J. Flowerdew[98], T. Fonseca Martin[16], A. Formica[135], A. Forti[81], D. Fortin[158a], D. Fournier[114], H. Fox[70], P. Francavilla[11], M. Franchini[19a,19b], S. Franchino[118a,118b], D. Francis[29], T. Frank[171], S. Franz[29], M. Fraternali[118a,118b], S. Fratina[119], S.T. French[27], C. Friedrich[41], F. Friedrich[43], R. Froeschl[29], D. Froidevaux[29], J.A. Frost[27], C. Fukunaga[155], E. Fullana Torregrosa[29], B.G. Fulsom[142], J. Fuster[166], C. Gabaldon[29], O. Gabizon[171], T. Gadfort[24], S. Gadomski[48], G. Gagliardi[49a,49b], P. Gagnon[59], C. Galea[97], E.J. Gallas[117], V. Gallo[16], B.J. Gallop[128], P. Gallus[124], K.K. Gan[108], Y.S. Gao[142,e], A. Gaponenko[14], F. Garberson[175], M. Garcia-Sciveres[14], C. García[166], J.E. García Navarro[166], R.W. Gardner[30], N. Garelli[29], H. Garitaonandia[104], V. Garonne[29], C. Gatti[46], G. Gaudio[118a], B. Gaur[140], L. Gauthier[135], P. Gauzzi[131a,131b], I.L. Gavrilenko[93], C. Gay[167], G. Gaycken[20], E.N. Gazis[9], P. Ge[32d], Z. Gecse[167], C.N.P. Gee[128], D.A.A. Geerts[104], Ch. Geich-Gimbel[20], K. Gellerstedt[145a,145b], C. Gemme[49a], A. Gemmell[52], M.H. Genest[54], S. Gentile[131a,131b], M. George[53], S. George[75], P. Gerlach[174], A. Gershon[152], C. Geweniger[57a], H. Ghazlane[134b], N. Ghodbane[33], B. Giacobbe[19a], S. Giagu[131a,131b], V. Giakoumopoulou[8], V. Giangiobbe[11], F. Gianotti[29], B. Gibbard[24], A. Gibson[157], S.M. Gibson[29], D. Gillberg[28], A.R. Gillman[128], D.M. Gingrich[2,d], J. Ginzburg[152], N. Giokaris[8], M.P. Giordani[163c], R. Giordano[101a,101b], F.M. Giorgi[15], P. Giovannini[98], P.F. Giraud[135], D. Giugni[88a], M. Giunta[92], P. Giusti[19a], B.K. Gjelsten[116], L.K. Gladilin[96],

JHEP11(2012)033

C. Glasman[79], J. Glatzer[47], A. Glazov[41], K.W. Glitza[174], G.L. Glonti[63], J.R. Goddard[74], J. Godfrey[141], J. Godlewski[29], M. Goebel[41], T. Göpfert[43], C. Goeringer[80], C. Gössling[42], S. Goldfarb[86], T. Golling[175], A. Gomes[123a,b], L.S. Gomez Fajardo[41], R. Gonçalo[75], J. Goncalves Pinto Firmino Da Costa[41], L. Gonella[20], S. Gonzalez[172], S. González de la Hoz[166], G. Gonzalez Parra[11], M.L. Gonzalez Silva[26], S. Gonzalez-Sevilla[48], J.J. Goodson[147], L. Goossens[29], P.A. Gorbounov[94], H.A. Gordon[24], I. Gorelov[102], G. Gorfine[174], B. Gorini[29], E. Gorini[71a,71b], A. Gorišek[73], E. Gornicki[38], B. Gosdzik[41], A.T. Goshaw[5], M. Gosselink[104], M.I. Gostkin[63], I. Gough Eschrich[162], M. Gouighri[134a], D. Goujdami[134c], M.P. Goulette[48], A.G. Goussiou[137], C. Goy[4], S. Gozpinar[22], I. Grabowska-Bold[37], P. Grafström[19a,19b], K-J. Grahn[41], F. Grancagnolo[71a], S. Grancagnolo[15], V. Grassi[147], V. Gratchev[120], N. Grau[34], H.M. Gray[29], J.A. Gray[147], E. Graziani[133a], O.G. Grebenyuk[120], T. Greenshaw[72], Z.D. Greenwood[24,m], K. Gregersen[35], I.M. Gregor[41], P. Grenier[142], J. Griffiths[7], N. Grigalashvili[63], A.A. Grillo[136], S. Grinstein[11], Y.V. Grishkevich[96], J.-F. Grivaz[114], E. Gross[171], J. Grosse-Knetter[53], J. Groth-Jensen[171], K. Grybel[140], D. Guest[175], C. Guicheney[33], S. Guindon[53], U. Gul[52], H. Guler[84,p], J. Gunther[124], B. Guo[157], J. Guo[34], P. Gutierrez[110], N. Guttman[152], O. Gutzwiller[172], C. Guyot[135], C. Gwenlan[117], C.B. Gwilliam[72], A. Haas[142], S. Haas[29], C. Haber[14], H.K. Hadavand[39], D.R. Hadley[17], P. Haefner[20], F. Hahn[29], S. Haider[29], Z. Hajduk[38], H. Hakobyan[176], D. Hall[117], J. Haller[53], K. Hamacher[174], P. Hamal[112], M. Hamer[53], A. Hamilton[144b,q], S. Hamilton[160], L. Han[32b], K. Hanagaki[115], K. Hanawa[159], M. Hance[14], C. Handel[80], P. Hanke[57a], J.R. Hansen[35], J.B. Hansen[35], J.D. Hansen[35], P.H. Hansen[35], P. Hansson[142], K. Hara[159], G.A. Hare[136], T. Harenberg[174], S. Harkusha[89], D. Harper[86], R.D. Harrington[45], O.M. Harris[137], J. Hartert[47], F. Hartjes[104], T. Haruyama[64], A. Harvey[55], S. Hasegawa[100], Y. Hasegawa[139], S. Hassani[135], S. Haug[16], M. Hauschild[29], R. Hauser[87], M. Havranek[20], C.M. Hawkes[17], R.J. Hawkings[29], A.D. Hawkins[78], D. Hawkins[162], T. Hayakawa[65], T. Hayashi[159], D. Hayden[75], C.P. Hays[117], H.S. Hayward[72], S.J. Haywood[128], M. He[32d], S.J. Head[17], V. Hedberg[78], L. Heelan[7], S. Heim[87], B. Heinemann[14], S. Heisterkamp[35], L. Helary[21], C. Heller[97], M. Heller[29], S. Hellman[145a,145b], D. Hellmich[20], C. Helsens[11], R.C.W. Henderson[70], M. Henke[57a], A. Henrichs[53], A.M. Henriques Correia[29], S. Henrot-Versille[114], C. Hensel[53], T. Henß[174], C.M. Hernandez[7], Y. Hernández Jiménez[166], R. Herrberg[15], G. Herten[47], R. Hertenberger[97], L. Hervas[29], G.G. Hesketh[76], N.P. Hessey[104], E. Higón-Rodriguez[166], J.C. Hill[27], K.H. Hiller[41], S. Hillert[20], S.J. Hillier[17], I. Hinchliffe[14], E. Hines[119], M. Hirose[115], F. Hirsch[42], D. Hirschbuehl[174], J. Hobbs[147], N. Hod[152], M.C. Hodgkinson[138], P. Hodgson[138], A. Hoecker[29], M.R. Hoeferkamp[102], J. Hoffman[39], D. Hoffmann[82], M. Hohlfeld[80], M. Holder[140], S.O. Holmgren[145a], T. Holy[126], J.L. Holzbauer[87], T.M. Hong[119], L. Hooft van Huysduynen[107], S. Horner[47], J-Y. Hostachy[54], S. Hou[150], A. Hoummada[134a], J. Howard[117], J. Howarth[81], I. Hristova[15], J. Hrivnac[114], T. Hryn'ova[4], P.J. Hsu[80], S.-C. Hsu[14], D. Hu[34], Z. Hubacek[126], F. Hubaut[82], F. Huegging[20], A. Huettmann[41], T.B. Huffman[117], E.W. Hughes[34], G. Hughes[70], M. Huhtinen[29], M. Hurwitz[14], U. Husemann[41], N. Huseynov[63,r], J. Huston[87], J. Huth[56], G. Iacobucci[48], G. Iakovidis[9], M. Ibbotson[81], I. Ibragimov[140], L. Iconomidou-Fayard[114], J. Idarraga[114], P. Iengo[101a], O. Igonkina[104], Y. Ikegami[64], M. Ikeno[64], D. Iliadis[153], N. Ilic[157], T. Ince[20], J. Inigo-Golfin[29], P. Ioannou[8], M. Iodice[133a], K. Iordanidou[8],

JHEP11(2012)033

V. Ippolito[131a,131b], A. Irles Quiles[166], C. Isaksson[165], M. Ishino[66], M. Ishitsuka[156], R. Ishmukhametov[39], C. Issever[117], S. Istin[18a], A.V. Ivashin[127], W. Iwanski[38], H. Iwasaki[64], J.M. Izen[40], V. Izzo[101a], B. Jackson[119], J.N. Jackson[72], P. Jackson[142], M.R. Jaekel[29], V. Jain[59], K. Jakobs[47], S. Jakobsen[35], T. Jakoubek[124], J. Jakubek[126], D.K. Jana[110], E. Jansen[76], H. Jansen[29], A. Jantsch[98], M. Janus[47], G. Jarlskog[78], L. Jeanty[56], I. Jen-La Plante[30], D. Jennens[85], P. Jenni[29], A.E. Loevschall-Jensen[35], P. Ježˇ[35], S. Jézéquel[4], M.K. Jha[19a], H. Ji[172], W. Ji[80], J. Jia[147], Y. Jiang[32b], M. Jimenez Belenguer[41], S. Jin[32a], O. Jinnouchi[156], M.D. Joergensen[35], D. Joffe[39], M. Johansen[145a,145b], K.E. Johansson[145a], P. Johansson[138], S. Johnert[41], K.A. Johns[6], K. Jon-And[145a,145b], G. Jones[169], R.W.L. Jones[70], T.J. Jones[72], C. Joram[29], P.M. Jorge[123a], K.D. Joshi[81], J. Jovicevic[146], T. Jovin[12b], X. Ju[172], C.A. Jung[42], R.M. Jungst[29], V. Juranek[124], P. Jussel[60], A. Juste Rozas[11], S. Kabana[16], M. Kaci[166], A. Kaczmarska[38], P. Kadlecik[35], M. Kado[114], H. Kagan[108], M. Kagan[56], E. Kajomovitz[151], S. Kalinin[174], L.V. Kalinovskaya[63], S. Kama[39], N. Kanaya[154], M. Kaneda[29], S. Kaneti[27], T. Kanno[156], V.A. Kantserov[95], J. Kanzaki[64], B. Kaplan[107], A. Kapliy[30], J. Kaplon[29], D. Kar[52], M. Karagounis[20], K. Karakostas[9], M. Karnevskiy[41], V. Kartvelishvili[70], A.N. Karyukhin[127], L. Kashif[172], G. Kasieczka[57b], R.D. Kass[108], A. Kastanas[13], M. Kataoka[4], Y. Kataoka[154], E. Katsoufis[9], J. Katzy[41], V. Kaushik[6], K. Kawagoe[68], T. Kawamoto[154], G. Kawamura[80], M.S. Kayl[104], S. Kazama[154], V.A. Kazanin[106], M.Y. Kazarinov[63], R. Keeler[168], R. Kehoe[39], M. Keil[53], G.D. Kekelidze[63], J.S. Keller[137], M. Kenyon[52], O. Kepka[124], N. Kerschen[29], B.P. Kerševan[73], S. Kersten[174], K. Kessoku[154], J. Keung[157], F. Khalil-zada[10], H. Khandanyan[145a,145b], A. Khanov[111], D. Kharchenko[63], A. Khodinov[95], A. Khomich[57a], T.J. Khoo[27], G. Khoriauli[20], A. Khoroshilov[174], V. Khovanskiy[94], E. Khramov[63], J. Khubua[50b], H. Kim[145a,145b], S.H. Kim[159], N. Kimura[170], O. Kind[15], B.T. King[72], M. King[65], R.S.B. King[117], J. Kirk[128], A.E. Kiryunin[98], T. Kishimoto[65], D. Kisielewska[37], T. Kitamura[65], T. Kittelmann[122], K. Kiuchi[159], E. Kladiva[143b], M. Klein[72], U. Klein[72], K. Kleinknecht[80], M. Klemetti[84], A. Klier[171], P. Klimek[145a,145b], A. Klimentov[24], R. Klingenberg[42], J.A. Klinger[81], E.B. Klinkby[35], T. Klioutchnikova[29], P.F. Klok[103], S. Klous[104], E.-E. Kluge[57a], T. Kluge[72], P. Kluit[104], S. Kluth[98], N.S. Knecht[157], E. Kneringer[60], E.B.F.G. Knoops[82], A. Knue[53], B.R. Ko[44], T. Kobayashi[154], M. Kobel[43], M. Kocian[142], P. Kodys[125], K. Köneke[29], A.C. König[103], S. Koenig[80], L. Köpke[80], F. Koetsveld[103], P. Koevesarki[20], T. Koffas[28], E. Koffeman[104], L.A. Kogan[117], S. Kohlmann[174], F. Kohn[53], Z. Kohout[126], T. Kohriki[64], T. Koi[142], G.M. Kolachev[106,*], H. Kolanoski[15], V. Kolesnikov[63], I. Koletsou[88a], J. Koll[87], M. Kollefrath[47], A.A. Komar[93], Y. Komori[154], T. Kondo[64], T. Kono[41,s], A.I. Kononov[47], R. Konoplich[107,t], N. Konstantinidis[76], S. Koperny[37], K. Korcyl[38], K. Kordas[153], A. Korn[117], A. Korol[106], I. Korolkov[11], E.V. Korolkova[138], V.A. Korotkov[127], O. Kortner[98], S. Kortner[98], V.V. Kostyukhin[20], S. Kotov[98], V.M. Kotov[63], A. Kotwal[44], C. Kourkoumelis[8], V. Kouskoura[153], A. Koutsman[158a], R. Kowalewski[168], T.Z. Kowalski[37], W. Kozanecki[135], A.S. Kozhin[127], V. Kral[126], V.A. Kramarenko[96], G. Kramberger[73], M.W. Krasny[77], A. Krasznahorkay[107], J.K. Kraus[20], S. Kreiss[107], F. Krejci[126], J. Kretzschmar[72], N. Krieger[53], P. Krieger[157], K. Kroeninger[53], H. Kroha[98], J. Kroll[119], J. Kroseberg[20], J. Krstic[12a], U. Kruchonak[63], H. Krüger[20], T. Kruker[16], N. Krumnack[62],

JHEP11(2012)033

Z.V. Krumshteyn[63], T. Kubota[85], S. Kuday[3a], S. Kuehn[47], A. Kugel[57c], T. Kuhl[41], D. Kuhn[60], V. Kukhtin[63], Y. Kulchitsky[89], S. Kuleshov[31b], C. Kummer[97], M. Kuna[77], J. Kunkle[119], A. Kupco[124], H. Kurashige[65], M. Kurata[159], Y.A. Kurochkin[89], V. Kus[124], E.S. Kuwertz[146], M. Kuze[156], J. Kvita[141], R. Kwee[15], A. La Rosa[48], L. La Rotonda[36a,36b], L. Labarga[79], J. Labbe[4], S. Lablak[134a], C. Lacasta[166], F. Lacava[131a,131b], H. Lacker[15], D. Lacour[77], V.R. Lacuesta[166], E. Ladygin[63], R. Lafaye[4], B. Laforge[77], T. Lagouri[79], S. Lai[47], E. Laisne[54], M. Lamanna[29], L. Lambourne[76], C.L. Lampen[6], W. Lampl[6], E. Lancon[135], U. Landgraf[47], M.P.J. Landon[74], J.L. Lane[81], V.S. Lang[57a], C. Lange[41], A.J. Lankford[162], F. Lanni[24], K. Lantzsch[174], S. Laplace[77], C. Lapoire[20], J.F. Laporte[135], T. Lari[88a], A. Larner[117], M. Lassnig[29], P. Laurelli[46], V. Lavorini[36a,36b], W. Lavrijsen[14], P. Laycock[72], O. Le Dortz[77], E. Le Guirriec[82], C. Le Maner[157], E. Le Menedeu[11], T. LeCompte[5], F. Ledroit-Guillon[54], H. Lee[104], J.S.H. Lee[115], S.C. Lee[150], L. Lee[175], M. Lefebvre[168], M. Legendre[135], F. Legger[97], C. Leggett[14], M. Lehmacher[20], G. Lehmann Miotto[29], X. Lei[6], M.A.L. Leite[23d], R. Leitner[125], D. Lellouch[171], B. Lemmer[53], V. Lendermann[57a], K.J.C. Leney[144b], T. Lenz[104], G. Lenzen[174], B. Lenzi[29], K. Leonhardt[43], S. Leontsinis[9], F. Lepold[57a], C. Leroy[92], J-R. Lessard[168], C.G. Lester[27], C.M. Lester[119], J. Levêque[4], D. Levin[86], L.J. Levinson[171], A. Lewis[117], G.H. Lewis[107], A.M. Leyko[20], M. Leyton[15], B. Li[82], H. Li[172,u], S. Li[32b,v], X. Li[86], Z. Liang[117,w], H. Liao[33], B. Liberti[132a], P. Lichard[29], M. Lichtnecker[97], K. Lie[164], W. Liebig[13], C. Limbach[20], A. Limosani[85], M. Limper[61], S.C. Lin[150,x], F. Linde[104], J.T. Linnemann[87], E. Lipeles[119], A. Lipniacka[13], T.M. Liss[164], D. Lissauer[24], A. Lister[48], A.M. Litke[136], C. Liu[28], D. Liu[150], H. Liu[86], J.B. Liu[86], L. Liu[86], M. Liu[32b], Y. Liu[32b], M. Livan[118a,118b], S.S.A. Livermore[117], A. Lleres[54], J. Llorente Merino[79], S.L. Lloyd[74], E. Lobodzinska[41], P. Loch[6], W.S. Lockman[136], T. Loddenkoetter[20], F.K. Loebinger[81], A. Loginov[175], C.W. Loh[167], T. Lohse[15], K. Lohwasser[47], M. Lokajicek[124], V.P. Lombardo[4], R.E. Long[70], L. Lopes[123a], D. Lopez Mateos[56], J. Lorenz[97], N. Lorenzo Martinez[114], M. Losada[161], P. Loscutoff[14], F. Lo Sterzo[131a,131b], M.J. Losty[158a,*], X. Lou[40], A. Lounis[114], K.F. Loureiro[161], J. Love[21], P.A. Love[70], A.J. Lowe[142,e], F. Lu[32a], H.J. Lubatti[137], C. Luci[131a,131b], A. Lucotte[54], A. Ludwig[43], D. Ludwig[41], I. Ludwig[47], J. Ludwig[47], F. Luehring[59], G. Luijckx[104], W. Lukas[60], D. Lumb[47], L. Luminari[131a], E. Lund[116], B. Lund-Jensen[146], B. Lundberg[78], J. Lundberg[145a,145b], O. Lundberg[145a,145b], J. Lundquist[35], M. Lungwitz[80], D. Lynn[24], E. Lytken[78], H. Ma[24], L.L. Ma[172], G. Maccarrone[46], A. Macchiolo[98], B. Maček[73], J. Machado Miguens[123a], R. Mackeprang[35], R.J. Madaras[14], H.J. Maddocks[70], W.F. Mader[43], R. Maenner[57c], T. Maeno[24], P. Mättig[174], S. Mättig[80], L. Magnoni[162], E. Magradze[53], K. Mahboubi[47], S. Mahmoud[72], G. Mahout[17], C. Maiani[135], C. Maidantchik[23a], A. Maio[123a,b], S. Majewski[24], Y. Makida[64], N. Makovec[114], P. Mal[135], B. Malaescu[29], Pa. Malecki[38], P. Malecki[38], V.P. Maleev[120], F. Malek[54], U. Mallik[61], D. Malon[5], C. Malone[142], S. Maltezos[9], V. Malyshev[106], S. Malyukov[29], R. Mameghani[97], J. Mamuzic[12b], A. Manabe[64], L. Mandelli[88a], I. Mandić[73], R. Mandrysch[15], J. Maneira[123a], A. Manfredini[98], P.S. Mangeard[87], L. Manhaes de Andrade Filho[23b], J.A. Manjarres Ramos[135], A. Mann[53], P.M. Manning[136], A. Manousakis-Katsikakis[8], B. Mansoulie[135], A. Mapelli[29], L. Mapelli[29], L. March[79], J.F. Marchand[28], F. Marchese[132a,132b], G. Marchiori[77], M. Marcisovsky[124], C.P. Marino[168], F. Marroquim[23a],

JHEP11(2012)033

Z. Marshall[29], F.K. Martens[157], L.F. Marti[16], S. Marti-Garcia[166], B. Martin[29], B. Martin[87], J.P. Martin[92], T.A. Martin[17], V.J. Martin[45], B. Martin dit Latour[48], S. Martin-Haugh[148], M. Martinez[11], V. Martinez Outschoorn[56], A.C. Martyniuk[168], M. Marx[81], F. Marzano[131a], A. Marzin[110], L. Masetti[80], T. Mashimo[154], R. Mashinistov[93], J. Masik[81], A.L. Maslennikov[106], I. Massa[19a,19b], G. Massaro[104], N. Massol[4], P. Mastrandrea[147], A. Mastroberardino[36a,36b], T. Masubuchi[154], P. Matricon[114], H. Matsunaga[154], T. Matsushita[65], C. Mattravers[117,c], J. Maurer[82], S.J. Maxfield[72], A. Mayne[138], R. Mazini[150], M. Mazur[20], L. Mazzaferro[132a,132b], M. Mazzanti[88a], J. Mc Donald[84], S.P. Mc Kee[86], A. McCarn[164], R.L. McCarthy[147], T.G. McCarthy[28], N.A. McCubbin[128], K.W. McFarlane[55,*], J.A. Mcfayden[138], G. Mchedlidze[50b], T. Mclaughlan[17], S.J. McMahon[128], R.A. McPherson[168,k], A. Meade[83], J. Mechnich[104], M. Mechtel[174], M. Medinnis[41], R. Meera-Lebbai[110], T. Meguro[115], R. Mehdiyev[92], S. Mehlhase[35], A. Mehta[72], K. Meier[57a], B. Meirose[78], C. Melachrinos[30], B.R. Mellado Garcia[172], F. Meloni[88a,88b], L. Mendoza Navas[161], Z. Meng[150,u], A. Mengarelli[19a,19b], S. Menke[98], E. Meoni[160], K.M. Mercurio[56], P. Mermod[48], L. Merola[101a,101b], C. Meroni[88a], F.S. Merritt[30], H. Merritt[108], A. Messina[29,y], J. Metcalfe[24], A.S. Mete[162], C. Meyer[80], C. Meyer[30], J-P. Meyer[135], J. Meyer[173], J. Meyer[53], T.C. Meyer[29], J. Miao[32d], S. Michal[29], L. Micu[25a], R.P. Middleton[128], S. Migas[72], L. Mijović[135], G. Mikenberg[171], M. Mikestikova[124], M. Mikuž[73], D.W. Miller[30], R.J. Miller[87], W.J. Mills[167], C. Mills[56], A. Milov[171], D.A. Milstead[145a,145b], D. Milstein[171], A.A. Minaenko[127], M. Miñano Moya[166], I.A. Minashvili[63], A.I. Mincer[107], B. Mindur[37], M. Mineev[63], Y. Ming[172], L.M. Mir[11], G. Mirabelli[131a], J. Mitrevski[136], V.A. Mitsou[166], S. Mitsui[64], P.S. Miyagawa[138], J.U. Mjörnmark[78], T. Moa[145a,145b], V. Moeller[27], K. Mönig[41], N. Möser[20], S. Mohapatra[147], W. Mohr[47], R. Moles-Valls[166], J. Monk[76], E. Monnier[82], J. Montejo Berlingen[11], F. Monticelli[69], S. Monzani[19a,19b], R.W. Moore[2], G.F. Moorhead[85], C. Mora Herrera[48], A. Moraes[52], N. Morange[135], J. Morel[53], G. Morello[36a,36b], D. Moreno[80], M. Moreno Llácer[166], P. Morettini[49a], M. Morgenstern[43], M. Morii[56], A.K. Morley[29], G. Mornacchi[29], J.D. Morris[74], L. Morvaj[100], H.G. Moser[98], M. Mosidze[50b], J. Moss[108], R. Mount[142], E. Mountricha[9,z], S.V. Mouraviev[93,*], E.J.W. Moyse[83], F. Mueller[57a], J. Mueller[122], K. Mueller[20], T.A. Müller[97], T. Mueller[80], D. Muenstermann[29], Y. Munwes[152], W.J. Murray[128], I. Mussche[104], E. Musto[101a,101b], A.G. Myagkov[127], M. Myska[124], J. Nadal[11], K. Nagai[159], R. Nagai[156], K. Nagano[64], A. Nagarkar[108], Y. Nagasaka[58], M. Nagel[98], A.M. Nairz[29], Y. Nakahama[29], K. Nakamura[154], T. Nakamura[154], I. Nakano[109], G. Nanava[20], A. Napier[160], R. Narayan[57b], M. Nash[76,c], T. Nattermann[20], T. Naumann[41], G. Navarro[161], H.A. Neal[86], P.Yu. Nechaeva[93], T.J. Neep[81], A. Negri[118a,118b], G. Negri[29], M. Negrini[19a], S. Nektarijevic[48], A. Nelson[162], T.K. Nelson[142], S. Nemecek[124], P. Nemethy[107], A.A. Nepomuceno[23a], M. Nessi[29,aa], M.S. Neubauer[164], M. Neumann[174], A. Neusiedl[80], R.M. Neves[107], P. Nevski[24], P.R. Newman[17], V. Nguyen Thi Hong[135], R.B. Nickerson[117], R. Nicolaidou[135], B. Nicquevert[29], F. Niedercorn[114], J. Nielsen[136], N. Nikiforou[34], A. Nikiforov[15], V. Nikolaenko[127], I. Nikolic-Audit[77], K. Nikolics[48], K. Nikolopoulos[17], H. Nilsen[47], P. Nilsson[7], Y. Ninomiya[154], A. Nisati[131a], R. Nisius[98], T. Nobe[156], L. Nodulman[5], M. Nomachi[115], I. Nomidis[153], S. Norberg[110], M. Nordberg[29], P.R. Norton[128], J. Novakova[125], M. Nozaki[64], L. Nozka[112], I.M. Nugent[158a], A.-

JHEP11(2012)033

E. Nuncio-Quiroz[20], G. Nunes Hanninger[85], T. Nunnemann[97], E. Nurse[76], B.J. O'Brien[45], S.W. O'Neale[17,*], D.C. O'Neil[141], V. O'Shea[52], L.B. Oakes[97], F.G. Oakham[28,d], H. Oberlack[98], J. Ocariz[77], A. Ochi[65], S. Oda[68], S. Odaka[64], J. Odier[82], H. Ogren[59], A. Oh[81], S.H. Oh[44], C.C. Ohm[29], T. Ohshima[100], H. Okawa[24], Y. Okumura[30], T. Okuyama[154], A. Olariu[25a], A.G. Olchevski[63], S.A. Olivares Pino[31a], M. Oliveira[123a,h], D. Oliveira Damazio[24], E. Oliver Garcia[166], D. Olivito[119], A. Olszewski[38], J. Olszowska[38], A. Onofre[123a,ab], P.U.E. Onyisi[30], C.J. Oram[158a], M.J. Oreglia[30], Y. Oren[152], D. Orestano[133a,133b], N. Orlando[71a,71b], I. Orlov[106], C. Oropeza Barrera[52], R.S. Orr[157], B. Osculati[49a,49b], R. Ospanov[119], C. Osuna[11], G. Otero y Garzon[26], J.P. Ottersbach[104], M. Ouchrif[134d], E.A. Ouellette[168], F. Ould-Saada[116], A. Ouraou[135], Q. Ouyang[32a], A. Ovcharova[14], M. Owen[81], S. Owen[138], V.E. Ozcan[18a], N. Ozturk[7], A. Pacheco Pages[11], C. Padilla Aranda[11], S. Pagan Griso[14], E. Paganis[138], C. Pahl[98], F. Paige[24], P. Pais[83], K. Pajchel[116], G. Palacino[158b], C.P. Paleari[6], S. Palestini[29], D. Pallin[33], A. Palma[123a], J.D. Palmer[17], Y.B. Pan[172], E. Panagiotopoulou[9], P. Pani[104], N. Panikashvili[86], S. Panitkin[24], D. Pantea[25a], A. Papadelis[145a], Th.D. Papadopoulou[9], A. Paramonov[5], D. Paredes Hernandez[33], W. Park[24,ac], M.A. Parker[27], F. Parodi[49a,49b], J.A. Parsons[34], U. Parzefall[47], S. Pashapour[53], E. Pasqualucci[131a], S. Passaggio[49a], A. Passeri[133a], F. Pastore[133a,133b,*], Fr. Pastore[75], G. Pásztor[48,ad], S. Pataraia[174], N. Patel[149], J.R. Pater[81], S. Patricelli[101a,101b], T. Pauly[29], M. Pecsy[143a], S. Pedraza Lopez[166], M.I. Pedraza Morales[172], S.V. Peleganchuk[106], D. Pelikan[165], H. Peng[32b], B. Penning[30], A. Penson[34], J. Penwell[59], M. Perantoni[23a], K. Perez[34,ae], T. Perez Cavalcanti[41], E. Perez Codina[158a], M.T. Pérez García-Estañ[166], V. Perez Reale[34], L. Perini[88a,88b], H. Pernegger[29], R. Perrino[71a], P. Perrodo[4], V.D. Peshekhonov[63], K. Peters[29], B.A. Petersen[29], J. Petersen[29], T.C. Petersen[35], E. Petit[4], A. Petridis[153], C. Petridou[153], E. Petrolo[131a], F. Petrucci[133a,133b], D. Petschull[41], M. Petteni[141], R. Pezoa[31b], A. Phan[85], P.W. Phillips[128], G. Piacquadio[29], A. Picazio[48], E. Piccaro[74], M. Piccinini[19a,19b], S.M. Piec[41], R. Piegaia[26], D.T. Pignotti[108], J.E. Pilcher[30], A.D. Pilkington[81], J. Pina[123a,b], M. Pinamonti[163a,163c], A. Pinder[117], J.L. Pinfold[2], B. Pinto[123a], C. Pizio[88a,88b], M. Plamondon[168], M.-A. Pleier[24], E. Plotnikova[63], A. Poblaguev[24], S. Poddar[57a], F. Podlyski[33], L. Poggioli[114], D. Pohl[20], M. Pohl[48], G. Polesello[118a], A. Policicchio[36a,36b], A. Polini[19a], J. Poll[74], V. Polychronakos[24], D. Pomeroy[22], K. Pommès[29], L. Pontecorvo[131a], B.G. Pope[87], G.A. Popeneciu[25a], D.S. Popovic[12a], A. Poppleton[29], X. Portell Bueso[29], G.E. Pospelov[98], S. Pospisil[126], I.N. Potrap[98], C.J. Potter[148], C.T. Potter[113], G. Poulard[29], J. Poveda[59], V. Pozdnyakov[63], R. Prabhu[76], P. Pralavorio[82], A. Pranko[14], S. Prasad[29], R. Pravahan[24], S. Prell[62], K. Pretzl[16], D. Price[59], J. Price[72], L.E. Price[5], D. Prieur[122], M. Primavera[71a], K. Prokofiev[107], F. Prokoshin[31b], S. Protopopescu[24], J. Proudfoot[5], X. Prudent[43], M. Przybycien[37], H. Przysiezniak[4], S. Psoroulas[20], E. Ptacek[113], E. Pueschel[83], J. Purdham[86], M. Purohit[24,ac], P. Puzo[114], Y. Pylypchenko[61], J. Qian[86], A. Quadt[53], D.R. Quarrie[14], W.B. Quayle[172], F. Quinonez[31a], M. Raas[103], V. Radescu[41], P. Radloff[113], T. Rador[18a], F. Ragusa[88a,88b], G. Rahal[177], A.M. Rahimi[108], D. Rahm[24], S. Rajagopalan[24], M. Rammensee[47], M. Rammes[140], A.S. Randle-Conde[39], K. Randrianarivony[28], F. Rauscher[97], T.C. Rave[47], M. Raymond[29], A.L. Read[116], D.M. Rebuzzi[118a,118b], A. Redelbach[173], G. Redlinger[24], R. Reece[119], K. Reeves[40],

JHEP11(2012)033

E. Reinherz-Aronis[152], A. Reinsch[113], I. Reisinger[42], C. Rembser[29], Z.L. Ren[150], A. Renaud[114], M. Rescigno[131a], S. Resconi[88a], B. Resende[135], P. Reznicek[97], R. Rezvani[157], R. Richter[98], E. Richter-Was[4,af], M. Ridel[77], M. Rijpstra[104], M. Rijssenbeek[147], A. Rimoldi[118a,118b], L. Rinaldi[19a], R.R. Rios[39], I. Riu[11], G. Rivoltella[88a,88b], F. Rizatdinova[111], E. Rizvi[74], S.H. Robertson[84,k], A. Robichaud-Veronneau[117], D. Robinson[27], J.E.M. Robinson[81], A. Robson[52], J.G. Rocha de Lima[105], C. Roda[121a,121b], D. Roda Dos Santos[29], A. Roe[53], S. Roe[29], O. Røhne[116], S. Rolli[160], A. Romaniouk[95], M. Romano[19a,19b], G. Romeo[26], E. Romero Adam[166], N. Rompotis[137], L. Roos[77], E. Ros[166], S. Rosati[131a], K. Rosbach[48], A. Rose[148], M. Rose[75], G.A. Rosenbaum[157], E.I. Rosenberg[62], P.L. Rosendahl[13], O. Rosenthal[140], L. Rosselet[48], V. Rossetti[11], E. Rossi[131a,131b], L.P. Rossi[49a], M. Rotaru[25a], I. Roth[171], J. Rothberg[137], D. Rousseau[114], C.R. Royon[135], A. Rozanov[82], Y. Rozen[151], X. Ruan[32a,ag], F. Rubbo[11], I. Rubinskiy[41], N. Ruckstuhl[104], V.I. Rud[96], C. Rudolph[43], G. Rudolph[60], F. Rühr[6], A. Ruiz-Martinez[62], L. Rumyantsev[63], Z. Rurikova[47], N.A. Rusakovich[63], J.P. Rutherfoord[6], C. Ruwiedel[14,*], P. Ruzicka[124], Y.F. Ryabov[120], M. Rybar[125], G. Rybkin[114], N.C. Ryder[117], A.F. Saavedra[149], I. Sadeh[152], H.F-W. Sadrozinski[136], R. Sadykov[63], F. Safai Tehrani[131a], H. Sakamoto[154], G. Salamanna[74], A. Salamon[132a], M. Saleem[110], D. Salek[29], D. Salihagic[98], A. Salnikov[142], J. Salt[166], B.M. Salvachua Ferrando[5], D. Salvatore[36a,36b], F. Salvatore[148], A. Salvucci[103], A. Salzburger[29], D. Sampsonidis[153], B.H. Samset[116], A. Sanchez[101a,101b], V. Sanchez Martinez[166], H. Sandaker[13], H.G. Sander[80], M.P. Sanders[97], M. Sandhoff[174], T. Sandoval[27], C. Sandoval[161], R. Sandstroem[98], D.P.C. Sankey[128], A. Sansoni[46], C. Santamarina Rios[84], C. Santoni[33], R. Santonico[132a,132b], H. Santos[123a], J.G. Saraiva[123a], T. Sarangi[172], E. Sarkisyan-Grinbaum[7], F. Sarri[121a,121b], G. Sartisohn[174], O. Sasaki[64], Y. Sasaki[154], N. Sasao[66], I. Satsounkevitch[89], G. Sauvage[4,*], E. Sauvan[4], J.B. Sauvan[114], P. Savard[157,d], V. Savinov[122], D.O. Savu[29], L. Sawyer[24,m], D.H. Saxon[52], J. Saxon[119], C. Sbarra[19a], A. Sbrizzi[19a,19b], D.A. Scannicchio[162], M. Scarcella[149], J. Schaarschmidt[114], P. Schacht[98], D. Schaefer[119], U. Schäfer[80], S. Schaepe[20], S. Schaetzel[57b], A.C. Schaffer[114], D. Schaile[97], R.D. Schamberger[147], A.G. Schamov[106], V. Scharf[57a], V.A. Schegelsky[120], D. Scheirich[86], M. Schernau[162], M.I. Scherzer[34], C. Schiavi[49a,49b], J. Schieck[97], M. Schioppa[36a,36b], S. Schlenker[29], E. Schmidt[47], K. Schmieden[20], C. Schmitt[80], S. Schmitt[57b], M. Schmitz[20], B. Schneider[16], U. Schnoor[43], A. Schoening[57b], A.L.S. Schorlemmer[53], M. Schott[29], D. Schouten[158a], J. Schovancova[124], M. Schram[84], C. Schroeder[80], N. Schroer[57c], M.J. Schultens[20], J. Schultes[174], H.-C. Schultz-Coulon[57a], H. Schulz[15], M. Schumacher[47], B.A. Schumm[136], Ph. Schune[135], C. Schwanenberger[81], A. Schwartzman[142], Ph. Schwegler[98], Ph. Schwemling[77], R. Schwienhorst[87], R. Schwierz[43], J. Schwindling[135], T. Schwindt[20], M. Schwoerer[4], G. Sciolla[22], W.G. Scott[128], J. Searcy[113], G. Sedov[41], E. Sedykh[120], S.C. Seidel[102], A. Seiden[136], F. Seifert[43], J.M. Seixas[23a], G. Sekhniaidze[101a], S.J. Sekula[39], K.E. Selbach[45], D.M. Seliverstov[120], B. Sellden[145a], G. Sellers[72], M. Seman[143b], N. Semprini-Cesari[19a,19b], C. Serfon[97], L. Serin[114], L. Serkin[53], R. Seuster[98], H. Severini[110], A. Sfyrla[29], E. Shabalina[53], M. Shamim[113], L.Y. Shan[32a], J.T. Shank[21], Q.T. Shao[85], M. Shapiro[14], P.B. Shatalov[94], K. Shaw[163a,163c], D. Sherman[175], P. Sherwood[76], A. Shibata[107], S. Shimizu[100], M. Shimojima[99], T. Shin[55], M. Shiyakova[63], A. Shmeleva[93], M.J. Shochet[30], D. Short[117],

JHEP11(2012)033

S. Shrestha[62], E. Shulga[95], M.A. Shupe[6], P. Sicho[124], A. Sidoti[131a], F. Siegert[47], Dj. Sijacki[12a], O. Silbert[171], J. Silva[123a], Y. Silver[152], D. Silverstein[142], S.B. Silverstein[145a], V. Simak[126], O. Simard[135], Lj. Simic[12a], S. Simion[114], E. Simioni[80], B. Simmons[76], R. Simoniello[88a,88b], M. Simonyan[35], P. Sinervo[157], N.B. Sinev[113], V. Sipica[140], G. Siragusa[173], A. Sircar[24], A.N. Sisakyan[63,*], S.Yu. Sivoklokov[96], J. Sjölin[145a,145b], T.B. Sjursen[13], L.A. Skinnari[14], H.P. Skottowe[56], K. Skovpen[106], P. Skubic[110], M. Slater[17], T. Slavicek[126], K. Sliwa[160], V. Smakhtin[171], B.H. Smart[45], S.Yu. Smirnov[95], Y. Smirnov[95], L.N. Smirnova[96], O. Smirnova[78], B.C. Smith[56], D. Smith[142], K.M. Smith[52], M. Smizanska[70], K. Smolek[126], A.A. Snesarev[93], S.W. Snow[81], J. Snow[110], S. Snyder[24], R. Sobie[168,k], J. Sodomka[126], A. Soffer[152], C.A. Solans[166], M. Solar[126], J. Solc[126], E.Yu. Soldatov[95], U. Soldevila[166], E. Solfaroli Camillocci[131a,131b], A.A. Solodkov[127], O.V. Solovyanov[127], V. Solovyev[120], N. Soni[85], V. Sopko[126], B. Sopko[126], M. Sosebee[7], R. Soualah[163a,163c], A. Soukharev[106], S. Spagnolo[71a,71b], F. Spanò[75], R. Spighi[19a], G. Spigo[29], R. Spiwoks[29], M. Spousta[125,ah], T. Spreitzer[157], B. Spurlock[7], R.D. St. Denis[52], J. Stahlman[119], R. Stamen[57a], E. Stanecka[38], R.W. Stanek[5], C. Stanescu[133a], M. Stanescu-Bellu[41], S. Stapnes[116], E.A. Starchenko[127], J. Stark[54], P. Staroba[124], P. Starovoitov[41], R. Staszewski[38], A. Staude[97], P. Stavina[143a,*], G. Steele[52], P. Steinbach[43], P. Steinberg[24], I. Stekl[126], B. Stelzer[141], H.J. Stelzer[87], O. Stelzer-Chilton[158a], H. Stenzel[51], S. Stern[98], G.A. Stewart[29], J.A. Stillings[20], M.C. Stockton[84], K. Stoerig[47], G. Stoicea[25a], S. Stonjek[98], P. Strachota[125], A.R. Stradling[7], A. Straessner[43], J. Strandberg[146], S. Strandberg[145a,145b], A. Strandlie[116], M. Strang[108], E. Strauss[142], M. Strauss[110], P. Strizenec[143b], R. Ströhmer[173], D.M. Strom[113], J.A. Strong[75,*], R. Stroynowski[39], J. Strube[128], B. Stugu[13], I. Stumer[24,*], J. Stupak[147], P. Sturm[174], N.A. Styles[41], D.A. Soh[150,w], D. Su[142], HS. Subramania[2], A. Succurro[11], Y. Sugaya[115], C. Suhr[105], M. Suk[125], V.V. Sulin[93], S. Sultansoy[3d], T. Sumida[66], X. Sun[54], J.E. Sundermann[47], K. Suruliz[138], G. Susinno[36a,36b], M.R. Sutton[148], Y. Suzuki[64], Y. Suzuki[65], M. Svatos[124], S. Swedish[167], I. Sykora[143a], T. Sykora[125], J. Sánchez[166], D. Ta[104], K. Tackmann[41], A. Taffard[162], R. Tafirout[158a], N. Taiblum[152], Y. Takahashi[100], H. Takai[24], R. Takashima[67], H. Takeda[65], T. Takeshita[139], Y. Takubo[64], M. Talby[82], A. Talyshev[106,f], M.C. Tamsett[24], J. Tanaka[154], R. Tanaka[114], S. Tanaka[130], S. Tanaka[64], A.J. Tanasijczuk[141], K. Tani[65], N. Tannoury[82], S. Tapprogge[80], D. Tardif[157], S. Tarem[151], F. Tarrade[28], G.F. Tartarelli[88a], P. Tas[125], M. Tasevsky[124], E. Tassi[36a,36b], M. Tatarkhanov[14], Y. Tayalati[134d], C. Taylor[76], F.E. Taylor[91], G.N. Taylor[85], W. Taylor[158b], M. Teinturier[114], F.A. Teischinger[29], M. Teixeira Dias Castanheira[74], P. Teixeira-Dias[75], K.K. Temming[47], H. Ten Kate[29], P.K. Teng[150], S. Terada[64], K. Terashi[154], J. Terron[79], M. Testa[46], R.J. Teuscher[157,k], J. Therhaag[20], T. Theveneaux-Pelzer[77], S. Thoma[47], J.P. Thomas[17], E.N. Thompson[34], P.D. Thompson[17], P.D. Thompson[157], A.S. Thompson[52], L.A. Thomsen[35], E. Thomson[119], M. Thomson[27], W.M. Thong[85], R.P. Thun[86], F. Tian[34], M.J. Tibbetts[14], T. Tic[124], V.O. Tikhomirov[93], Y.A. Tikhonov[106,f], S. Timoshenko[95], P. Tipton[175], S. Tisserant[82], T. Todorov[4], S. Todorova-Nova[160], B. Toggerson[162], J. Tojo[68], S. Tokár[143a], K. Tokushuku[64], K. Tollefson[87], M. Tomoto[100], L. Tompkins[30], K. Toms[102], A. Tonoyan[13], C. Topfel[16], N.D. Topilin[63], I. Torchiani[29], E. Torrence[113], H. Torres[77], E. Torró Pastor[166], J. Toth[82,ad], F. Touchard[82], D.R. Tovey[138], T. Trefzger[173],

JHEP11(2012)033

L. Tremblet[29], A. Tricoli[29], I.M. Trigger[158a], S. Trincaz-Duvoid[77], M.F. Tripiana[69], N. Triplett[24], W. Trischuk[157], B. Trocmé[54], C. Troncon[88a], M. Trottier-McDonald[141], M. Trzebinski[38], A. Trzupek[38], C. Tsarouchas[29], J.C-L. Tseng[117], M. Tsiakiris[104], P.V. Tsiareshka[89], D. Tsionou[4,ai], G. Tsipolitis[9], S. Tsiskaridze[11], V. Tsiskaridze[47], E.G. Tskhadadze[50a], I.I. Tsukerman[94], V. Tsulaia[14], J.-W. Tsung[20], S. Tsuno[64], D. Tsybychev[147], A. Tua[138], A. Tudorache[25a], V. Tudorache[25a], J.M. Tuggle[30], M. Turala[38], D. Turecek[126], I. Turk Cakir[3e], E. Turlay[104], R. Turra[88a,88b], P.M. Tuts[34], A. Tykhonov[73], M. Tylmad[145a,145b], M. Tyndel[128], G. Tzanakos[8], K. Uchida[20], I. Ueda[154], R. Ueno[28], M. Ugland[13], M. Uhlenbrock[20], M. Uhrmacher[53], F. Ukegawa[159], G. Unal[29], A. Undrus[24], G. Unel[162], Y. Unno[64], D. Urbaniec[34], G. Usai[7], M. Uslenghi[118a,118b], L. Vacavant[82], V. Vacek[126], B. Vachon[84], S. Vahsen[14], J. Valenta[124], S. Valentinetti[19a,19b], A. Valero[166], S. Valkar[125], E. Valladolid Gallego[166], S. Vallecorsa[151], J.A. Valls Ferrer[166], P.C. Van Der Deijl[104], R. van der Geer[104], H. van der Graaf[104], R. Van Der Leeuw[104], E. van der Poel[104], D. van der Ster[29], N. van Eldik[29], P. van Gemmeren[5], I. van Vulpen[104], M. Vanadia[98], W. Vandelli[29], A. Vaniachine[5], P. Vankov[41], F. Vannucci[77], R. Vari[131a], T. Varol[83], D. Varouchas[14], A. Vartapetian[7], K.E. Varvell[149], V.I. Vassilakopoulos[55], F. Vazeille[33], T. Vazquez Schroeder[53], G. Vegni[88a,88b], J.J. Veillet[114], F. Veloso[123a], R. Veness[29], S. Veneziano[131a], A. Ventura[71a,71b], D. Ventura[83], M. Venturi[47], N. Venturi[157], V. Vercesi[118a], M. Verducci[137], W. Verkerke[104], J.C. Vermeulen[104], A. Vest[43], M.C. Vetterli[141,d], I. Vichou[164], T. Vickey[144b,aj], O.E. Vickey Boeriu[144b], G.H.A. Viehhauser[117], S. Viel[167], M. Villa[19a,19b], M. Villaplana Perez[166], E. Vilucchi[46], M.G. Vincter[28], E. Vinek[29], V.B. Vinogradov[63], M. Virchaux[135,*], J. Virzi[14], O. Vitells[171], M. Viti[41], I. Vivarelli[47], F. Vives Vaque[2], S. Vlachos[9], D. Vladoiu[97], M. Vlasak[126], A. Vogel[20], P. Vokac[126], G. Volpi[46], M. Volpi[85], G. Volpini[88a], H. von der Schmitt[98], H. von Radziewski[47], E. von Toerne[20], V. Vorobel[125], V. Vorwerk[11], M. Vos[166], R. Voss[29], T.T. Voss[174], J.H. Vossebeld[72], N. Vranjes[135], M. Vranjes Milosavljevic[104], V. Vrba[124], M. Vreeswijk[104], T. Vu Anh[47], R. Vuillermet[29], I. Vukotic[30], W. Wagner[174], P. Wagner[119], H. Wahlen[174], S. Wahrmund[43], J. Wakabayashi[100], S. Walch[86], J. Walder[70], R. Walker[97], W. Walkowiak[140], R. Wall[175], P. Waller[72], B. Walsh[175], C. Wang[44], H. Wang[172], H. Wang[32b,ak], J. Wang[150], J. Wang[54], R. Wang[102], S.M. Wang[150], T. Wang[20], A. Warburton[84], C.P. Ward[27], M. Warsinsky[47], A. Washbrook[45], C. Wasicki[41], I. Watanabe[65], P.M. Watkins[17], A.T. Watson[17], I.J. Watson[149], M.F. Watson[17], G. Watts[137], S. Watts[81], A.T. Waugh[149], B.M. Waugh[76], M.S. Weber[16], P. Weber[53], A.R. Weidberg[117], P. Weigell[98], J. Weingarten[53], C. Weiser[47], H. Wellenstein[22], P.S. Wells[29], T. Wenaus[24], D. Wendland[15], Z. Weng[150,w], T. Wengler[29], S. Wenig[29], N. Wermes[20], M. Werner[47], P. Werner[29], M. Werth[162], M. Wessels[57a], J. Wetter[160], C. Weydert[54], K. Whalen[28], S.J. Wheeler-Ellis[162], A. White[7], M.J. White[85], S. White[121a,121b], S.R. Whitehead[117], D. Whiteson[162], D. Whittington[59], F. Wicek[114], D. Wicke[174], F.J. Wickens[128], W. Wiedenmann[172], M. Wielers[128], P. Wienemann[20], C. Wiglesworth[74], L.A.M. Wiik-Fuchs[47], P.A. Wijeratne[76], A. Wildauer[98], M.A. Wildt[41,s], I. Wilhelm[125], H.G. Wilkens[29], J.Z. Will[97], E. Williams[34], H.H. Williams[119], W. Willis[34], S. Willocq[83], J.A. Wilson[17], M.G. Wilson[142], A. Wilson[86], I. Wingerter-Seez[4], S. Winkelmann[47], F. Winklmeier[29], M. Wittgen[142], S.J. Wollstadt[80], M.W. Wolter[38],

JHEP11(2012)033

H. Wolters[123a,h], W.C. Wong[40], G. Wooden[86], B.K. Wosiek[38], J. Wotschack[29], M.J. Woudstra[81], K.W. Wozniak[38], K. Wraight[52], M. Wright[52], B. Wrona[72], S.L. Wu[172], X. Wu[48], Y. Wu[32b,al], E. Wulf[34], B.M. Wynne[45], S. Xella[35], M. Xiao[135], S. Xie[47], C. Xu[32b,z], D. Xu[138], B. Yabsley[149], S. Yacoob[144a,am], M. Yamada[64], H. Yamaguchi[154], A. Yamamoto[64], K. Yamamoto[62], S. Yamamoto[154], T. Yamamura[154], T. Yamanaka[154], J. Yamaoka[44], T. Yamazaki[154], Y. Yamazaki[65], Z. Yan[21], H. Yang[86], U.K. Yang[81], Y. Yang[59], Z. Yang[145a,145b], S. Yanush[90], L. Yao[32a], Y. Yao[14], Y. Yasu[64], G.V. Ybeles Smit[129], J. Ye[39], S. Ye[24], M. Yilmaz[3c], R. Yoosoofmiya[122], K. Yorita[170], R. Yoshida[5], C. Young[142], C.J. Young[117], S. Youssef[21], D. Yu[24], J. Yu[7], J. Yu[111], L. Yuan[65], A. Yurkewicz[105], M. Byszewski[29], B. Zabinski[38], R. Zaidan[61], A.M. Zaitsev[127], Z. Zajacova[29], L. Zanello[131a,131b], D. Zanzi[98], A. Zaytsev[106], C. Zeitnitz[174], M. Zeman[124], A. Zemla[38], C. Zendler[20], O. Zenin[127], T. Ženiš[143a], Z. Zinonos[121a,121b], S. Zenz[14], D. Zerwas[114], G. Zevi della Porta[56], Z. Zhan[32d], D. Zhang[32b,ak], H. Zhang[87], J. Zhang[5], X. Zhang[32d], Z. Zhang[114], L. Zhao[107], T. Zhao[137], Z. Zhao[32b], A. Zhemchugov[63], J. Zhong[117], B. Zhou[86], N. Zhou[162], Y. Zhou[150], C.G. Zhu[32d], H. Zhu[41], J. Zhu[86], Y. Zhu[32b], X. Zhuang[97], V. Zhuravlov[98], D. Zieminska[59], N.I. Zimin[63], R. Zimmermann[20], S. Zimmermann[20], S. Zimmermann[47], M. Ziolkowski[140], R. Zitoun[4], L. Živković[34], V.V. Zmouchko[127,*], G. Zobernig[172], A. Zoccoli[19a,19b], M. zur Nedden[15], V. Zutshi[105] and L. Zwalinski[29]

[1]: Physics Department, SUNY Albany, Albany NY, United States of America
[2]: Department of Physics, University of Alberta, Edmonton AB, Canada
[3]: [(a)]Department of Physics, Ankara University, Ankara; [(b)]Department of Physics, Dumlupinar University, Kutahya; [(c)]Department of Physics, Gazi University, Ankara; [(d)]Division of Physics, TOBB University of Economics and Technology, Ankara; [(e)]Turkish Atomic Energy Authority, Ankara, Turkey
[4]: LAPP, CNRS/IN2P3 and Université de Savoie, Annecy-le-Vieux, France
[5]: High Energy Physics Division, Argonne National Laboratory, Argonne IL, United States of America
[6]: Department of Physics, University of Arizona, Tucson AZ, United States of America
[7]: Department of Physics, The University of Texas at Arlington, Arlington TX, United States of America
[8]: Physics Department, University of Athens, Athens, Greece
[9]: Physics Department, National Technical University of Athens, Zografou, Greece
[10]: Institute of Physics, Azerbaijan Academy of Sciences, Baku, Azerbaijan
[11]: Institut de Física d'Altes Energies and Departament de Física de la Universitat Autònoma de Barcelona and ICREA, Barcelona, Spain
[12]: [(a)]Institute of Physics, University of Belgrade, Belgrade; [(b)]Vinca Institute of Nuclear Sciences, University of Belgrade, Belgrade, Serbia
[13]: Department for Physics and Technology, University of Bergen, Bergen, Norway
[14]: Physics Division, Lawrence Berkeley National Laboratory and University of California, Berkeley CA, United States of America

JHEP11(2012)033

[15]: Department of Physics, Humboldt University, Berlin, Germany
[16]: Albert Einstein Center for Fundamental Physics and Laboratory for High Energy Physics, University of Bern, Bern, Switzerland
[17]: School of Physics and Astronomy, University of Birmingham, Birmingham, United Kingdom
[18]: [(a)]Department of Physics, Bogazici University, Istanbul; [(b)]Division of Physics, Dogus University, Istanbul; [(c)]Department of Physics Engineering, Gaziantep University, Gaziantep; [(d)]Department of Physics, Istanbul Technical University, Istanbul, Turkey
[19]: [(a)]INFN Sezione di Bologna; [(b)]Dipartimento di Fisica, Università di Bologna, Bologna, Italy
[20]: Physikalisches Institut, University of Bonn, Bonn, Germany
[21]: Department of Physics, Boston University, Boston MA, United States of America
[22]: Department of Physics, Brandeis University, Waltham MA, United States of America
[23]: [(a)]Universidade Federal do Rio De Janeiro COPPE/EE/IF, Rio de Janeiro; [(b)]Federal University of Juiz de Fora (UFJF), Juiz de Fora; [(c)]Federal University of Sao Joao del Rei (UFSJ), Sao Joao del Rei; [(d)]Instituto de Fisica, Universidade de Sao Paulo, Sao Paulo, Brazil
[24]: Physics Department, Brookhaven National Laboratory, Upton NY, United States of America
[25]: [(a)]National Institute of Physics and Nuclear Engineering, Bucharest; [(b)]University Politehnica Bucharest, Bucharest; [(c)]West University in Timisoara, Timisoara, Romania
[26]: Departamento de Física, Universidad de Buenos Aires, Buenos Aires, Argentina
[27]: Cavendish Laboratory, University of Cambridge, Cambridge, United Kingdom
[28]: Department of Physics, Carleton University, Ottawa ON, Canada
[29]: CERN, Geneva, Switzerland
[30]: Enrico Fermi Institute, University of Chicago, Chicago IL, United States of America
[31]: [(a)]Departamento de Física, Pontificia Universidad Católica de Chile, Santiago; [(b)]Departamento de Física, Universidad Técnica Federico Santa María, Valparaíso, Chile
[32]: [(a)]Institute of High Energy Physics, Chinese Academy of Sciences, Beijing; [(b)]Department of Modern Physics, University of Science and Technology of China, Anhui; [(c)]Department of Physics, Nanjing University, Jiangsu; [(d)]School of Physics, Shandong University, Shandong, China
[33]: Laboratoire de Physique Corpusculaire, Clermont Université and Université Blaise Pascal and CNRS/IN2P3, Aubiere Cedex, France
[34]: Nevis Laboratory, Columbia University, Irvington NY, United States of America
[35]: Niels Bohr Institute, University of Copenhagen, Kobenhavn, Denmark
[36]: [(a)]INFN Gruppo Collegato di Cosenza; [(b)]Dipartimento di Fisica, Università della Calabria, Arcavata di Rende, Italy
[37]: AGH University of Science and Technology, Faculty of Physics and Applied Computer Science, Krakow, Poland

JHEP11(2012)033

[38]: The Henryk Niewodniczanski Institute of Nuclear Physics, Polish Academy of Sciences, Krakow, Poland
[39]: Physics Department, Southern Methodist University, Dallas TX, United States of America
[40]: Physics Department, University of Texas at Dallas, Richardson TX, United States of America
[41]: DESY, Hamburg and Zeuthen, Germany
[42]: Institut für Experimentelle Physik IV, Technische Universität Dortmund, Dortmund, Germany
[43]: Institut für Kern- und Teilchenphysik, Technical University Dresden, Dresden, Germany
[44]: Department of Physics, Duke University, Durham NC, United States of America
[45]: SUPA - School of Physics and Astronomy, University of Edinburgh, Edinburgh, United Kingdom
[46]: INFN Laboratori Nazionali di Frascati, Frascati, Italy
[47]: Fakultät für Mathematik und Physik, Albert-Ludwigs-Universität, Freiburg, Germany
[48]: Section de Physique, Université de Genève, Geneva, Switzerland
[49]: [(a)]INFN Sezione di Genova; [(b)]Dipartimento di Fisica, Università di Genova, Genova, Italy
[50]: [(a)]E. Andronikashvili Institute of Physics, Tbilisi State University, Tbilisi; [(b)]High Energy Physics Institute, Tbilisi State University, Tbilisi, Georgia
[51]: II Physikalisches Institut, Justus-Liebig-Universität Giessen, Giessen, Germany
[52]: SUPA - School of Physics and Astronomy, University of Glasgow, Glasgow, United Kingdom
[53]: II Physikalisches Institut, Georg-August-Universität, Göttingen, Germany
[54]: Laboratoire de Physique Subatomique et de Cosmologie, Université Joseph Fourier and CNRS/IN2P3 and Institut National Polytechnique de Grenoble, Grenoble, France
[55]: Department of Physics, Hampton University, Hampton VA, United States of America
[56]: Laboratory for Particle Physics and Cosmology, Harvard University, Cambridge MA, United States of America
[57]: [(a)]Kirchhoff-Institut für Physik, Ruprecht-Karls-Universität Heidelberg, Heidelberg; [(b)]Physikalisches Institut, Ruprecht-Karls-Universität Heidelberg, Heidelberg; [(c)]ZITI Institut für technische Informatik, Ruprecht-Karls-Universität Heidelberg, Mannheim, Germany
[58]: Faculty of Applied Information Science, Hiroshima Institute of Technology, Hiroshima, Japan
[59]: Department of Physics, Indiana University, Bloomington IN, United States of America
[60]: Institut für Astro- und Teilchenphysik, Leopold-Franzens-Universität, Innsbruck, Austria
[61]: University of Iowa, Iowa City IA, United States of America

JHEP11(2012)033

[62]: Department of Physics and Astronomy, Iowa State University, Ames IA, United States of America
[63]: Joint Institute for Nuclear Research, JINR Dubna, Dubna, Russia
[64]: KEK, High Energy Accelerator Research Organization, Tsukuba, Japan
[65]: Graduate School of Science, Kobe University, Kobe, Japan
[66]: Faculty of Science, Kyoto University, Kyoto, Japan
[67]: Kyoto University of Education, Kyoto, Japan
[68]: Department of Physics, Kyushu University, Fukuoka, Japan
[69]: Instituto de Física La Plata, Universidad Nacional de La Plata and CONICET, La Plata, Argentina
[70]: Physics Department, Lancaster University, Lancaster, United Kingdom
[71]: [(a)]INFN Sezione di Lecce; [(b)]Dipartimento di Matematica e Fisica, Università del Salento, Lecce, Italy
[72]: Oliver Lodge Laboratory, University of Liverpool, Liverpool, United Kingdom
[73]: Department of Physics, Jožef Stefan Institute and University of Ljubljana, Ljubljana, Slovenia
[74]: School of Physics and Astronomy, Queen Mary University of London, London, United Kingdom
[75]: Department of Physics, Royal Holloway University of London, Surrey, United Kingdom
[76]: Department of Physics and Astronomy, University College London, London, United Kingdom
[77]: Laboratoire de Physique Nucléaire et de Hautes Energies, UPMC and Université Paris-Diderot and CNRS/IN2P3, Paris, France
[78]: Fysiska institutionen, Lunds universitet, Lund, Sweden
[79]: Departamento de Fisica Teorica C-15, Universidad Autonoma de Madrid, Madrid, Spain
[80]: Institut für Physik, Universität Mainz, Mainz, Germany
[81]: School of Physics and Astronomy, University of Manchester, Manchester, United Kingdom
[82]: CPPM, Aix-Marseille Université and CNRS/IN2P3, Marseille, France
[83]: Department of Physics, University of Massachusetts, Amherst MA, United States of America
[84]: Department of Physics, McGill University, Montreal QC, Canada
[85]: School of Physics, University of Melbourne, Victoria, Australia
[86]: Department of Physics, The University of Michigan, Ann Arbor MI, United States of America
[87]: Department of Physics and Astronomy, Michigan State University, East Lansing MI, United States of America
[88]: [(a)]INFN Sezione di Milano; [(b)]Dipartimento di Fisica, Università di Milano, Milano, Italy
[89]: B.I. Stepanov Institute of Physics, National Academy of Sciences of Belarus, Minsk, Republic of Belarus

JHEP11(2012)033

[90]: National Scientific and Educational Centre for Particle and High Energy Physics, Minsk, Republic of Belarus
[91]: Department of Physics, Massachusetts Institute of Technology, Cambridge MA, United States of America
[92]: Group of Particle Physics, University of Montreal, Montreal QC, Canada
[93]: P.N. Lebedev Institute of Physics, Academy of Sciences, Moscow, Russia
[94]: Institute for Theoretical and Experimental Physics (ITEP), Moscow, Russia
[95]: Moscow Engineering and Physics Institute (MEPhI), Moscow, Russia
[96]: Skobeltsyn Institute of Nuclear Physics, Lomonosov Moscow State University, Moscow, Russia
[97]: Fakultät für Physik, Ludwig-Maximilians-Universität München, München, Germany
[98]: Max-Planck-Institut für Physik (Werner-Heisenberg-Institut), München, Germany
[99]: Nagasaki Institute of Applied Science, Nagasaki, Japan
[100]: Graduate School of Science and Kobayashi-Maskawa Institute, Nagoya University, Nagoya, Japan
[101]: [(a)]INFN Sezione di Napoli; [(b)]Dipartimento di Scienze Fisiche, Università di Napoli, Napoli, Italy
[102]: Department of Physics and Astronomy, University of New Mexico, Albuquerque NM, United States of America
[103]: Institute for Mathematics, Astrophysics and Particle Physics, Radboud University Nijmegen/Nikhef, Nijmegen, Netherlands
[104]: Nikhef National Institute for Subatomic Physics and University of Amsterdam, Amsterdam, Netherlands
[105]: Department of Physics, Northern Illinois University, DeKalb IL, United States of America
[106]: Budker Institute of Nuclear Physics, SB RAS, Novosibirsk, Russia
[107]: Department of Physics, New York University, New York NY, United States of America
[108]: Ohio State University, Columbus OH, United States of America
[109]: Faculty of Science, Okayama University, Okayama, Japan
[110]: Homer L. Dodge Department of Physics and Astronomy, University of Oklahoma, Norman OK, United States of America
[111]: Department of Physics, Oklahoma State University, Stillwater OK, United States of America
[112]: Palacký University, RCPTM, Olomouc, Czech Republic
[113]: Center for High Energy Physics, University of Oregon, Eugene OR, United States of America
[114]: LAL, Université Paris-Sud and CNRS/IN2P3, Orsay, France
[115]: Graduate School of Science, Osaka University, Osaka, Japan
[116]: Department of Physics, University of Oslo, Oslo, Norway
[117]: Department of Physics, Oxford University, Oxford, United Kingdom
[118]: [(a)]INFN Sezione di Pavia; [(b)]Dipartimento di Fisica, Università di Pavia, Pavia, Italy

JHEP11(2012)033

[119]: Department of Physics, University of Pennsylvania, Philadelphia PA, United States of America
[120]: Petersburg Nuclear Physics Institute, Gatchina, Russia
[121]: [(a)]INFN Sezione di Pisa; [(b)]Dipartimento di Fisica E. Fermi, Università di Pisa, Pisa, Italy
[122]: Department of Physics and Astronomy, University of Pittsburgh, Pittsburgh PA, United States of America
[123]: [(a)]Laboratorio de Instrumentacao e Fisica Experimental de Particulas - LIP, Lisboa, Portugal; [(b)]Departamento de Fisica Teorica y del Cosmos and CAFPE, Universidad de Granada, Granada, Spain
[124]: Institute of Physics, Academy of Sciences of the Czech Republic, Praha, Czech Republic
[125]: Faculty of Mathematics and Physics, Charles University in Prague, Praha, Czech Republic
[126]: Czech Technical University in Prague, Praha, Czech Republic
[127]: State Research Center Institute for High Energy Physics, Protvino, Russia
[128]: Particle Physics Department, Rutherford Appleton Laboratory, Didcot, United Kingdom
[129]: Physics Department, University of Regina, Regina SK, Canada
[130]: Ritsumeikan University, Kusatsu, Shiga, Japan
[131]: [(a)]INFN Sezione di Roma I; [(b)]Dipartimento di Fisica, Università La Sapienza, Roma, Italy
[132]: [(a)]INFN Sezione di Roma Tor Vergata; [(b)]Dipartimento di Fisica, Università di Roma Tor Vergata, Roma, Italy
[133]: [(a)]INFN Sezione di Roma Tre; [(b)]Dipartimento di Fisica, Università Roma Tre, Roma, Italy
[134]: [(a)]Faculté des Sciences Ain Chock, Réseau Universitaire de Physique des Hautes Energies - Université Hassan II, Casablanca; [(b)]Centre National de l'Energie des Sciences Techniques Nucleaires, Rabat; [(c)]Faculté des Sciences Semlalia, Université Cadi Ayyad, LPHEA-Marrakech; [(d)]Faculté des Sciences, Université Mohamed Premier and LPTPM, Oujda; [(e)]Faculté des sciences, Université Mohammed V-Agdal, Rabat, Morocco
[135]: DSM/IRFU (Institut de Recherches sur les Lois Fondamentales de l'Univers), CEA Saclay (Commissariat a l'Energie Atomique), Gif-sur-Yvette, France
[136]: Santa Cruz Institute for Particle Physics, University of California Santa Cruz, Santa Cruz CA, United States of America
[137]: Department of Physics, University of Washington, Seattle WA, United States of America
[138]: Department of Physics and Astronomy, University of Sheffield, Sheffield, United Kingdom
[139]: Department of Physics, Shinshu University, Nagano, Japan
[140]: Fachbereich Physik, Universität Siegen, Siegen, Germany
[141]: Department of Physics, Simon Fraser University, Burnaby BC, Canada

JHEP11(2012)033

[142]: SLAC National Accelerator Laboratory, Stanford CA, United States of America
[143]: [(a)]Faculty of Mathematics, Physics & Informatics, Comenius University, Bratislava; [(b)]Department of Subnuclear Physics, Institute of Experimental Physics of the Slovak Academy of Sciences, Kosice, Slovak Republic
[144]: [(a)]Department of Physics, University of Johannesburg, Johannesburg; [(b)]School of Physics, University of the Witwatersrand, Johannesburg, South Africa
[145]: [(a)]Department of Physics, Stockholm University; [(b)]The Oskar Klein Centre, Stockholm, Sweden
[146]: Physics Department, Royal Institute of Technology, Stockholm, Sweden
[147]: Departments of Physics & Astronomy and Chemistry, Stony Brook University, Stony Brook NY, United States of America
[148]: Department of Physics and Astronomy, University of Sussex, Brighton, United Kingdom
[149]: School of Physics, University of Sydney, Sydney, Australia
[150]: Institute of Physics, Academia Sinica, Taipei, Taiwan
[151]: Department of Physics, Technion: Israel Institute of Technology, Haifa, Israel
[152]: Raymond and Beverly Sackler School of Physics and Astronomy, Tel Aviv University, Tel Aviv, Israel
[153]: Department of Physics, Aristotle University of Thessaloniki, Thessaloniki, Greece
[154]: International Center for Elementary Particle Physics and Department of Physics, The University of Tokyo, Tokyo, Japan
[155]: Graduate School of Science and Technology, Tokyo Metropolitan University, Tokyo, Japan
[156]: Department of Physics, Tokyo Institute of Technology, Tokyo, Japan
[157]: Department of Physics, University of Toronto, Toronto ON, Canada
[158]: [(a)]TRIUMF, Vancouver BC; [(b)]Department of Physics and Astronomy, York University, Toronto ON, Canada
[159]: Institute of Pure and Applied Sciences, University of Tsukuba,1-1-1 Tennodai, Tsukuba, Ibaraki 305-8571, Japan
[160]: Science and Technology Center, Tufts University, Medford MA, United States of America
[161]: Centro de Investigaciones, Universidad Antonio Narino, Bogota, Colombia
[162]: Department of Physics and Astronomy, University of California Irvine, Irvine CA, United States of America
[163]: [(a)]INFN Gruppo Collegato di Udine; [(b)]ICTP, Trieste; [(c)]Dipartimento di Chimica, Fisica e Ambiente, Università di Udine, Udine, Italy
[164]: Department of Physics, University of Illinois, Urbana IL, United States of America
[165]: Department of Physics and Astronomy, University of Uppsala, Uppsala, Sweden
[166]: Instituto de Física Corpuscular (IFIC) and Departamento de Física Atómica, Molecular y Nuclear and Departamento de Ingeniería Electrónica and Instituto de Microelectrónica de Barcelona (IMB-CNM), University of Valencia and CSIC, Valencia, Spain
[167]: Department of Physics, University of British Columbia, Vancouver BC, Canada

JHEP11(2012)033

[168]: Department of Physics and Astronomy, University of Victoria, Victoria BC, Canada
[169]: Department of Physics, University of Warwick, Coventry, United Kingdom
[170]: Waseda University, Tokyo, Japan
[171]: Department of Particle Physics, The Weizmann Institute of Science, Rehovot, Israel
[172]: Department of Physics, University of Wisconsin, Madison WI, United States of America
[173]: Fakultät für Physik und Astronomie, Julius-Maximilians-Universität, Würzburg, Germany
[174]: Fachbereich C Physik, Bergische Universität Wuppertal, Wuppertal, Germany
[175]: Department of Physics, Yale University, New Haven CT, United States of America
[176]: Yerevan Physics Institute, Yerevan, Armenia
[177]: Domaine scientifique de la Doua, Centre de Calcul CNRS/IN2P3, Villeurbanne Cedex, France
[a]: Also at Laboratorio de Instrumentacao e Fisica Experimental de Particulas - LIP, Lisboa, Portugal
[b]: Also at Faculdade de Ciencias and CFNUL, Universidade de Lisboa, Lisboa, Portugal
[c]: Also at Particle Physics Department, Rutherford Appleton Laboratory, Didcot, United Kingdom
[d]: Also at TRIUMF, Vancouver BC, Canada
[e]: Also at Department of Physics, California State University, Fresno CA, United States of America
[f]: Also at Novosibirsk State University, Novosibirsk, Russia
[g]: Also at Fermilab, Batavia IL, United States of America
[h]: Also at Department of Physics, University of Coimbra, Coimbra, Portugal
[i]: Also at Department of Physics, UASLP, San Luis Potosi, Mexico
[j]: Also at Università di Napoli Parthenope, Napoli, Italy
[k]: Also at Institute of Particle Physics (IPP), Canada
[l]: Also at Department of Physics, Middle East Technical University, Ankara, Turkey
[m]: Also at Louisiana Tech University, Ruston LA, United States of America
[n]: Also at Dep Fisica and CEFITEC of Faculdade de Ciencias e Tecnologia, Universidade Nova de Lisboa, Caparica, Portugal
[o]: Also at Department of Physics and Astronomy, University College London, London, United Kingdom
[p]: Also at Group of Particle Physics, University of Montreal, Montreal QC, Canada
[q]: Also at Department of Physics, University of Cape Town, Cape Town, South Africa
[r]: Also at Institute of Physics, Azerbaijan Academy of Sciences, Baku, Azerbaijan
[s]: Also at Institut für Experimentalphysik, Universität Hamburg, Hamburg, Germany
[t]: Also at Manhattan College, New York NY, United States of America
[u]: Also at School of Physics, Shandong University, Shandong, China
[v]: Also at CPPM, Aix-Marseille Université and CNRS/IN2P3, Marseille, France
[w]: Also at School of Physics and Engineering, Sun Yat-sen University, Guanzhou, China
[x]: Also at Academia Sinica Grid Computing, Institute of Physics, Academia Sinica, Taipei, Taiwan

JHEP11(2012)033

[y]: Also at Dipartimento di Fisica, Università La Sapienza, Roma, Italy
[z]: Also at DSM/IRFU (Institut de Recherches sur les Lois Fondamentales de l'Univers), CEA Saclay (Commissariat a l'Energie Atomique), Gif-sur-Yvette, France
[aa]: Also at section de Physique, Université de Genève, Geneva, Switzerland
[ab]: Also at Departamento de Fisica, Universidade de Minho, Braga, Portugal
[ac]: Also at Department of Physics and Astronomy, University of South Carolina, Columbia SC, United States of America
[ad]: Also at Institute for Particle and Nuclear Physics, Wigner Research Centre for Physics, Budapest, Hungary
[ae]: Also at California Institute of Technology, Pasadena CA, United States of America
[af]: Also at Institute of Physics, Jagiellonian University, Krakow, Poland
[ag]: Also at LAL, Université Paris-Sud and CNRS/IN2P3, Orsay, France
[ah]: Also at Nevis Laboratory, Columbia University, Irvington NY, United States of America
[ai]: Also at Department of Physics and Astronomy, University of Sheffield, Sheffield, United Kingdom
[aj]: Also at Department of Physics, Oxford University, Oxford, United Kingdom
[ak]: Also at Institute of Physics, Academia Sinica, Taipei, Taiwan
[al]: Also at Department of Physics, The University of Michigan, Ann Arbor MI, United States of America
[am]: Also at Discipline of Physics, University of KwaZulu-Natal, Durban, South Africa
[*]: Deceased

JHEP11(2012)033